UCGE Reports

Number 20199

Department of Geomatics Engineering

Study of Interference Effects on GPS Signal Acquisition

(URL: http://www.geomatics.ucalgary.ca/links/GradTheses.html)

by

Sameet Mangesh Deshpande

July 2004

UNIVERSITY OF CALGARY

Study of Interference Effects on GPS Signal Acquisition

by

Sameet Mangesh Deshpande

A THESIS

SUBMITTED TO THE FACULTY OF GRADUATE STUDIES

IN PARTIAL FULFILMENT OF THE REQUIREMENTS FOR THE

DEGREE OF MASTER OF SCIENCE

DEPARTMENT OF GEOMATICS ENGINEERING

CALGARY, ALBERTA

JULY, 2004

Abstract

Interference and jamming is one of the major concerns in using the Global Positioning System (GPS) for critical applications. The GPS system has advantages over the narrow-band navigation systems since GPS signals are spread-spectrum signals and receiver design techniques can eliminate most of the interference signals. Any signal or its harmonics near the GPS L1 and L2 frequencies are a potential source of interference. The interference signals outside GPS frequency band can be filtered out either by a GPS antenna or a receiver front-end. Interference signals within the GPS frequency bandwidth are difficult to isolate using the filters. These signals need to be mitigated either by the acquisition process or the tracking process. This thesis investigates possible interference mitigation by the acquisition process.

Acquisition methods were implemented as a part of the correlator in a software receiver and used for analysis. Interference resulting from sampling in the receiver front-end and cross-correlation between the GPS Gold codes were studied. Aliasing effect introduces a loss of 2-3 dB in the acquisition gain and causes false locks for smaller sampling frequencies at a wider precorrelation bandwidth. The cross-correlation between the GPS Gold codes causes problems for the signal acquisition below -135 dBm.

Different radio frequency (RF) interference signals were studied to analyze their effect on the acquisition process. Adaptive predetection integration (up to 100 ms) was performed to determine the possible tolerance to the RF interference signals. A continuous wave (CW) interference hinders the acquisition more compared to any other RF signals such as swept CW, amplitude modulated (AM), frequency modulated (FM) or broadband noise. An RF signal level of 15-25 dB above the GPS signal level was found sufficient to jam the acquisition process.

Acknowledgements

I would like to thank Dr. Elizabeth Cannon for her guidance, support and encouragement throughout my research. I would also like to thank my fellow graduate students in the PLAN group for their help during my studies and making my stay in Calgary enjoyable. I would also like to thank Dr. Jayanta Kumar Ray, Muralikrishna, and Rakesh Nayak for their encouragement and help during my studies. Accord Software and Systems Pvt. Ltd. is thanked for introducing me to field of GPS and encouraging me to continue my education.

Last but not the least; I am grateful to my family and friends for their encouragement and motivation throughout my career.

Dedicated to my parents

Table of Contents

List of Tables

List of Figures and Illustrations

List of Abbreviations

GPS	Global Positioning System
FCC	Federal Communications Commissions
RF	Radio Frequency
TTFF	Time-To-First-Fix
DFT	Discrete Fourier transform
PLAN	Position, Location, and Navigation
CW	Continuous Wave
AM	Amplitude Modulation
FM	Frequency Modulation
VHF	Very High Frequency
VOR	VHF Omni-directional Radio
LORAN	Long-range RAdio Navigation
RADAR	RAdio Detection And Ranging
NAVSTAR	NAVigation Satellite Timing And Ranging
SPS	Standard Positioning Service
PPS	Precise Positioning Service
C/A	Coarse-Acquisition
TOA	Time Of Arrival
CDMA	Code Division Multiple Access
PRN	Pseudo Random Noise
DS	Direct Sequence
BPSK	Binary Phase Shift Keying
SV	Space Vehicle
NDU	Navigation Data Unit
PN	Pseudo Noise
IF	Intermediate Frequency
AGC	Automatic Gain Control
ADC	Analog-to-Digital Converter
PLL	Phase Lock Loop
FLL	Frequency Lock Loop
DLL	Delay Lock Loop
C/No	Carrier-to-Noise
ASIC	Application Specific Integrated Circuit
DSP	Digital Signal Processors
FPGA	Field Programmable Gate Arrays
FFT	Fast Fourier Transform
SNR	Signal-to-Noise Ratio
VCO	Voltage Controlled Oscillator
NCO	Numeric Controlled Oscillator
RFI	RF Interference
RAIM	Receiver Autonomous Integrity Monitoring
FDI	False Detection Identification
EIRP	Effective Isotropic Radiated Power

ATC	Air Traffic Control
J/N	Jammer-to-Noise
J/S	Jammer-to-Signal
FAA	Federal Aviation Authority
DGPS	Differential GPS
SA	Selective Availability
HTS	High Temperature Superconducting
RT	Room Temperature
NF	Noise Figure
LNA	Low Noise Amplifier
FPRA	Fixed Rejection Pattern Antenna
DF	Direction Finder
AOA	Angle Of Arrival
CRPA	Controlled Rejection Pattern Antenna
TDOA	Time Differences Of Arrival
ARLAS	Aircraft RFI Localization And Avoidance System
PDCB	Pulse Duty Cycle – Blanker
HAGR	High-Gain Advanced GPS Receiver
LOS	Line-Of-Sight
STAP	Space-Time Adaptive Processor
DOA	Direction Of Arrival
DOF	Degrees Of Freedom
SFAP	Space-Frequency Adaptive Processing
ISU	Interference Suppression Unit
BPF	Band Pass Filter
LPF	Low Pass Filter
PDF	Probability Density Function
SF	Sampling Frequency
TV	Television
RMS	Root Mean Square
IFFT	Inverse FFT
dBW	deciBel per Watt
dB	deciBel
dBm	deciBel per milliwatt
E911	Enhanced 911
SAW	Surface Acoustic Wave
I	Inphase
Q	Quadrature
GIDL	Generalized Interference Detection and Location
GNSS	Global Navigation Satellite System
PC	Personal Computer
DoD	Department of Defense
CWI	Continuous Wave Interference
MOPS	Minimum Operational Performance Standards
COTS	Commerical-Off-The-Shelf
SF	Sampling Frequency

PN	Pseudo Noise
WAAS	Wide Area Augmentation System

CHAPTER 1: INTRODUCTION

1.1 Background

The Global Positioning System (GPS) has become a critical part of the navigation infrastructure not only within the United States but also in other nations around the world [Paddan et al., 2003]. Traditionally the GPS was designed for applications where the satellite visibility was not an issue. These GPS receivers were required to have an acquisition sensitivity (minimum signal strength detectable) of -130 dBm [ICD, 2003]. With the E-911 mandate from the Federal Communications Commissions (FCC), it has become necessary to provide positions under all kinds of environments [FCC, 2003]. Indoor and urban canyon environments typically attenuate the GPS signal by about 20-25 dB [MacGougan, 2003]. Thus a signal strength of -150 dBm should be able to be acquired and tracked by a GPS receiver to provide position. A GPS signal below the -135 dBm power level is categorized as a weak signal [Tsui and Lin, 2001]. GPS receivers designed to operate at nominal GPS signal strengths are referred to as standard GPS receivers, while the receivers designed for weak signal environments are called the high-sensitivity receivers [Tsui and Bao, 2000].

A GPS receiver must detect the presence of the GPS signal to track and decode the information from the GPS signal required for position computation [Kaplan, 1996]. Tracking of the signals is possible only after they have been acquired, so acquisition is the first step in the GPS signal processing scheme. The acquisition process must ensure

that the signal is acquired at the correct code phase and carrier frequency [Spilker and Parkinson, 1996]. A GPS receiver should be capable of giving a reasonably correct position (within 5-10 m) in the presence of interference and multipath signals. Thus, the GPS receiver should be capable of mitigating the effects of Radio Frequency (RF) interference and multipath signals [Maenpa et al., 1997].

Any radio navigation system can be disrupted by an interference of high power and GPS is no exception. Although the GPS frequency bands are protected by the FCC frequency assignments, there is still a chance of spurious unintentional and intentional interference [Spilker and Parkinson, 1996]. RF interference (RFI) is a major source for the degradation of GPS accuracy and reliability. The interference signals must be mitigated to prevent the GPS receiver from giving erroneous information. This becomes important when the GPS is being used for critical applications [RTCA, 2001]. RFI mitigation can be done at various stages in the GPS receiver. Interference signals can be filtered out either by the GPS antenna or the front-end section of the GPS receiver [Littlepage, 1999]. The GPS signal processing and navigation algorithms can be modified to estimate the interference effect and detect the interference source [Macabiau et al., 2001].

1.2 Relevant Research

GPS signal acquisition has been extensively studied since the launch of the GPS program. A simple time domain correlation approach was widely used in the first generation GPS receivers [Spilker and Parkinson, 1996]. The time domain correlation methods were sequential in nature and simple for hardware implementation. The implementation

aspects of the signal acquisition schemes using Field Programmable Gate Arrays (FPGA) have been extensively studied by Gunawardena [2000], Alaqeeli and Starzyk [2001] and Alaqeeli [2002]. The GPS receiver manufacturers have used different technologies and modifications of this scheme in their receivers and most of these methods are the intellectual property (IP) of the respective companies. Van Nee and Conen [1991] pioneered the study of GPS signal acquisition in the frequency domain whereby they developed a circular convolution technique to speed up the acquisition process. Tsui and Bao [2000] improved the scheme to use only half the GPS signal spectrum for acquisition. Frequency domain methods allow the correlator section of the GPS receiver to be implemented in software. Software receiver design and development was studied by Akos et al. [2001], Burns et al. [2002] and Ledvina et al. [2003].

The use of the GPS in weak signal environments such as urban canyons, forest areas and indoors developed a need to acquire the GPS signals about 20-25 dB below the nominal signal strength. Chansarkar [2000], Choi et al. [2002] and Lin et al. [2002] developed techniques to extend the signal integration period during acquisition beyond the navigation data bit duration to increase the acquisition sensitivity. Tsui and Lin [2001] developed a scheme to have different thresholds for signal detection under different environments. Weak signal acquisition is required to provide a Doppler estimate within the bandwidth of the tracking loops. Tsui and Bao [2000] and Akopian et al. [2002] developed fine frequency estimation methods to acquire the signals with a resolution up to 1 Hz.

GPS is rapidly becoming the most widely used navigation system in automobile navigation, personal navigation, defence applications, timing applications and atmospheric studies. Methods of improving its accuracy through the use of Differential GPS (DGPS) has further opened up applications in precision navigation, including air, sea, and land. These applications require GPS to provide a reliable and accurate solution, however the system is vulnerable to low power interference from RF signals in the GPS frequency band [Littlepage, 1999]. Unintentional interference and jamming are two of the major concerns in using the GPS for various critical applications [Kaplan, 1996]. The Federal Aviation Authority (FAA) sponsored various tests to determine the vulnerability of GPS receivers to RFI allowing it to establish the interference tolerance standards for GPS receivers in civil aviation. These tests were focused on the coarse/acquisition (C/A) code receiver tracking degradation and loss of lock under different interference conditions. RFI effects on GPS signals have been extensively studied by researchers since the time of designing the GPS system (1970s).

Johannessen et al. [1990] studied potential sources of interference for the GPS and provided some solutions for civil aviation applications. Littlepage [1999] analyzed the effect of various interference signals on the use of the GPS for civil applications. RTCA [2001] established the minimum operational performance standards (MOPS) for the GPS/WAAS receivers under interference conditions based on the results from the FAA tests. Erlandson and Fraizer [2002] studied the effect of RFI signals on GPS in marine applications. Buck and Sellick [1997] analyzed the interference caused by television (TV) signals.

Different RFI mitigation techniques have been developed over the years by different researchers. These techniques can be classified into five categories

1. Antenna gain variation
2. RF filtering
3. Interference location
4. Sampling and Automatic Gain Control (AGC)
5. RFI mitigation in tracking

Antenna gain can be varied to provide a zero gain in the direction of the interference signal. This ensures that the interference signal is not captured by the GPS antenna. Different adaptive antenna arrays have been developed to achieve this goal. Bond and Brading [2000] developed a direction finder (DF) location vector to null the gain for interference signals. Kunysz [2001] developed a controlled rejection pattern antenna (CRPA) array to provide better tolerance to various kinds of interference signals. Navsys Inc. first developed a commercial GPS antenna to include spatial signal processing. Brown et al. [2000] further enhanced the antenna to detect the presence of interference signals and to estimate its direction. Moore and Gupta [2001] analyzed antenna arrays equipped with a space-time adaptive processor (STAP) to provide interference mitigation. The drawbacks in a STAP antenna were overcome using space-frequency adaptive processing (SFAP) [Gupta and Moore, 2001]. Vaccaro and Fante [2000] studied the different adaptive processing algorithms under an interference environment to determine the best methods available for the GPS antenna design.

RF filtering can be used to filter out interference signals outside the GPS frequency band. These filters should have a sharp cut-off outside the GPS bandwidth, low loss in the pass band and high rejection in the stop band. Escobar and Harper [2001] designed some high temperature superconducting (HTS) filters to provide the interference mitigation for tactical mobile applications.

Locating and nullifying the source(s) of the interference can realize the mitigation of the errors. Various interference localization techniques have been developed for determining the source(s) of the interference. Gormov et al. [2000] developed an inverse long range radio navigation (LORAN) method to estimate the direction of the jammer location. Brown et al. [1999] developed a time difference of arrival (TDOA) method to determine location of a large number of jammer sources. Shau-Shinu and Enge [2001] developed the RFI location method using a network of distributed sensors. The advantage of using a network of distributed sensors is that no sensor motion is required and is robust to sensor failures.

Bastide et al. [2003] studied the AGC to use it as a tool for interference assessment. An AGC is an accurate indicator of the noise in the receiver and variations of its threshold levels can be used to determine the presence of an interference signal. Blanking of the GPS signal using the AGC can be used to eliminate pulse interference. Hegarty et al. [2000] studied the effect of pulse interference on the AGC and designed a technique to suppress the pulse signal and determine the loss of signal during blanking. Leica Inc.

developed an RFI mitigation technique using multi-level sampling. Maenpa et al. [1997] analyzed the technique and found it suitable to minimize in-band interference.

Macabiau et al. [2001] devised a multi-correlator technique for detecting continuous wave (CW) interference. Manz et al. [2000] developed a technique to mitigate interference in the phase lock loop (PLL) provided the user is stationary and has a stable clock. Cooper and Daly [1997] developed a technique of preprocessing the GPS signal to remove the interference components using a PLL before passing the signal to the GPS tracking loops. These techniques were effective in mitigating CW interference but are not suitable for different interference signals.

A software receiver allows flexibility in dealing with interference. The exploitation of spectrum transforms as well as other mathematical tools are more feasible in software than in traditional hardware receivers. The accuracy of this representation is a function of the signal bandwidth, sampling rate and quantization error. Cutright et al. [2003] developed a frequency domain approach using a software receiver to mitigate RFI. Burns et al. [2002] evaluated software receiver interference mitigation by varying the number of bits in an Analog-to-Digital converter (ADC).

A considerable amount of research has been done on the GPS signal acquisition process and various RFI mitigation techniques. GPS signal acquisition has been studied for feasibility in hardware and software implementation, weak signal environments and fine frequency estimation. RFI mitigation at various stages in a GPS receiver from the GPS

antenna to the navigation solution has been studied extensively except for the acquisition process. RFI mitigation in the acquisition process has not been the focus of study mainly because of the few parameters controlling the acquisition process. This research studies the effect of the RFI signals in the acquisition process of a GPS receiver.

1.3 Research Objectives

The primary objective of this research is to analyze the effect of various RFI signals on the GPS signal acquisition process. The analysis will be done in terms of the variation in the noise power and the signal-to-noise ratio (SNR) in the acquisition process under different interference conditions. The tolerance to the various interference power levels for different adaptive predetection integration period is also evaluated.

To achieve this objective, first several acquisition schemes for the L1 C/A-code will be implemented for this research as a part of a software GPS receiver. The software GPS receiver is being developed by the Positioning, Location and Navigation (PLAN) group at the University of Calgary. The acquisition schemes will be analyzed in terms of mean acquisition time, acquisition gain and ability to acquire the correct signals. The effect of various acquisition parameters like sampling frequency and predetection integration time on the acquisition process will be studied.

The effect of CW, swept CW, broadband noise, pulsed interference, amplitude modulated (AM) and frequency modulated (FM) signals on the acquisition process will be

investigated. The research will be limited to a stationary scenario and interference frequencies within the GPS frequency band.

1.4 Thesis Outline

Chapter 2 gives an overview of the GPS and its error sources. GPS measurements and their signal structure are explained in brief. C/A-code generation and its auto correlation and cross-correlation properties are explained.

Chapter 3 discusses the GPS receiver architecture. It presents an overview of the work done on a software receiver. It also discusses various acquisition schemes and acquisition detection methods. Research done on weak signal acquisition is presented and the various acquisition performance parameters are also discussed.

Chapter 4 gives an overview of RFI and its effects. It discusses various interference signals and GPS jamming methods. RFI mitigation strategies are discussed briefly.

Chapter 5 discusses the basic acquisition results using GPS simulator data and real GPS data. An analysis of various parameters on the GPS acquisition process is discussed as well as the impact of sampling frequency and predetection integration time.

Chapter 6 presents the effects of various interference signals on GPS acquisition. CW, swept CW, broadband noise, pulsed interference, AM and FM signals are evaluated.

Adaptive predetection integration is performed to determine the interference tolerance possible.

Chapter 7 gives the conclusions obtained from the research and provides recommendations for future work.

CHAPTER 2: GPS SYSTEM OVERVIEW

This chapter gives a brief overview of the GPS system, various GPS measurements and their signal structure. It also discusses C/A-code generation and its auto correlation and cross correlation properties.

2.1 GPS System

The GPS is a satellite-based positioning system capable of providing a user position anywhere in the world. This system was developed by the Department of Defense (DoD) to support the military forces of the United States of America by providing world-wide, real-time positions [Parkinson et al., 1995]. GPS can be used for civilian applications even though it was developed for military applications [Spilker and Parkinson, 1996]. The system currently consists of 27 (nominally 24) satellites which provide continuous information for the user to compute position, velocity and time (PVT). The satellites orbit about 28,000 km above the Earth's surface and have an orbital period of 11 hr 58 m [ICD, 2003]. The GPS functions on the concept of one-way Time-of-Arrival (TOA) ranging whereby the user determines the TOA of the GPS signal transmitted by the GPS satellites. These ranges are used by the user to compute the navigation solution. A 3D position computation requires the range information from at least three satellites [Kaplan, 1996]. However, the GPS receiver clock is not generally synchronized with the satellite clocks and hence an additional measurement is required to solve the receiver clock offset.

GPS provides different accuracy levels for civilian and military users. Civilian users have access to the C/A-code which provides the Standard Positioning Service (SPS). Military users use a Precise (P)-code to get the Precise Positioning Service (PPS). The P-code is encrypted and hence not available for civilian users. The SPS provides an accuracy of 36 m (2D RMS 95%) in the horizontal plane and 77 m (95%) in the vertical direction [Stenbit, 2001] although recent field tests show accuracies of 5-10 m (1-σ RMS) [MacGougan, 2003]. GPS operates on two signal frequencies using code division multiple access (CDMA) technology to transmit the ranging codes [ICD, 2003]. The GPS signal structure is discussed in Section 2.3.

2.2 GPS Observations and Error Sources

Three different types of positioning information can be extracted from a GPS satellite signal, namely a pseudorange measurement, a carrier phase measurement, and the Doppler.

2.2.1 Pseudorange

A pseudorange is a range measurement between the GPS satellite and the user. This range measurement has inherent errors which make it different from the true range [Kaplan, 1996]. The pseudorange is a measure of the time delay required to align the GPS signal received from the satellite with the local GPS signal generated by the receiver. This time delay is converted into a distance measurement using the speed of light. The receiver clock and satellite clock are not synchronized which introduces an

error in the range. Hence the measured range is different from the true range and is called a pseudorange [Spilker and Parkinson, 1996]. The pseudorange is instantly available to compute position information and is given by Equation (2.1) [Wells et al., 1986].

$$p(t) = \rho(t) + d_{orb} + c\big(dt(t) - dT(t)\big) + d_{trop}(t) + d_{iono}(t) + \varepsilon_p \qquad 2.1$$

where

- $p(t)$ is the pseudorange measurement at time t (m),
- $\rho(t)$ is the true distance between satellite and receiver (m),
- d_{orb} is the orbital error (m),
- c is the speed of light (m/s),
- $dt(t)$ is the satellite clock error (s),
- $dT(t)$ is the receiver clock error (s),
- $d_{trop}(t)$ is the tropospheric error (m),
- $d_{iono}(t)$ is the ionospheric error (m), and
- ε_p is the code multipath and measurement noise (m).

2.2.2 Carrier Phase

A carrier phase measurement is a range measurement computed from the GPS carrier signal information. The total number of the carrier cycles from the GPS satellites to the user are measured and converted into a range measurement using the carrier wavelength [Kaplan, 1996]. The receiver cannot determine the number of integer cycles before the signal is acquired. This is referred to as the integer cycle ambiguity. This ambiguity must

be resolved before the carrier phase measurement can be used for position computation. It can be represented by Equation (2.2) [Wells et al., 1986].

$$\theta(t) = -\lambda\varphi(t) = \rho(t) + d_{orb} + c\left(dt(t) - dT(t)\right) + d_{trop}(t) - d_{iono}(t) + \lambda N + \varepsilon_{\theta} \qquad 2.2$$

where

$\theta(t)$ is the carrier phase measurement at time t (m),

$\varphi(t)$ is the carrier phase measurement (cycles),

λ is the carrier wavelength (m/cycle),

N is the integer carrier phase ambiguity (cycles), and

ε_{θ} is the carrier multipath and measurement noise (m).

The definitions of the other symbols are the same as in Equation (2.1). The carrier phase measurement with the ambiguity resolved to the correct integer provides a very accurate range measurement and is used to provide centimetre-level position accuracies.

2.2.3 Doppler

The Doppler is a measure of the instantaneous rate of the GPS carrier phase and is the instantaneous Doppler frequency shift of the incoming carrier. The Doppler shift results from the relative motion between the receiver and the satellite. The major role of the Doppler measurement in the navigation process is to compute a velocity estimate.

2.2.4 GPS Errors

GPS measurements have various errors including satellite clock errors, orbital errors, atmospheric errors, receiver clock error, multipath and interference [Wells et al., 1986]. The satellite clock error is the drift in the satellite clock with respect to the GPS time reference. The GPS master control station synchronizes the satellite clock with the GPS clock during the upload of the navigation information, and this offset is transmitted in the navigation message. The satellite orbital error is the difference between the satellite's position using the ephemeris and the actual values [ICD, 2003].

When the GPS signal travels through the troposphere its path will bend slightly due to the refractivity of the troposphere [Kaplan, 1996]. The change of the refractivity from free space to the troposphere causes the speed of the GPS signal to slow down which results in a delay of the GPS signal. This tropospheric delay is a function of the temperature, pressure, and relative humidity [Spilker and Parkinson, 1996]. Hopfield [1969] and Saastamoinen [1972] have developed different tropospheric delay models which can reduce the tropospheric error by about 90%.

The ionosphere is the layer of the atmosphere that extends from 60 to over 1000 km of height above the Earth's surface. It is an important source of range and range-rate errors for GPS users requiring high-accuracy measurements [Tsui and Bao, 2000]. The ionospheric variation is generally large compared to the troposphere and is more difficult to model. Ionospheric error can be eliminated using dual frequency measurements from

GPS. The single frequency ionospheric (Klobuchar) model described in ICD [2003] can reduce the ionospheric error by 50%. Ionospheric error can be further reduced using better ionospheric estimation models and Wide Area Augmentation Systems (WAAS) can be used to provide ionospheric corrections to reduce the error [Lachapelle, 2002].

The user clock is often inaccurate and not synchronized with the GPS clock, which results in the user clock error. The approximate magnitudes of the different errors are listed in Table 2.1.

Table 2.1: GPS error sources [Lachapelle, 2002]

GPS error source	**Error magnitude (1 σ) (m)**
Satellite clock and orbital errors	2.3
Ionosphere on L1	7.0
Troposphere	0.2
Code multipath	0.01-10
Code noise	0.6
Carrier multipath	50×10^{-3}
Carrier noise	$0.2\text{-}2 \times 10^{-3}$

All errors except multipath and noise can be reduced using techniques such as single-differencing, double-differencing and DGPS corrections [Lachapelle, 2002]. Multipath is the error caused by the reflected GPS signals entering the receiver front-end and mixing with the direct signal [Braasch and Van Grass, 1991]. Its effect will be more pronounced for static receivers close to large reflectors. It is specific to a receiver/antenna and

depends on the surrounding environment. Hence care has to be taken while installing GPS receivers for static applications, such as reference stations.

2.3 GPS Signal Structure Overview

The current GPS signal structure was developed specifically for positioning purpose and since it was developed for military application it also required a good resistance to jamming signals [Parkinson et al., 1995]. The spread spectrum concept was used to transmit ranging codes to provide the desired anti-jamming performance. A pseudo random noise (PRN) sequence with a high chipping rate was used to transmit the navigation information on to the GPS frequencies [ICD, 2003]. Spread spectrum signals have power below the noise level and can be recovered only with an appropriate spreading code. The two spreading codes used in the GPS signal are the C/A-code and P-code. These spreading codes were selected from a family of Gold codes [Kaplan, 1996]. Each satellite transmits the signal on the two frequencies (L1 and L2) with the P-code present on both the frequencies. The C/A-code is transmitted only on the L1 frequency. The CDMA technique of transmitting different spreading code for each satellite on the same frequency is used in the GPS to distinguish the signals from the different satellites [ICD, 2003]. Figure 2.1 represents the current GPS signal structure. The basics of spread spectrum and CDMA are discussed briefly in Sections 2.3.1 and 2.3.2.

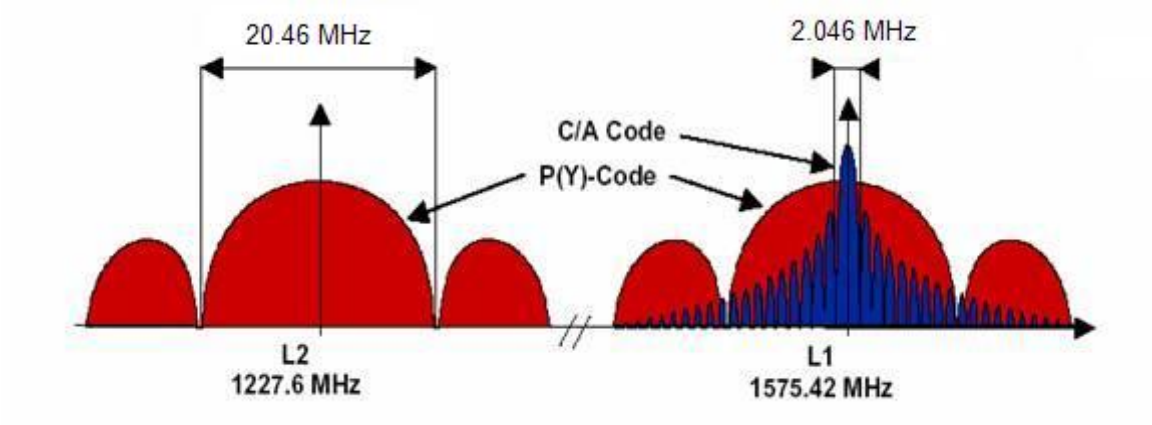

Figure 2.1: GPS signal spectrum

2.3.1 Spread Spectrum Basics

The spread spectrum concept consists of transmitting the information over a large bandwidth and using a PRN sequence to spread the information [Peterson et al., 1995]. The amount of bandwidth required for transmission is determined by the PRN sequence bandwidth. All modulation techniques which use a bandwidth wider than required for transmission are not spread spectrum techniques. The spread spectrum technique is useful for long distance communication with less interference problems [Kaplan, 1996]. During recovery of the spread spectrum signal, any interference signal is spread thereby reducing its power level below the noise. Spread spectrum solves two important communication problems namely pulse jamming and low probability of detection [Peterson et al., 1995]. The pulse jammer power level is reduced during signal recovery in the spread spectrum method. The spread spectrum can be recovered only when the PRN signal used for spreading is known [Peterson et al., 1995]. This reduces the chance of signal detection by other users in the same frequency band.

A direct sequence (DS) spread spectrum is used for the GPS signals. It consists of modulating the information signal using a spreading carrier signal [Peterson et al., 1995]. A binary phase shift keying (BPSK) signal is used to spread (modulate) the navigation data signal. The BPSK signal is a square wave (±1) and the phase of the modulated signal changes by 180 degrees with a change in the sign of the signal. Consider a data modulated carrier signal, S(t), given in Equation (2.3).

$$S(t) = A\cos(\omega t + \Phi(t)) \tag{2.3}$$

where

A is the amplitude of the carrier signal (volts),

ω is the carrier frequency (Hz), and

Φ is the data modulation signal.

BPSK spreading is performed by multiplying the S(t) by a function c(t), which represents the spreading waveform and the resulting signal, $S_t(t)$, is given in Equation (2.4).

$$S_t(t) = Ac(t)\cos(\omega t + \Phi(t)) \tag{2.4}$$

This spread spectrum signal is then transmitted and is received by the receiver after a delay of T. To recover the signal, the receiver must replicate the spreading signal used at the transmitter and match the phase of the spreading signal. The received signal, $S_r(t)$, is given in Equation (2.5).

$$S_r(t) = Ac(t-T)\cos(\omega t + \Phi(t-T) + \phi) \tag{2.5}$$

where

ϕ is the random phase error (radians).

The spreading signal, c(t), has values of ±1, which when multiplied with the received signal c(t-T) will have a value of one when the phase of the replica signal matches the

incoming signal. This allows for the recovery of the information in Equation (2.5) except for some random phase error [Tsui and Bao, 2000]. A similar concept is used in the GPS for transmission and recovery of the information.

2.3.2 Code Division Multiple Access

A CDMA system is one in which different transmitters transmit the information on the same carrier frequency using different spreading codes to distinguish each transmitter. The spreading codes used are a set of orthogonal or near-orthogonal codes [Kaplan, 1996]. An orthogonal code has a zero correlation with the other codes used in the system. The GPS uses the CDMA technology to transmit information from the GPS satellites at the same centre frequency which gives rise to the possibility of interference among the codes [Tsui and Bao, 2000]. The codes do not have zero cross-correlation due to side lobes of the codes and hence there is a possibility of a cross-correlation peak, resulting from correlation between same or different codes, being higher than the autocorrelation peak when the desired signal is weak.

2.3.3 GPS Signal Structure

GPS satellites transmit on two frequencies in the L-band of the frequency spectrum called L1 and L2 signals. The L1 signal is the primary frequency and is transmitted at 1.57542 GHz and L2 is the secondary frequency and is transmitted at 1.2276 GHz. The GPS signal is a BPSK DS spread spectrum signal [ICD, 2003]. The two carrier frequencies are modulated by the spread spectrum codes with a unique PRN associated

with each space vehicle (SV). The signals are further modulated by a 50 Hz navigation data message [ICD, 2003]. The C/A and P-codes are in phase quadrature with each other on the L1 frequency. A C/A-code is 1023 bits long and is available to civilian users. A P-code is one week long code and the structure of the P-code is known. It is reserved for military applications and hence is encrypted using a Y-code. This encrypted code is transmitted instead of the P-code on both frequencies [ICD, 2003].

Figure 2.2 shows a block diagram of the GPS satellite transmitter unit. The GPS satellite uses a 10.23 MHz reference clock to generate both the L1 and L2 frequencies. This clock is usually a cesium clock and generates a clock frequency slightly lower than 10.23 MHz to account for the relativistic effect [Spilker and Parkinson, 1996]. The GPS signal broadcast on the L1 and L2 frequencies have the signal structure given in Equations (2.6) and (2.7) [Kaplan, 1996].

$$L_1(t) = A_1 P(t) N(t) \cos(2\pi f_1 t) + A_1 C/A(t) N(t) \sin(2\pi f_1 t) \qquad 2.6$$

$$L_2(t) = A_2 P(t) N(t) \cos(2\pi f_2 t) \qquad 2.7$$

where

A_1 is the L1 signal amplitude,

A_2 is the L2 signal amplitude,

$P(t)$ is the P-code,

$C/A(t)$ is the C/A-code,

$N(t)$ is the navigation data,

$\cos(2\pi f_1 t), \cos(2\pi f_2 t), \sin(2\pi f_1 t)$ are the unmodulated L_1 and L_2 signals, and

$L_1(t)$ and $L_2(t)$ are the modulated L_1 and L_2 signals.

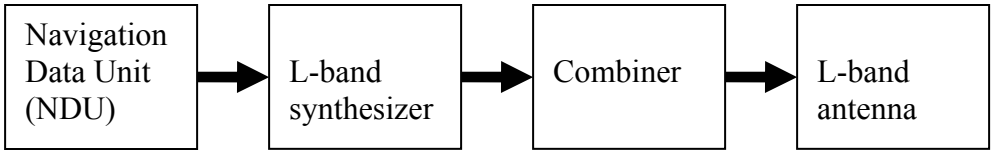

Figure 2.2: GPS satellite transmitter unit [Spilker and Parkinson, 1996]

The navigation data unit (NDU) generates the cosine and sine of the carrier signal which are modulated by a 50 Hz navigation data signal. This modulated signal is then spread using the C/A-code and the P(Y)-code [Kaplan, 1996]. The NDU block performs the function of modulating the signal, and the synthesizer is used to manipulate the signals according to the bandwidth specifications of the signal. For the L1 signal, the combiner combines the C/A-code and the P(Y)-code signals onto one signal. Both the L1 and the L2 signals are transmitted to the Earth using an L-band antenna.

2.4 C/A Code Generation

A block diagram of the C/A-code generator is shown in Figure 2.3. The C/A-code is generated using a linear code generator. Linear code generators can be described by a polynomial of the form $1 + \sum_{i=0}^{n} X^i$, where X^i means that the output of the i^{th} cell of the n-stage shift register is used as the input to a modulo-2 adder and the 1 means that the output of the adder is fed to the first cell [Tsui and Bao, 2000]. The C/A-code generator consists of two 10-bit shift registers (G1 and G2), which generate a maximum length pseudo noise (PN) codes with length of $2^{10} - 1 = 1023$ bits. The only state the shift register must not get into is an all-zero state. The shift registers can be described by the polynomials $G1 = 1 + X^3 + X^{10}$ and $G2 = 1 + X^2 + X^3 + X^6 + X^8 + X^9 + X^{10}$ [ICD, 2003].

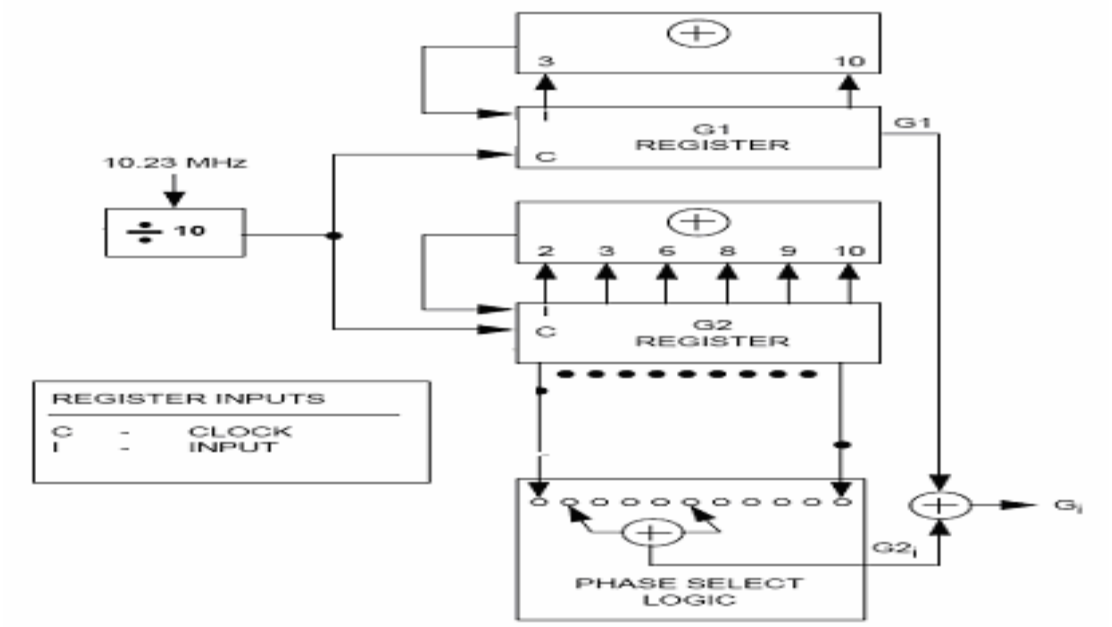

Figure 2.3: GPS C/A code generator [ICD, 2003]

The unique C/A-code for each SV is a result of the exclusive-or of a delayed version of the G2 output sequence and the G1 direct output sequence. The delay effect in the G2 PRN code is obtained by the exclusive-or of the selected positions of two taps whose output is called G21. This is because a PN code sequence has the property that when added to a phase-shifted version of the same code it does not change but obtains another phase [Tsui and Bao, 2000]. The function of the two taps on the G2 shift register is to shift the code phase in G2 with respect to the code phase in G1 without the need for an additional shift register to perform this delay. Each PRN code is associated with two tap positions on the G2 register. Table 2.2 describes these tap positions for all defined GPS PRN numbers and also specifies the equivalent delay in the C/A-code chips [ICD, 2003]. The chipping rate for the C/A-code is 1.023 MHz and hence the C/A-code repeats every millisecond.

The first 32 of these PRN numbers are reserved for the GPS satellites and the remaining PRNs (33 to 37) are reserved for other uses such as ground transmissions. The generation of the P-code is more complex than the C/A-code. P-code generators use four 12-bit shift registers and their sequences are combined to generate the P-code. The sequence generated is 38 weeks long which is partitioned into 37 unique sequences that are truncated at the end of one week. Each week long code represents the P-code for the GPS satellites [ICD, 2003]. The P-code is not a part of this research and hence the generation of the P-code is not discussed in detail.

Table 2.2: GPS C/A-code delay [ICD, 2003]

PRN number	C/A code tap selection	C/A code delay (chips)	PRN number	C/A code tap selection	C/A code delay (chips)
1	2Θ6	5	20	4Θ7	472
2	3Θ7	6	21	5Θ8	473
3	4Θ8	7	22	6Θ9	474
4	5Θ9	8	23	1Θ3	509
5	1Θ9	17	24	4Θ6	512
6	2Θ10	18	25	5Θ7	513
7	1Θ8	139	26	6Θ8	514
8	2Θ9	140	27	7Θ9	515
9	3Θ10	141	28	8Θ10	516
10	2Θ3	251	29	1Θ6	859
11	3Θ4	252	30	2Θ7	860
12	5Θ6	254	31	3Θ8	861
13	6Θ7	255	32	4Θ9	862
14	7Θ8	256	33	5Θ10	863
15	8Θ9	257	34	4Θ10	950
16	9Θ10	258	35	1Θ7	947
17	1Θ4	469	36	2Θ8	948
18	2Θ5	470	37	4Θ10	950
19	3Θ6	471			

Θ Exclusive-OR operator

2.5 C/A Code Correlation Properties

This section discusses the correlation properties of the C/A-code and their probability of occurrence.

2.5.1 Auto Correlation

The C/A-code correlation properties are fundamental to the signal acquisition and demodulation processes in a GPS receiver [Spilker and Parkinson, 1996]. The correlation of a code with itself is called autocorrelation, while the correlation between two codes is called cross-correlation. The autocorrelation function involves replicating the code and then shifting its phase while multiplying it with the original function. When the phases of the two signals match, the maximum correlation is obtained. The autocorrelation function for a Pseudo Noise (PN) sequence, PN(t), whose amplitude is ±A, chipping period is T_c and period is NT_c is given by Equation (2.8) [Macabiau et al., 2001].

$$R(\tau) = \frac{1}{T_c}\int_0^{T_c} PN(t)PN(t+\tau)dt \qquad 2.8$$

A PN sequence of length $N = 2^n-1$, where n is the number of shift register stages used to generate the sequence is called a maximum length sequence [Kaplan, 1996]. The autocorrelation function yields $-A^2/N$ outside the correlation interval because the number of negative values (-1) is always one greater than number of positive values (+1) in a maximum length PN sequence [Peterson et al., 1995]. An autocorrelation function for a

maximum length PN sequence is the infinite series of triangular functions with period NT_c. The negative correlation amplitude ($-A^2/N$) is obtained when the phase shift,τ, is greater than $\pm T_c$, (or multiples of $\pm T_c(N\pm1)$) and represents a dc term in the series [Macabiau et al., 2001].

GPS PRN codes have periodic correlation triangles and a peak spectrum that has similar characteristics to the maximum length PN sequences [Kaplan, 1996]. However the GPS codes are not maximum length PN sequences. A simple 10-bit linear code generator can generate 1023 sequences but all the autocorrelation functions have considerable power in the side lobes which affects the signal detection at low signal strengths. This problem was overcome by combining sequences from two 10-bit shift registers (G1 and G2) to generate the C/A-code [Spilker and Parkinson, 1996]. The combination of two sequences from the C/A-code generator yields 1023 possible combinations. The correlation properties of these sequences were studied and 32 codes with the best cross-correlation properties were selected for the GPS satellites [Kaplan, 1996].

The autocorrelation function of the GPS C/A-code has the same period and shape in the correlation domain as the maximum length PN sequences. However, there are small correlation values in the interval between the maximum correlation intervals. These small fluctuations in the autocorrelation function of the C/A-code result in the deviation of the line spectrum from the sin(x)/x envelope [Spilker and Parkinson, 1996]. The 1 KHz line spectrum spacing is the same for all the C/A-codes and the 10-bit maximum length sequence code. The ratio of power in each of the C/A-code line spectrum to the total

power can fluctuate by nearly 8 dB with respect to the -30 dB levels that would be obtained if every line contained the same power [Kaplan, 1996]. The autocorrelation for PRN 12 is shown in the Figure 2.4.

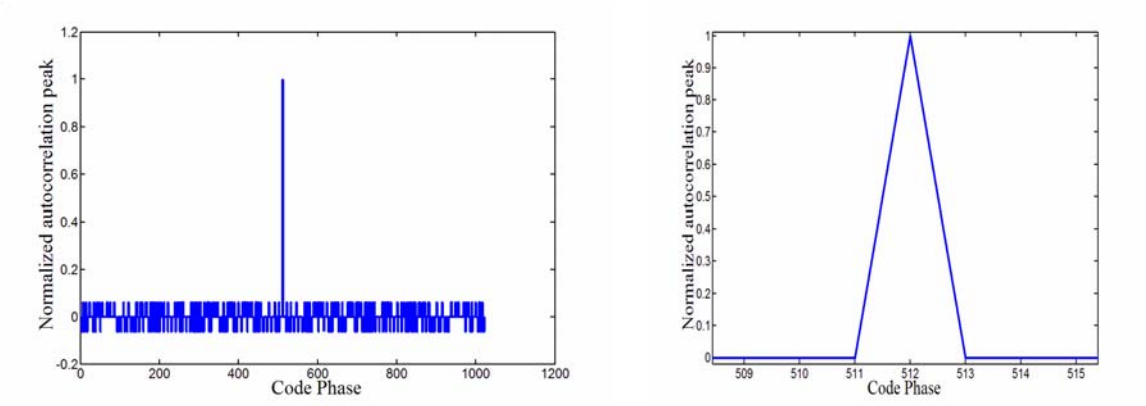

(a) chip level (b) zoomed around the peak

Figure 2.4: Autocorrelation plot for SV 12

2.5.2 Cross Correlation

A GPS receiver should generate a replica of the GPS PRN code and shift its phase to align with the PRN code for each SV. The PRN codes for different satellites should have poor cross-correlation properties among them to allow acquisition of the correct PRN signal. The GPS C/A-code length is 1023 chips which causes the cross-correlation properties to be poor for some codes. The C/A-code autocorrelation peaks are higher than cross-correlation peaks by just 21-24 dB, which can cause false acquisition [Kaplan, 1996]. Table 2.3 lists the C/A-code cross correlation power probabilities.

Table 2.3: Cross correlation probability of C/A code [Kaplan, 1996]

Cumulative Probability of Occurrence	Cross correlation for any two codes (dB)
0.23	-23.9
0.50	-24.2
0.99	-60.2

The P-code is not a maximum length sequence but since its period is very long its autocorrelation and cross-correlation properties are almost ideal. The cross-correlation peak between the P-codes is 127 dB lower than the autocorrelation peak, which is much better compared to 24 dB difference for the C/A-codes [Kaplan, 1996]. The autocorrelation function of the P-code has similar characteristics to the C/A-code. The study of P-code is not a part of this research and hence the correlation properties of the P-code will not be discussed.

CHAPTER 3: GPS RECEIVER ARCHITECTURE AND SOFTWARE RECEIVER DESIGN

This chapter discusses the architecture of a conventional GPS receiver and it presents an overview of the work done on a software receiver. Research done on the acquisition process including weak signal acquisition, is presented and various acquisition performance parameters are also discussed.

3.1 Conventional GPS Receiver Architecture

A conventional GPS receiver consists of three blocks which process the incoming GPS signal in three different frequency ranges. The RF section operates on the incoming GPS signals at the GHz frequency range, the signal processing section operates on the signal at the MHz/KHz frequency range and the data processing section operates at the Hz frequency range. A conventional GPS Receiver block diagram is shown in Figure 3.1.

The RF section is responsible for receiving the GPS signal from the antenna and down converting it to an intermediate frequency (IF) [Kaplan, 1996]. The down conversion process can be performed in a single stage or in multiple stages. Each stage consists of a local oscillator, mixer and band pass filter to eliminate the undesired mixer product. The RF section amplifies the signal and also determines its precorrelation bandwidth. The IF signal is sampled at a desired sampling rate using an AGC and an ADC [Tsui and Bao, 2000].

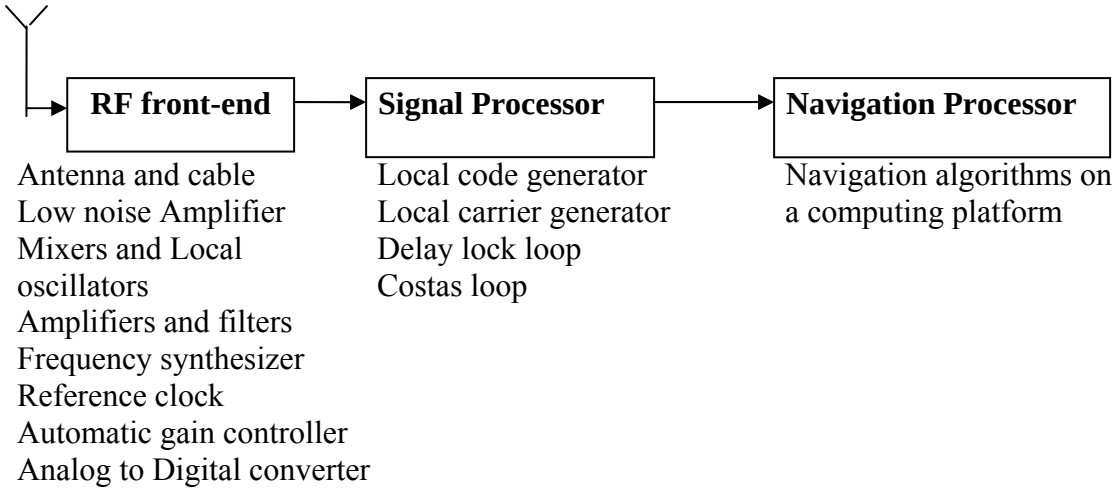

Figure 3.1: GPS receiver architecture

The signal processor acquires and tracks the signals and determines the navigation data bit value. Acquisition involves performing a two-dimensional search in the code and Doppler range. It involves a carrier wipe-off wherein the carrier from the incoming GPS signal is removed and code wipe-off wherein the PRN code from the incoming GPS signal is removed. Once the carrier is wiped off, the residual frequency component is the Doppler. The acquisition process must replicate both the carrier and code of the satellite in order to acquire it (the signal match for success is two-dimensional). To acquire the signal, correlation is done over a period called the predetection integration period, which is chosen depending on the acquisition scheme, time-to-first-fix (TTFF) requirement, data bit prediction and Doppler frequency [Tsui and Bao, 2000]. When the replica signal correctly matches the code and Doppler of the received signal, a GPS signal peak is obtained. This peak is easily distinguishable from other peaks at the nominal power (-130 dBm) and allows signal acquisition. The GPS signal acquisition process is explained in detail in Section 3.3.

Once the signal is acquired, the tracking loops are used to keep lock on the signal and to detect the navigation data bit transitions. A PLL and a Frequency lock loop (FLL) are used to track the carrier signal whereas a Delay lock loop (DLL) is used to track the code phase [Spilker and Parkinson, 1996]. This section generates the pseudorange and the Doppler measurements, computes the Carrier-to-Noise (C/No) ratio of the signal to determine signal quality and determines the thresholds for the acquisition and tracking process. It also extracts the raw navigation data from the data bits collected.

The navigation processor extracts the navigation information from the raw data bits collected, computes satellite positions and uses them to compute the user's PVT information. Present day GPS receivers combine the receiver blocks to reduce cost and size and to have a greater level of integration [Ray, 2003]. Advances in GPS receiver technology have made it possible to have a 12-channel receiver with the capability of computing the navigation information at a 10 Hz rate, being smaller in size than a credit card, and affordable to an average customer (less than $100).

3.2 Software Receiver

Traditionally, a GPS receiver has the RF and signal processing sections implemented in hardware. The signal processor (usually called the correlator) is generally realized in an Application Specific Integrated Circuit (ASIC). Realizing the correlator in software requires access to the digitized output of the RF section. With the increasing power of microprocessors and in particular digital signal processors (DSP), it has become possible to implement a software-based GPS receiver having only the RF section as the hardware

part [Ledvina et al., 2003]. Since the data is processed in software, a modification to the existing processing algorithms involves changing and recompiling of the source code as opposed to the change of the hardware design of the ASIC [Akos et al., 2001].

A software receiver can be customized more easily than a hardware receiver and is a useful research tool to analyze the effect of the following acquisition parameters

1. Predetection Integration Time: The predetection integration time can be varied to determine the amount of acquisition gain obtained and the sensitivity improvement realized [Ledvina et al., 2003].
2. Sampling Frequency: The sampling frequency can be varied to determine the aliasing effect and the processing power requirement. In a real-time software receiver, the sampling frequency also determines the memory requirements.
3. Data Wipe Off: To increase the integration period over the navigation data bit duration, the navigation data bit transition should be determined and the navigation data bit value should be predicted. Different data prediction methods can be implemented and analyzed [Tsui and Lin, 2001].
4. Fine Frequency Estimation: To get a fine estimate of the Doppler, averaging and squaring of the signal are performed using a coarse estimate of the Doppler and code delay. Then a fast Fourier transform (FFT) is performed to obtain a better estimate for the Doppler [Akopian et al., 2002].

3.3 GPS Acquisition

A GPS receiver must detect the presence of GPS signals to track and decode the information for the position computation. A receiver replicates the GPS signal with different PRN codes and performs correlation with the incoming signal. The correlation process yields various peaks that are compared with a detection threshold to test for acquisition success.

The replica signal must match the incoming signal both in code and Doppler. The code phase varies due to the range change between the satellite and the receiver. Doppler variation is due to the relative motion between the satellite and the receiver [Kaplan, 1996]. The role of the acquisition is to provide a coarse estimate of the code phase and the Doppler to the tracking loops. The satellite motion induces a Doppler within ±5 KHz from the GPS L1 frequency [Tsui and Bao, 2000]. User dynamics and clock drift introduce an additional Doppler in the GPS signal. The acquisition Doppler search range should be expanded to include these uncertainties to enable proper acquisition. The code phase search range extends from 1 to 1023 chips (of the C/A-code). The acquisition process searches the signal for a particular value of the code phase and Doppler frequency over a certain period of time called the predetection integration time. The acquisition time is determined by the predetection integration period and the number of cells (obtained from code phase and Doppler range) to search. The GPS receiver can compute visible satellites from approximate knowledge of the receiver position, the GPS

time and the almanac which reduces the number of satellites to be searched and speeds up the TTFF.

There have been various acquisition methods developed to acquire GPS signals and a few of them are discussed below.

3.3.1 Time Domain Correlation (cell by cell search)

This is the conventional method for acquisition [Kaplan, 1996]. The search range is divided into cells, wherein each cell represents a particular code delay and Doppler frequency. Correlation is performed in each cell for the predetection integration period and the correlation value is compared against the threshold. If it exceeds the threshold, the satellite is declared as acquired otherwise the search is continued into the next cell. The total number of cells to be searched is given by the number of code delay cells times the number of Doppler bins. This method is simple and best suited for hardware implementation [Tsui and Bao, 2000]. This method performs a sequential search and is time consuming for a software receiver implementation.

3.3.2 Circular Convolution (FFT method)

In this method, the signal is transformed from the time domain to the frequency domain using a Discrete Fourier Transform (DFT) [Van Nee and Conen, 1991]. This method uses the correlation property of the Fourier transform. The property states that the correlation of two sequences in the time domain is the same as the inverse Fourier transform of the

convolution of the Fourier transform of the two sequences. For a particular Doppler bin, the correlation of the two sequences performed at all code phase shifts is the same as the inverse Fourier transform of the product of the Fourier transform of the two sequences. Thus, this method reduces the acquisition search range to one-dimension.

The cells are searched in parallel by taking the FFT of the incoming and the local signal which reduces the acquisition time. The steps involved in this scheme are [Van Nee and Conen, 1991]:

1. Collect the sampled IF signal for the desired coherent integration period: x(t)
2. Take the FFT of the input signal: X(F)
3. Generate the local PRN code for the same coherent integration period and modulate it with the carrier (IF + desired Doppler) and sample it at the same sampling frequency: y(t)
4. Take the FFT of the local signal: Y(F)
5. Perform convolution in the frequency domain: Z(F) = (conjugate X(F)) * Y(F)
6. Transform the convoluted signal in the time domain: z(t) = IFFT(Z(F))
7. Compute the absolute value of the signal z(t), where z(t) represents the correlation of the input signal with the local signal for that Doppler and all possible code phase shifts.
8. Find the peak of the absolute value of z(t) and compare it against the noise threshold. If the peak is greater than the detection threshold, a signal is present. The detection threshold gives an indication of the noise power present. The computation of the detection threshold is explained in Section 5.2. If a signal is

not detected, the procedure is repeated for all possible Doppler values. The detection threshold is optimally based on the noise spectral power density and the allowable probability of false acquisition.

3.3.3 Modified Circular Convolution

This method is same as the circular convolution method (discussed in the Section 3.3.2) except for the length of the FFT which is reduced by half [Tsui and Bao, 2000]. The C/A-code and P-code are transmitted in phase quadrature with each other on the L1 frequency. Hence most of the C/A-code information is contained in the in-phase part of the GPS spectrum. The second half of the spectrum contains little signal information. Hence, this method takes only half the spectrum and performs the correlation [Tsui and Bao, 2000]. The use of half of the spectrum results in a lower number of FFT points. This reduces the FFT processing time and the acquisition time. There is a loss of 1.1 dB determined from simulation analysis, which is due to a loss of the signal information in the other half of the GPS spectrum [Tsui and Bao, 2000].

3.3.4 Delay and Multiply Approach

In this method, the frequency information is eliminated in the input signal and only a code delay has to be searched [Spilker and Parkinson, 1996]. The input signal is multiplied by the delayed version of itself, which eliminates the frequency information but at the same time converts the PRN sequence into a new code. Thus autocorrelation and cross-correlation of the new code have to be performed to determine the code delay.

The problem with this method is that the noise is raised when the input signal is multiplied with its delayed version [Tsui and Bao, 2000]. This method is not useful for acquiring weak signals and hence is not suitable for high-sensitivity receivers.

3.4 Acquisition Detector

The correlation process in acquisition yields correlation peaks. The correlation peak should be above the noise level in the acquisition process to allow the signal to be detected. Noise power computation is an important step in the acquisition process. It is then used to compute the detection threshold. The detection threshold is the minimum value which the correlation peak should exceed for the acquisition process to declare the signal as acquired [Ward, 1996]. An acquisition detector is used to determine the presence of the signal. Most GPS receivers use a multiple trial (M of N / Tong detector) approach compared to a single trial (Binary detector) approach [Kaplan, 1996].

In the binary detector the specified false detection probability along with the noise spectral power are used to determine the threshold. If the correlation value is larger than the threshold, the signal is declared as present [Ward, 1996].

The M of N detector takes N envelopes and compares them to the threshold of each cell. If M or more exceed the threshold, then the signal is declared as present. If not, the signal is declared as absent and the search is repeated for the next cell [Kaplan, 1996].

The Tong detector makes use of an up/down counter to keep a count of the number of times the correlation value has exceeded the threshold. A minimum value of the counter needs to be determined above which the Tong detector declares the signal as present. This value is usually determined by simulations and is a trade off between the search speed and the false detection probability [Spilker and Parkinson, 1996]. There is a limit on the number of times a particular cell is searched before declaring the signal as absent. For weak signals the minimum value of the counter should be kept higher compared to that for strong signals.

3.5 Fine Frequency Estimation

The acquisition process gives a coarse estimate of the Doppler frequency. The tracking loop bandwidth is usually a few Hertz and hence the Doppler frequency estimate should be within the bandwidth of the tracking loop. To obtain a fine estimate of the Doppler frequency, the coherent integration period has to be increased.

The Doppler frequency resolution is given by the inverse of the coherent integration time [Tsui and Lin, 2001]. To obtain a 1 Hz resolution, the coherent integration time has to be one second. The coherent integration time is limited by the navigation data bit transition instant and the Doppler frequency variation. The navigation data bit transition imposes a limit of 20 ms for the coherent integration. The Doppler frequency variation over the coherent integration period causes the correlation value to be multiplied by the sinc signal [Ward, 1996]. This reduces the total correlation value and may even cancel the

correlation value. Hence a coarse estimate of the Doppler frequency is determined first to allow fine frequency estimation.

Tsui and Lin [2001] proposed a method to obtain the fine estimate of the Doppler. The phase of the residual signal after carrier wipe-off (using a coarse Doppler estimate) is determined at two instants. The phase difference between the two instants over the time period between the instants gives the fine estimate of the Doppler.

Akopian et al. [2002] developed a method to obtain a fine resolution of the Doppler frequency. A coarse estimate of the Doppler is determined using standard acquisition techniques (discussed in Section 3.3) and is used to wipe off the carrier. The resulting samples are squared to remove the navigation data and are integrated over the desired integration time. A FFT is performed to get a fine estimate of the Doppler. The integration time decides the resolution of the Doppler.

3.6 Weak Signal Acquisition

The navigation data bit duration puts a limit on the coherent integration period. This limit puts a constraint on the processing signal gain in the acquisition process which determines the GPS signal level that can be acquired [Ward, 1996]. To acquire weak signals the predetection integration time has to be extended beyond 20 ms. A method of achieving this is to perform coherent integration for 20 ms and non-coherent integration for the desired duration [Choi et al., 2002]. Non-coherent integration squares and sums the signal across the coherent integration periods. This allows for a coherent integration

time to be less than 20 ms and a predetection integration time beyond 20 ms. Non-coherent integration introduces a squaring loss which can be reduced by multiplying the adjacent coherent integration samples over the desired period [Chansarkar, 2000].

Lin et al. [2002] proposed an incoherent integration scheme to reduce the squaring loss present in non-coherent integration. In this scheme, the absolute amplitudes of the coherent integrations are summed up instead of squaring before summation which reduces squaring loss. Multiple thresholds for detection with different coefficients based on the false detection probability were chosen to compensate for the power loss during the correlation due to the Doppler frequency mismatch and the code phase transition.

For a high-sensitivity GPS receiver, the desired acquisition sensitivity is -180 dBW. The nominal noise spectral density in a GPS receiver is usually -204 dBW-Hz. For a precorrelation bandwidth of 2 MHz, the noise contained in this bandwidth is -204 + 63 = -141 dBW and hence the SNR at this sensitivity is -180-(-141) = -39 dB. To detect the signal, the required SNR is about 14 dB and hence the correlation process should provide a gain of 14-(-39) = 53 dB. In addition to this, there are receiver implementation losses such as quantization loss, frequency mismatch loss, code delay mismatch loss and RF bandwidth loss, which together can be around 2 dB [Ray, 2003]. Hence the required correlation gain is 53+2 = 55 dB. The coherent integration gain is given by $10\log_{10}$ (1023 * coherent integration period). For example, with 20 ms coherent integration, the gain obtained is 43 dB. So the SNR before non-coherent integration is -39-2+ 43 = 2 dB. Non-coherent integration introduces a squaring loss of 3 dB for an SNR of 2 dB [Ray, 2003]

and hence the required gain is 14-2-(-3) = 15 dB. Non-coherent integration should provide for this 15 dB gain. The non-coherent integration period is given by $10^{(\text{gain needed}/10)}$, i.e. $10^{(15/10)} = 32$ times the coherent integration of 20 ms. In this manner, the coherent and non-coherent integration periods can be chosen. Thus each cell will take 640 ms (32 * 20 ms) to be searched. To reduce the TTFF, a parallel correlator can be used and multiple cells can be searched at the same time.

3.7 Satellite Search

The TTFF can be reduced by properly organizing the order in which the satellites are searched. If almanac (less than 4 month old), time (accurate up to 10 min) and user position (accurate up to 100 km) are available, then the list of visible satellites can be computed and satellites can be searched in descending order of their elevation angle. If any of this information is not available, the list of visible satellites cannot be computed. In that case, a sky search has to be performed. The order in which the satellites are searched during a sky search will determine the TTFF [Pietilä and Syrjärinne, 2000]. Hence, the order has to be carefully chosen to reduce the TTFF. A few methods to select the order of satellites to be searched are:

1. Sequential order from PRN number 1 to 32 [Ward, 1996].
2. Random selection [Kaplan, 1996].
3. Satellites in orbital plane-wise [Pietilä and Syrjärinne, 2000].
4. Statistical distance measure between satellites and building up a tree with different levels such as 4, 8 12 and so on [Pietilä and Syrjärinne, 2000].

3.8 GPS Tracking

The tracking process follows from the acquisition process and keeps the lock on the signal and generates the measurements. The receiver should keep track of the carrier and code phase of the incoming satellite signals. The tracking loops consist of a loop filter, discriminator and either a voltage controlled oscillator (VCO) or a numeric controlled oscillator (NCO). A VCO or NCO generates the local signal to match the incoming signal. The difference between the incoming signal and a local signal is averaged in the loop filter and then passed to the discriminator to determine the error. The discriminator output gives an error which is fed back to the VCO/NCO to correct the generation of the local signal [Kaplan, 1996]. The tracking process also detects for the loss of lock on the satellite signal. If there is a loss of lock, the signal has to be reacquired through the acquisition process.

An FLL outperforms a PLL under dynamic stress and RFI conditions while a PLL gives better measurement accuracy than the FLL [Kaplan, 1996]. An FLL-assisted-PLL solves the GPS receiver designer's dilemma when faced with the need for both the dynamics robustness of the FLL plus the accuracy performance of the PLL [Ward, 1998]. A well-designed code tracking DLL will track at considerably lower levels of C/No than the carrier tracking loop in an unaided (stand-alone) GPS receiver. Since both the code and carrier tracking loops must successfully track their respective signals in order for the unaided GPS receiver to operate, it is sufficient to analyze only the weaker (carrier)

tracking loop to determine the overall receiver tracking threshold (effective C/No below which the carrier tracking is no longer successful).

3.9 Acquisition Performance Parameters

Acquisition is performed for each satellite over the code phase and Doppler range. A predetection integration time is a combination of the coherent and non-coherent integration time. The coherent integration time algebraically adds up the signal and noise while the non-coherent integration time performs the absolute sum of the signal and noise across coherent integration periods [Tsui and Lin, 2001]. The predetection bandwidth is obtained as the inverse of the coherent integration period. It determines the number of Doppler bins to be searched over the complete Doppler search range and decreases as the coherent integration period increases [Ward, 1996]. An increase in the coherent integration period accumulates more signals and allows the noise to average out thereby increasing the SNR. However, an increase in the coherent integration period reduces the predetection integration bandwidth thereby increasing the number of Doppler bins [Tsui and Lin, 2001]. This increases the number of cells to be searched which along with an increase in the coherent integration time increases the total acquisition time at the cost of a higher SNR. The optimum value of the coherent integration time should be chosen to meet the gain and time requirements of the acquisition.

Non-coherent integration is used to increase the gain while keeping the coherent integration time as small as possible [Choi et al., 2002]. It adds up the signal and noise across the coherent integration periods, thereby increasing both the signal and noise

power. The amount of increase in the signal power is linear while the noise power does not add up linearly. Noise is white Gaussian in nature and varies across coherent integration periods [Kaplan, 1996].

The quality of the acquisition is usually judged by its mean acquisition time, acquisition sensitivity (cold, warm and hot starts), and its false alarm and missed detection probabilities [Lin et al., 2002]. The acquisition performance is characterized by the acquisition gain, the mean acquisition time and memory requirements.

Acquisition gain is the ratio of the correct signal peak to the detection threshold and depends on the length of the predetection integration period. The gain is lower in the weak signal environments, under multipath and in interference conditions [Tsui and Bao, 2000]. It gives an indication of the allowable increase in the noise power before the failure of the acquisition process. It is usually expressed in terms of decibels (dB) or SNR.

The mean time for acquisition is determined by the predetection integration period, the number of Doppler bins and the code phase cells. The total Doppler search range is determined by the satellite motion, the receiver clock offset and the receiver dynamics [Kaplan, 1996]. The acquisition search range can be reduced if the approximate values of the Doppler and code phase are known a priori. Acquisition has to be as quick as possible to allow the GPS receiver to provide a navigation solution almost instantly after power on.

Embedded systems have limited the amount of memory available for processing so the available memory has to be efficiently distributed among various GPS processing blocks. In this context, the memory consumed by the acquisition process becomes significant. The acquisition process should utilize as few memory locations as possible. This can be achieved by using a smaller coherent integration time or averaging of samples considered for detection.

CHAPTER 4: RFI: EFFECTS AND MITIGATION STRATEGIES

This chapter discusses various interference types and their effects on the GPS signal processing. Different jamming techniques and interference mitigation strategies are also discussed.

4.1 Interference Signals

RFI is a major source for degradation of the GPS accuracy and reliability. Since there are other sources of errors which further degrade GPS accuracy, this makes RFI mitigation more difficult. GPS satellites and users are mobile which make it difficult to integrate the signals over long periods of time to average out the effects of noise. Satellite and user motion introduce Doppler effects, slow power fluctuations (due to changes in the effective antenna gain and path loss) and fast power changes (due to multipath fading, blockage and shadowing) [Heppe and Ward, 2003]. A Doppler fluctuation makes it difficult to distinguish between user motion and receiver clock drift. Power fluctuations make it difficult to determine the thresholds for acquisition and tracking. Atmospheric errors introduce range and range-rate errors.

RFI and jamming are two major concerns in using GPS to provide a reliable solution [Kaplan, 1996]. Unintentional interference can be caused by RF transmitters, harmonics of ground transmitters, radar signals and accidental transmission of signals in the wrong frequency band [Spilker and Parkinson, 1996]. The signals, or the harmonics of the signals, near the GPS frequencies (L1 and L2), are potential sources of interference.

Interference can also be caused by ionospheric scintillation and evil waveforms transmitted by the GPS satellites themselves [Geyer and Fraizer, 1999]. Pulsed interference can result from radar signals in nearby frequency bands which are not properly filtered [Littlepage, 1999]. Table 4.1 summarizes various types of RFI with a few interference sources shown in Figure 4.1.

Table 4.1: Types of RFI and possible sources [Kaplan, 1996]

Type	Typical source
Wideband-Gaussian	Intentional noise jammers
Wideband phase/frequency modulation	Television transmitter's harmonics or near-band microwave link transmitters
Wideband-spread spectrum	Intentional spread spectrum jammers or near-field of pseudolites
Wideband pulse	Radar transmitters
Narrowband phase/frequency modulation	AM stations transmitter's harmonics
Narrowband swept continuous wave	Intentional CW jammers or FM stations transmitter's harmonics
Narrowband continuous wave	Intentional CW jammers or near-band unmodulated transmitter's carriers

CW interference can be either a pure tone or a narrow band modulated signal such as AM or FM [Macabiau et al., 2001]. It distorts the signal spectrum and affects the carrier tracking loop. A carrier tracking loop will lock onto the interference frequency for a pure tone signal (provided the CW power level is considerably high) generating erroneous carrier phase and Doppler measurements. Broadband noise increases the amount of noise in the GPS spectrum without distorting the signal spectrum [Heppe and Ward, 2003]. Swept CW interference is more damaging than CW interference because it can cover multiple Doppler frequencies and affect more than one receiver channel at the same time.

Pulse interference can cause malfunctioning of the AGC which affects the tracking loops [Hegarty et al., 2000].

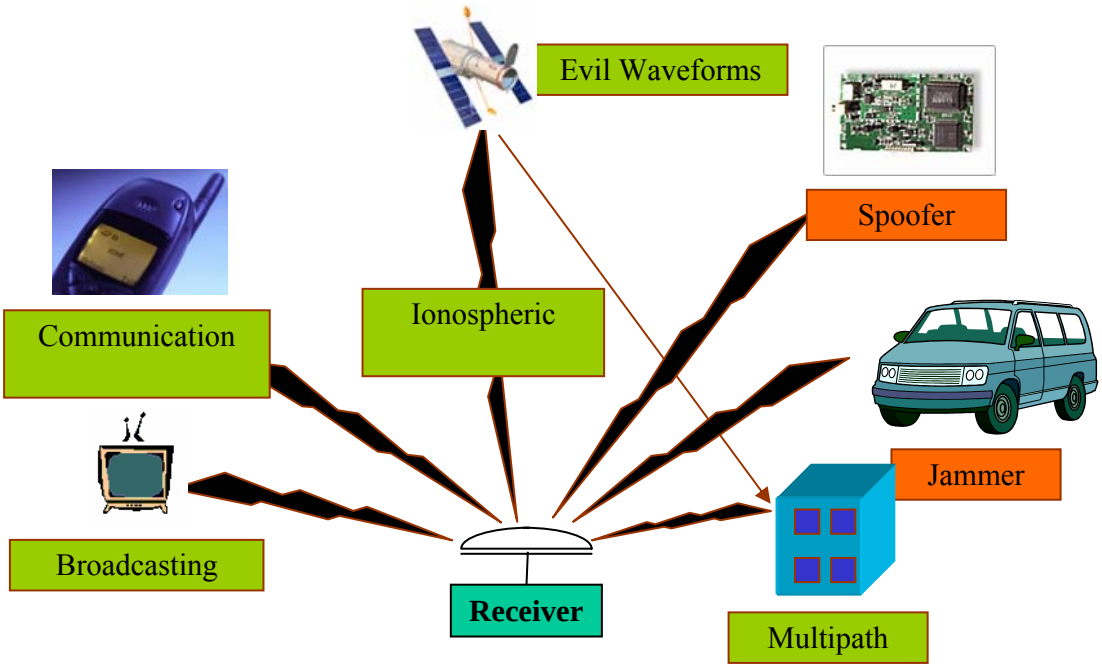

Figure 4.1: Some sources of RF interference

An AM and FM radio broadcast transmitter's high-order harmonic emissions fall close to the GPS L1 frequency and cause interference. RFI likelihood is considered minimal for AM radio broadcasts since the harmonic order (985) is high [Erlandson and Fraizer, 2002]. For an FM broadcast the harmonic order (15 to 18) is lower and the maximum effective isotropic radiated power (EIRP) is higher (50 to 60 dBW) [Macabiau et al., 2001]. Analog TV broadcast maximum EIRP limits are higher than FM and the harmonic orders are lower (2 to 9 for RFI signals within 2 MHz of the GPS L1 frequency) and the predicted minimum separation radius exceeds 100 miles [Buck and Sellick, 1997]. Thus FM and TV signals will cause interference in the GPS receiver. Buck and Sellick [1997] analyzed the effects of the harmonics of the TV signals interfering with GPS frequencies and they were found to be in the L1 signal spectrum causing a non-linear effect. The

strongest suspected interference signal was at 525.25 MHz (video carrier of a local TV station). Thus the 1575.75 MHz signal was the third harmonic of the local station video carrier. The GPS L1 frequency divided by three is 525.14 MHz and the transmitted TV signal's lower side band suppression was at 524.50 MHz thereby allowing full power at this frequency. This jump in power would produce a high level of interference resulting in a reduced SNR. Filters were found to be effective in eliminating these interference signals by having high attenuation for the undesired signals. The TV and Air Traffic Control (ATC) frequencies have high transmitter powers and their harmonics fall in the GPS L1 frequency band. Table 4.2 lists the various TV and ATC frequency harmonics falling in the GPS frequency band.

Table 4.2: TV and ATC harmonics in GPS frequency band [Buck and Sellick, 1997]

Harmonic	Band (MHz)	Usage
2	787.199 – 787.222	Broadcasting
3	524.799 – 525.481	Broadcasting
4	393.599 – 394.111	Fixed/mobile
5	314.879 – 315.289	Fixed/mobile
6	262.400 – 262.741	Fixed/mobile
7	224.914 – 225.206	Broadcasting
8	196.800 – 197.055	Broadcasting
9	174.933 – 175.160	Broadcasting
10	157.440 – 157.644	Broadcasting
11	143.127 – 143.313	Fixed/mobile
12	131.200 – 131.370	ATC
13	121.107 – 121.265	ATC
14	112.457 – 112.603	VOR
15	104.960 – 105.096	Broadcasting

The best protection for a GPS receiver is to use RF filtering to exclude the unwanted interference. Spurious transmissions from RF transmitters in the GPS frequency band should be measured to allow its suppression [Johannessen et al., 1990].

4.2 Interference Effects

RFI has the same effect on GPS acquisition or tracking as signal blockage, foliage attenuation, ionospheric scintillation and multipath, which is to reduce the C/No for all the GPS signals. A jammer reduces the SNR of the GPS signals affecting acquisition and tracking of the signals in the GPS receiver. Spoofing is another form of interference which transmits a stronger version of the GPS signal to capture the receiver loops and fool the receiver [Heppe and Ward, 2003]. Pseudolites operating at close range to a receiver can jam the GPS receiver. The primary aspect of the GPS architecture that makes it vulnerable is the low power of the signal that is actually below the noise floor until it is de-spread with an appropriate PRN code. The RFI effect depends on the details of receiver design, especially the front-end bandwidth and early-late spacing in the discriminator [Macabiau et al., 2001]. It has a different effect on the code tracking accuracy than it does on some other aspects of the GPS receiver [Geyer and Fraizer, 1999]. Several types of perturbations like the thermal noise, atmospheric disturbances, multipath and interference can affect the GPS signal. Geyer and Fraizer [1999] conducted tests on a C/A-code receiver for the FAA to determine the vulnerability of the GPS receivers to RFI. This allowed the FAA to establish interference standards for GPS receivers used in civil aviation. These tests were focused on the C/A-code receiver's

tracking degradation and loss of lock under different interference conditions. The GPS was found vulnerable to very high frequency (VHF) transmissions and CW interference.

RFI detection should be given high priority because it provides an instantaneous warning of the potential loss of GPS integrity. It can be detected using a jamming-to-noise (J/N) power ratio meter [Kaplan, 1996]. The J/N meter is implemented in the AGC of the GPS receiver front-end. This meter keeps a check on the thermal noise level and any signal different from it, is detected as the presence of the interference signal.

The C/No for a SV signal without interference is termed as unjammed C/No [Kaplan, 1996]. The difference between the unjammed C/No and the acquisition or the tracking threshold gives an indication of the possible interference tolerance and is termed as effective C/No. The unjammed C/No and the effective C/No are used to compute the maximum jammer-to-signal (J/S) level at the receiver input from which the RFI power can be determined. The unjammed C/No depends upon the GPS receiver parameters and is computed from Equation (4.1) [Kaplan, 1996].

$$C/No = Sr + Ga - 10\log(kTo) - Nf - L \ (dB-Hz) \qquad 4.1$$

where

Sr	is the received GPS signal power (dBW),
Ga	is the antenna gain towards the SV (dBic),
10log(kTo)	is the thermal noise density (dB-Hz) ≅ -204 dBW-Hz,
k	is the Boltzmann's constant (watt-sec/K) = 1.30 x 10^{-23},
To	is the thermal noise reference temperature (K) = 290 K,

Nf is the noise figure of the receiver (dB), and

L is the implementation loss plus ADC loss (dB).

Signal information is lost during conversion of the signal from analog to digital by the ADC which is referred to as the ADC loss. The level to which the unjammed C/No is reduced by the RFI is called the equivalent C/No power density ratio. The equivalent C/No power density ratio is related to unjammed C/No and J/S as given by Equation (4.2) [Kaplan, 1996].

$$[C/No]_{eq} = ((C/No)^{-1} + (J/S)/QR))^{-1} \quad \text{(power ratio)} \qquad 4.2$$

where

C/No is the unjammed carrier-to-noise power in a 1 Hz bandwidth expressed as a ratio,

J/S is the jammer-to-signal power expressed as a ratio,

R is the GPS PRN code chipping rate (chips/sec), which is 1.023×10^6 chips for the C/A code and 10.23×10^6 chips for the P code, and

Q is the spread spectrum processing gain adjustment factor, and is 1 for narrow band jammer, 1.5 for wide spread spectrum jammer and 2 for wideband Gaussian noise jammer.

Equation (4.2) can be expressed in terms of dB-Hz (Equation (4.3)) and rearranged to obtain J/S (Equation (4.4)) [Kaplan, 1996].

$$[C/No]_{eq} = -10\log[10^{-(C/No)/10} + 10^{(J/S)/10}/QR](dB-Hz) \qquad 4.3$$

$$J/S = 10\log[QR\,(10^{-([C/No]eq)/10} - 10^{-(C/No)/10})](dB) \qquad 4.4$$

For an C/A-code receiver, Sr = -159.6 dBW and assuming the antenna has unity gain toward the SV (Ga = 0), a noise figure of 4 dB and an implementation loss of 2 dB, then the unjammed C/No is 38.4 dB-Hz. For Q=2, and assuming an equivalent C/No threshold of 28 dB-Hz, the J/S = 34.7 dB [Kaplan, 1996]. This tolerance looks good in terms of dB but when converted to the actual signal power it is just 3 pW. The RF transmitter transmits signals with high power levels (in terms of Watts) and hence the harmonics of these signals will have power levels greater than 3 pW. This will result in jamming of the GPS receiver and hence RFI detection and mitigation is important in a GPS receiver.

A number of techniques have been designed to increase the robustness of GPS receiver to RFI signals [Littlepage, 1999]. RFI can be mitigated at various stages of the GPS receiver from the instant of receiving the GPS signals by the antenna to the position computation instant. RFI signals will have full effect when the interference signal is unobstructed and the antenna provides adequate gain to the signal.

4.3 GPS Jammer

Jamming or spoofing is a form of an intentional interference. Jamming can be of the form of signal denial (which prevents acquisition and tracking of the GPS signal) or signal deception (which fools the receiver to mistake an interference signal as the GPS signal) [Heppe and Ward, 2003]. A simple jammer can be constructed to generate a CW, AM or FM interference. Jammer design becomes complex when a range of jamming types are to be generated from the same source. A brute force jamming method introduces broadband noise or CW jamming to prevent lock on the satellites. An intelligent jammer uses different types of interference signals to attack the GPS receiver. Pulse signals can be

used to attack the AGC and tracking loops and a swept CW signal can capture all receiver channels by exploiting C/A-code spectral lines. The frequency of these signals can be varied to reduce the chance of jammer detection [Cutright et al., 2003]. The effect of jamming on the RF front-end is to create additional spurious signals and tones which disrupt receiver operations. Jamming forces the low noise amplifier (LNA) into saturation and yields spurious signals. It forces the AGC to respond at incorrect operating points by exploiting the tracking loop constant and signal suppression in the ADC [Heppe and Ward, 2003].

Interference signals within the GPS C/A-code bandwidth are termed as Narrowband interference [Kaplan, 1996]. Narrowband interference signals are potentially more dangerous than expected due to the line spectrum of the Gold codes used for ranging. They could coincide with a strong spectral line which results in a larger residual line in the carrier tracking loop [Macabiau et al., 2001]. The CW interference effect on tracking can be detected due to the Doppler variation between the satellite and a user. A broadband RFI averages the spectral lines and causes an asymptotic effect like a sinc function [Kaplan, 1996]. The effective interference signal power at the receiver can be determined using a link budget knowing the power transmitted by the interference source and is calculated using Equation (4.5) [Heppe and Ward, 2003].

$$\text{Received RFI} = \text{EIRP} - \text{Path loss} + \text{Antenna Gain} \qquad 4.5$$

The EIRP represents the effective power transmitted by the source. The signal is weakened by the path loss as it propagates through space. The path loss can be calculated by Equation (4.6).

$$\text{Path Loss (dB)} = 31.8 + 20\log(f) + 20\log(\rho) \quad 4.6$$

where

f is the frequency in MHz, and

ρ is the range in km.

The antenna gain impacts the amount of interference received by the receiver. It can be designed to provide attenuation in the direction of the interference signal provided the direction is known [Bond and Brading, 2000].

GPS jammers are available commercially at low cost compared to the GPS receivers and these jammers can transmit different types of waveforms. The most difficult interference waveform for the GPS receivers to mitigate is broadband noise [Kaplan, 1996]. Since the GPS signal is a spread spectrum signal; a narrow band pass filter in the receiver front-end that removes the jamming signal will remove only a small portion of the GPS signal while removing the narrow band jamming signals. The GPS signal has a low power level which makes it vulnerable to jamming over long distances. Brown et al. (1999) analyzed the effect of a single 4-Watt CW jammer on the GPS acquisition in a GPS receiver. The results illustrated in Figure 4.2 deny the C/A-code acquisition for a J/S ratio of 22 dB. GPS tracking was jammed when the jammer was close to the receiver (1 km) while acquisition was jammed over a larger distance. Airborne users are more affected by a ground-based jammer than ground-based GPS users as they have a direct line-of-sight (LOS) to the jammer over significant distances (up to 145 km) as shown in Figure 4.2.

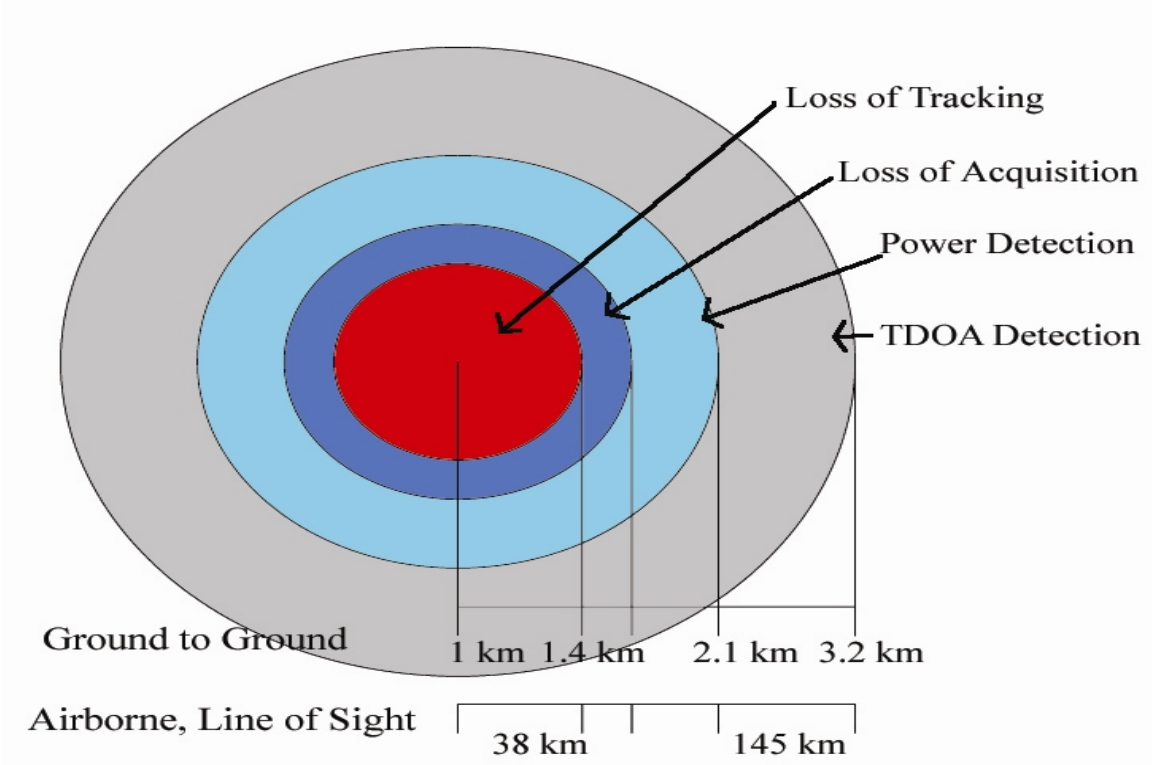

Figure 4.2: Effective range of single 4-watt GPS jammer [Brown et al., 1999]

A GPS receiver can be successfully jammed by generating interference signals that match the Doppler and by offsetting the jammer to a maximum spectral line of the C/A-code. The correlation process of a CW line and a PRN code will spread the CW line, but the mixing process at certain strong C/A-code lines results in the RFI line being less suppressed than other frequencies [Johnston, 1999]. The net result is that CW interference can leak through the correlation process at this strong line. Johnston [1999] performed experiments on CW and swept frequency interference using a commercial off-the-shelf (COTS) NavSymm/Navstar XR5-M 12 channel GPS receiver used in conjunction with Navstar software version 3.7. DGPS was used to remove the effects of

Selective Availability (SA) to obtain the error due to the jamming. The results showed that CW jamming gave a maximum position error of 23 km while the swept frequency gave an error of 220 m for a J/S ratio of 35 dB.

4.3.1 Simple Jammers

A simple jammer is one which generates interference signals without the knowledge of the GPS receiver design [Heppe and Ward, 2003]. It usually generates one type of interference signal like broadband noise, CW, etc. A brute force broadband noise jammer uses a simple noise source combined with an up-converter, an amplifier and an antenna [Spilker and Parkinson, 1996]. This causes increased tracking jitter, cycle clips and loss of lock. It is effective over short ranges and the goal is to deny the GPS signal. Acquisition can be disrupted at 3-4 times the range at which tracking is lost [Heppe and Ward, 2003]. It is low cost and affects all the receivers within its effective range. The jammer power should be high to affect over a long range but it also increases the probability of detection.

A CW jammer is simply a tone frequency generator at GPS frequencies. Its purpose is to capture the carrier tracking loop of the receiver and to mislead the user. A high power CW signal can cause the tracking loop to appear as stable but will generate erroneous measurements [Johannessen et al., 1990]. It is effective over medium ranges, is low cost, and affects all the receivers within its range. The disadvantage is that it is easier to detect than a broadband noise jammer and can be filtered out prior to correlation during acquisition or tracking [Burns et al., 2002].

4.3.2 Intelligent Jammers

A jammer designed with the knowledge of the GPS receiver architecture is called an intelligent jammer [Heppe and Ward, 2003]. An intelligent jammer generates complex waveforms like pulse signals or sweep CW signals making the RFI detection difficult. For example a pulsed noise jammer is more complex in design than a CW jammer. The key parameters in design are the pulse duration, duty cycle and amplifier efficiency. The intention of a pulse jammer is to disrupt tracking and data demodulation. The pulses are designed to match the time constant of the AGC and this can give 10's of dB advantage to the jammer [Hegarty et al., 2000]. A pulse jammer requires less power since the signal is not continuous which makes it more difficult to detect. Its disadvantage is that it requires a high power amplifier and the knowledge of the receiver design to affect the AGC [Heppe and Ward, 2003]. Knowledge of the receiver architecture can help design a pulse jammer to keep the receiver constantly in acquisition mode even though the jammer is never constantly on.

A swept CW (chirped jammer) allows the capture of the carrier tracking loops for all signals despite the Doppler difference [Johnston, 1999]. This jammer can be used to attack rapidly moving vehicles and can be turned off to save power after the receiver has been jammed [Heppe and Ward, 2003]. Knowledge of the receiver's reacquisition time is used to determine the on/off period of the jammer. An interference signal close to the receiver's IF is difficult to isolate using hardware techniques. A frequency hopping jammer is similar to a CW or pulse jammer whose frequency is varied in steps over the

desired bandwidth of the signal. The frequency variation makes it difficult to detect the interference signal [Heppe and Ward, 2003]. The frequency variation rate can be changed to make it more difficult to detect.

4.3.3 Spoofers

Spoofing is an intentional jamming signal similar in nature to the GPS signal. It can be of two types: navigation and data link signals [Kaplan, 1996]. Navigation spoofers transmit false GPS signals at a high power to fool the receiver and capture it. This will introduce large errors in the GPS measurements and will provide an erroneous navigation solution. These false GPS signals should be carefully designed to be able to fool the receiver [Heppe and Ward, 2003]. Data link spoofers capture the navigation data signal and require about an extra 10 dB of power compared to the navigation spoofers. The navigation data is spoofed to provide erroneous information about the range accuracy, GPS time, satellite positions and their health. Both the spoofing signals can be combined to severely degrade GPS solution [Heppe and Ward, 2003].

Spoofing requires capturing of the tracking loops and eliminating the actual GPS signals. Therefore, spoofer must track the receiver trajectory and generate signals to match the GPS signals. Once the receiver starts tracking the spoofed signals, their power can be increased to eliminate the GPS signals and then the erroneous information can be transmitted to fool the receiver. The spoofer should track the GPS signal and the receiver's motion to have a tight closed loop signal generation [Heppe and Ward, 2003]. Receiver autonomous integrity monitoring (RAIM) and false detection and identification

(FDI) methods in a GPS receiver can be used to isolate the erroneous GPS measurements when there are more than four measurements. Hence the spoofer should spoof all the satellite signals to throw the receiver off its trajectory [Spilker and Parkinson, 1996].

4.3.4 Pseudolites

The GPS signal power varies about 20% between the satellites at the horizon and at high elevations [Kaplan, 1996]. The antenna gain pattern is usually designed to ensure the GPS signal strength does not vary much between the satellites. The use of pseudolites to augment GPS satellites gives rise to the near-far problem [Madhani and Axelrad, 2001]. A pseudolite signal has a large power variation when it is close to the GPS receiver. A pseudolite designed to provide a GPS signal level at a distance of 50 km would provide about 60 dB more power at a distance of 50 m from the receiver [Madhani and Axelrad, 2001]. This near-far problem can be overcome using different methods classified into three categories namely signal pulsing, frequency offsets and the use of different PRN codes. Signal pulsing consists of transmitting the pseudolite signal in terms of the pulse which decreases the average power of the pseudolite signal. The pseudolite signals can be transmitted at a frequency outside the GPS frequency band which requires changes to be made in the receiver front-end [Ndili, 1994].

Madhani and Axelrad [2001] developed a successive interference cancellation approach to overcome the near-far problem in the pseudolites. This approach identifies and eliminates the strongest component in the received signal. The next strongest component is then identified and cancelled. This is repeated until all the signals are separated. The

strongest signal is removed first since it is easy to acquire and its removal gives the most benefit for the remaining weak satellite signals.

4.4 RFI Mitigation Methods

GPS has an advantage over narrow-band navigation systems with respect to unintentional interference due to the following reasons. The GPS signals are spread-spectrum signals and receiver design techniques can reduce the effect of most of the interference signals [Kaplan, 1996]. A GPS navigation solution is usually over determined and RAIM/FDI methods can be used to isolate erroneous information [Spilker and Parkinson, 1996]. The correlation process in a GPS receiver de-spreads the GPS signal and spreads any interference signal present which reduces the interference power and provides some protection against interference signals. However, a high power interference signal can distort the correlation peak or give rise to the correlation peak at incorrect estimates [Heppe and Ward, 2003]. The main strategy for any interference mitigation method is to eliminate the interference signal or reduce the interference signal to white Gaussian noise, so that there is only an increase in noise without distortion of the GPS signal spectrum [Cooper and Daly, 1997].

4.4.1 RF Filtering

GPS receivers operating close to RF broadcasting devices like TV stations, high power transmitters will suffer from out-of-band interference [Escobar and Harper, 2001]. To eliminate out-of-band interference high performance RF filters are used between the

antenna and the receivers. These RF filters are required to have a sharp cut-off outside the GPS bandwidth, low loss in the pass band and high rejection in the stop band. Superconducting Technology Inc. constructed a set of HTS filters for the L1 and L2 frequencies along with a cryogenically cooled LNA. The use of cryogenic technology decreases the loss in the filter improving its performance. This improvement in the performance allows for the use of normal filters after the LNA without much affect on the Noise Figure (NF) of the receiver front-end [Escobar and Harper, 2001]. The development of surface acoustic wave (SAW) filters has reduced the size, weight, cost and cooling requirements for the filters.

4.4.2 Adaptive Antenna Array

A GPS antenna captures the GPS signal and feeds it to a receiver. Any interference signal in the GPS frequency band is also picked up by the antenna [Bond and Brading, 2000]. RFI can be eliminated by providing a zero antenna gain in the direction of the interference signal. Antenna gain pattern cannot be modified for a single element antenna without changing its orientation [Kunsyz, 2001]. It can be varied by using an array of antenna elements. An adaptive antenna array works on this basic concept of providing a zero gain to the interference signal. The adaptive antenna arrays can be either fixed rejection pattern antenna (FRPA) or CRPA. Both these antenna arrays consist of an adaptive processor to combine signals from different antenna elements. The manner in which the signals from the different antenna elements are combined can be varied to change the overall gain pattern of the array.

The FRPA system consists of an array of three conventional antenna elements and a vector processor which contains the adaptive antenna RF circuits and a processor [Littlepage, 1999]. A minimum of three elements are required to determine the interference location in both the azimuth and elevation and to provide a uniform azimuth accuracy throughout the area visible to the antenna. The spacing between the antenna elements is important to avoid directional ambiguities [Bond and Brading, 2000]. The interference direction is determined from the angle of arrival (AOA) and array theory. The DF algorithm checks the results across the antenna pairs to ensure consistency and to trap the errors [Bond and Brading, 2000]. The number of antenna elements in the array determines the number of the interference sources that can be eliminated. FRPAs provide substantial jammer suppression at a relatively low cost but they are vulnerable to the distributed broadnoise jammers [Kunsz, 2001]. This problem can be overcome using spatial filtering (adaptive nulling) provided by the CRPAs [Littlepage, 1999].

Kunysz [2001] designed a compact, dual GPS frequency L1/L2, multi-element CRPA array. Each antenna element consists of an aperture coupled spiral slot array which reduces the mutual coupling between the adjacent elements. This provides better tolerance towards the interference or a multipath signal and helps to reduce the size of the array. This antenna was successfully found to mitigate a wideband jammer and multipath signals in standard surveying, marine and arctic applications.

4.4.3 Interference Localization

RFI can be mitigated provided the direction and nature of the interference signal is known. Interference localization is to determine the direction of the interference signal [Brown et al., 1999]. There are several ways to implement interference localization such as interferometry, TDOA systems, spatial spectrum estimation, phase antenna arrays, etc. The interferometrical approach uses a concept of direction finding to localize the interference source. It employs a group of signal recognition and direction finding equipment to locate the interference source. This technique is useful for locating a small number of jammers but is not practical to locate a large number [Brown et al., 1999].

TDOA techniques can be used to locate a large number of jammers. The time delay of the interference signal reaching the multiple antennas can be used to determine the location of the interference source [Gormov et al., 2000]. Doppler measurements from each antenna are used to determine the satellite motion and to isolate any other signal, but these measurements provide erroneous information when the carrier drifts or is intentionally dithered. The direction finding techniques using the antenna arrays are limited in the number of separate jammers that can be located [Brown et al., 1999].

Many simultaneous measurements are necessary to quickly and accurately locate a large number of jammers and spoofers [Shau-Shinu and Enge, 2001]. A simple method is to use the C/No information from a GPS receiver to determine the jammer location. The satellite signal strength, and the GPS time and location of the receiver can be used to

determine the jammer location [Brown et al., 1999]. This method is effective when there is a large variation in the C/No as a function of the distance from the jammer. However, it is less effective in estimating the location of low power interference signals. RFI source location can be estimated using a network of distributed sensors rather than a single sensor [Shau-Shinu and Enge, 2001]. The network approach to locate the RFI source requires no sensor motion and is robust to sensor failures.

Shau-Shinu and Enge [2001] developed an aircraft RFI localization and avoidance system (ARLAS) to reduce the interference in aviation applications. The system uses a GPS antenna mounted on the top of an aircraft to determine the interference location. The SNR of the received GPS signal is calculated by the GPS receiver under different values of roll, pitch and heading which are measured from the gyros. This information along with the vertical gain information of the GPS antenna is used to estimate the direction to the interference source.

4.4.4 AGC as Interference Mitigation Tool

GPS signals received by the antenna have an inherent thermal noise present in them. This thermal noise is determined by the AGC and is used to determine the thresholds for quantization. Bastide et al. [2003] studied the AGC as a tool for interference assessment. An AGC provides an accurate indication of the thermal noise in the receiver. These noise levels can be used to determine the presence of interference. Any interference signal will increase the noise power in the receiver which can be detected using the AGC.

Bastide et al. [2003] devised a Chi-square test to detect the presence of interference using the distribution of the ADC bins.

4.4.5 Pulse Blanking

Pulse interference signals affect GPS receivers depending on its characteristics such as power, duty cycle and pulse width [Hegarty et al., 2000]. They will continue to affect the receiver components even in it's off state because the components have a recovery period to resume their normal operation. These signals tend to saturate the RF stages, the AGC and the ADC in a receiver front-end. Slow AGCs will be severely affected by pulse interference. These AGCs are slow to respond and will incorrectly determine the quantization levels, which will result in improper sampling [Hegarty et al., 2000]. A fast AGC along with an increase in the number of quantization levels will solve this problem. Hegarty et al. [2000] devised a technique to eliminate pulse interference through blanking. In this method, whenever the pulse interference is detected, the ADC outputs a zero thereby eliminating the interference signal. However this introduces a signal loss at the samples where the pulse interference was detected. Perfect blanking for a single strong-pulsed signal will result in SNR degradation of 10log(1-PDCB) where PDCB (pulse duty cycle – blanker) is the duty cycle of the blanking signal. This SNR degradation follows from the fact that when strong pulses are present, blanking completely suppresses the desired signal (20log (1-PDCB) SNR degradation) and thermal noise (10log (1-PDCB) SNR gain) [Hegarty et al., 2000].

4.4.6 Spatial Signal Processing

Navsys Inc. pioneered the first commercial receiver to include spatial signal processing; the high-gain advanced GPS Receiver (HAGR). This receiver uses digital spatial processing to combine signals from the antenna (up to 16) elements. Brown et al. [2000] further enhanced the HAGR to detect the presence of the interference signals and to estimate its direction. The AOA of the interference signal is determined using the cross-correlation between multiple antenna elements. A cross-correlation value higher than the noise power indicates the presence of an additional interference signal. This technique was found capable of detecting CW interference above a -129 dBm power level and a broadband interference above -125 dBm [Brown et al., 2000].

4.4.7 Space Time Adaptive Processing (STAP)

Antenna arrays equipped with a STAP can null multiple RFI signals arriving from different directions without previous knowledge of the interference type or the direction of arrival (DOA) [Moore and Gupta, 2001]. An antenna array with L elements and N taps for each element will capture LN signals and feed it to the STAP. The STAP adjusts the coefficients for each tap and the array element to provide a zero gain in the direction of the interference. For this antenna, there are LN-1 DOF available and hence it can eliminate up to LN-1 independent RFI sources. Moore and Gupta [2001] demonstrated that a wideband RFI source could consume multiple spatial DOF depending on the interference power and bandwidth. The STAP is required to process matrices of order LNxLN and was found to distort the desired GPS signal introducing significant errors in

the navigation solution under severe jamming conditions. This problem was overcome using a SFAP [Gupta and Moore, 2001].

4.4.8 Spatial Frequency Adaptive Processing

SFAP is an alternative solution to the STAP whereby signals from the antenna elements are processed in the frequency domain. STAP and SFAP are equivalent if the tap spacing is equal to the sampling interval [Gupta and Moore, 2001]. The SFAP performance can be improved by using a window function to multiply the time domain samples before transforming them into the frequency domain. The window function (e.g. Blackman window) should have low side lobes to provide better performance. The narrowband SFAP does not distort any of the desired signals as observed in the STAP [Gupta and Moore, 2001].

4.4.9 RFI Mitigation in the GPS Correlator

Macabiau et al. [2001] devised a multicorrelator technique for the CW interference detection. A multicorrelator receiver provides correlation values of the incoming signal with several delayed replicas of the same local code in a single tracking channel. CW interference disturbs the in-phase and quadrature correlator outputs of the tracking loop and this effect varies as the spacing between the correlators' changes. This variation in the correlator outputs is used to determine the frequency of the CW interference.

Manz et al. [2000] developed a technique to mitigate the RFI in the PLL. This method can be used only if the user is stationary and has a stable clock. The amount of thermal noise present in the PLL is determined and the variation of the noise power in the PLL is studied. An increase in the PLL noise due to interference is equated with the noise power injected into the PLL. The ratio of the interference power to the C/A-code signal power is determined which indicates the interference power required to jam the PLL. A narrow PLL bandwidth increases the probability of tracking the correlation side lobes. The standard algorithm used to detect the 25 Hz side lobes can be modified to detect the 12.5 and 8.33 Hz side lobes [Tsui and Bao, 2000]. The narrow PLL bandwidth improved the CW interference rejection performance in a GPS receiver.

Cooper and Daly [1997] developed a technique of preprocessing the GPS signals to remove the interference components before passing them to the GPS correlator. The frequency of the interference signal is determined using frequency domain techniques and a PLL is used to generate the replica interference signal. The AGC in the receiver front-end is used to determine the instant at which the interference signal is present. This interference signal is mixed with the local interference signal (generated by the PLL) to cancel the interference signal. The locally generated interference signal can be differenced from the incoming signal, noise and interference to give signal and noise only, thus cancelling the interference [Cooper and Daly, 1997]. A single PLL can eliminate a single interference signal and hence multiple PLLs are required to eliminate multiple interference signals.

4.4.10 Multilevel Sampling

Leica GPS Inc. developed a technology to mitigate the RFI using a multi-level sampling technique. It employs an adaptive ADC wherein the ADC sampling threshold levels are dynamically controlled by the processor to maintain a statistical frequency which is determined using the quantization thresholds and quantized samples. This technique also improves in-band rejection of the narrowband interference signals [Maenpa et al., 1997]. SAW filters can be used to eliminate the out-of-band interference.

Braasch et al. [1997] analysed an interference suppression unit (ISU), developed by Electro-Radiation Inc., which provides significant interference tolerance. It is effective against different types of interference and can be used with any patch antenna. It was shown to be effective in suppressing an additional 20 dB of broadband noise and narrowband interference compared to stand alone GPS receivers.

4.4.11 Advantage of a Software Receiver

A software receiver allows flexibility in dealing with interference. The exploitation of the spectrum transforms, and other mathematical tools, is more feasible in software than in traditional hardware receivers [Cutright et al. 2003]. Software receivers can look at the signal in different domains and can process a block of data rather than individual samples. This allows for direct filtering of the RFI signals thereby minimizing the effects of RFI. Cutright et al. [2003] developed a frequency domain approach to mitigate the RFI in a software receiver. This method transforms the IF signal into the frequency domain

and removes the bias from the spectrum. The bias might be introduced by the receiver front-end bandwidth. The detection threshold is determined to separate the noise and the interference signals. The frequency bins exceeding the threshold are identified and they contain the RFI. These bins are set to zero to remove the interference signal and are transformed back into the time domain. The new signal is free from RFI and is passed to the software correlator. This algorithm is useful for isolating narrow in-band and pulse interference [Cutright et al., 2003]. However, wideband interference cannot be easily separated from the signal.

Burns et al. [2002] evaluated interference mitigation in a software receiver by varying the number of bits in the ADC. The tracking accuracy of the receiver in the presence of interference was chosen as the criteria for determining the success of the interference mitigation. The interference signals were introduced after the receiver started tracking the satellite. The FFT of the incoming data was studied to determine the frequency components with interference. These bins were removed to eliminate the interference signals [Burns et al., 2002]. The signal is better represented with a higher number of the ADC levels and allows for a better estimation of the frequency components containing the interference.

RFI mitigation methods discussed above try to mitigate the interference at various processing stages in the GPS receiver. RFI mitigation at antenna reception eliminates the interference signal before it can enter the receiver. RF filters are essential to eliminate the interference signals outside the GPS frequency band. CW interference can be reduced by

preprocessing the IF signal before passing it to the GPS correlator. A swept CW affects all the receiver channels which can be reduced using adaptive notch filters. A blanking method can be used to remove pulse interference. A robust solution to the GPS jamming will always require a variety of anti-jam technologies [Heppe and Ward, 2003].

CHAPTER 5: ACQUISITION: IMPLEMENTATION AND RESULTS

This chapter discusses two acquisition schemes (circular convolution and modified circular convolution) suitable for software receiver implementation. Different acquisition performance parameters are studied using these two schemes.

5.1 Acquisition Implementation

The acquisition process is used to detect the presence of a signal and provide coarse estimates of the code phase and Doppler to the tracking process. It exploits the autocorrelation and cross-correlation properties of the GPS PRN codes to acquire the signal. A block diagram of the acquisition process is shown in Figure 5.1. All the blocks except the acquisition detector and the acquisition manager are common to the tracking process. The acquisition and tracking processes form the core blocks of the correlator in a GPS receiver. Different modules in the acquisition process are discussed below.

Acquisition manager: This module manages the various blocks of the acquisition process and specifies the parameters of operation to each block. It decides the PRN to be searched and the predetection integration time for each cell search. It also specifies the Doppler and code phase range to be searched for the corresponding PRN along with the parameters to compute the detection threshold for acquisition.

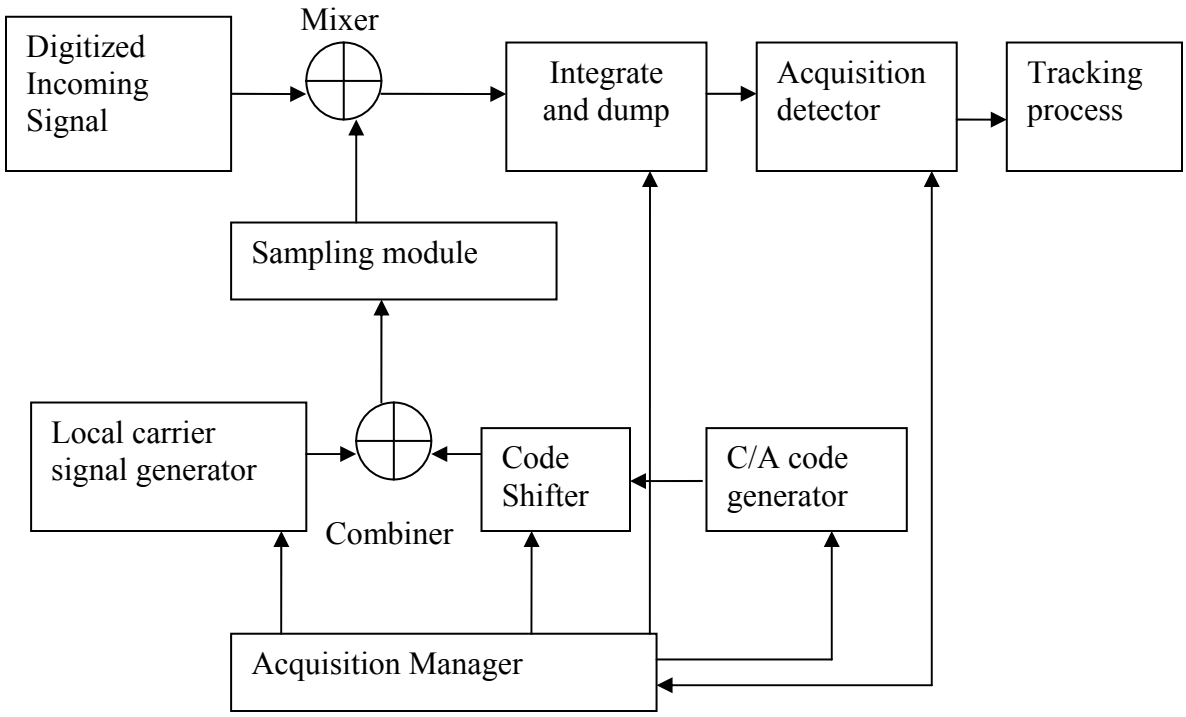

Figure 5.1: Block diagram of the GPS acquisition process

Local carrier signal generator: This module is used to generate the carrier to match the frequency of the incoming IF signal. It generates a carrier signal with frequency as the sum of the receiver IF and the Doppler frequency to be searched. It generates both the in-phase and quadrature components of the carrier signal. The Doppler frequency is modified after all the cells for that particular Doppler are searched with no success.

C/A-code generator: C/A-code generation is explained in Section 2.4. This module generates the C/A-code for the desired PRN number. The C/A-code generator should be capable of generating the code for all GPS satellites.

Code shifter: This module is used to shift the C/A-code by the code phase amount to be searched. The code phase should be properly matched with the incoming signal to acquire it.

Combiner: This module is used to combine the signals applied at its input. The carrier signal is combined with the shifted C/A-code to obtain a local replica of the incoming signal.

Sampling module: The incoming IF signal is sampled at an appropriate sampling frequency chosen to avoid the aliasing effect and to reduce processing power. The sampling signal used to sample the incoming signal must match in phase with the local signal. If there is a phase mismatch, there will be incorrect representation of the local signal with the incoming signal which will yield incorrect results.

Mixer: It mixes the incoming signal with a local replica signal to perform carrier and code wipe off. The resulting signal consists of two components with frequencies as the sum and the difference of the two signals. Correlation is performed during the code wipe off which yields a correlation peak. The acquisition detector determines whether the correlation peak is correct. The high frequency component at the mixer output needs to be eliminated and the low frequency component should be processed to determine if the acquisition is a success.

Integrate and dump: This section integrates the mixer output and acts as a low pass filter (LPF) to eliminate the high frequency component. The integrated signal is combined across the integration periods before passing it to the acquisition detector.

Acquisition detector: This module is used to detect the presence of the GPS signal. Noise computation is an important part of the acquisition process. Detection threshold computation is explained in Section 5.2 and is the minimum noise level which the correlation peak should exceed to be detected as a signal. It should be optimally chosen to avoid a false lock and to allow weak signal acquisition. A signal is acquired when the correlation peak exceeds the detection threshold and estimates of the code phase and Doppler of the cell under search are passed to the tracking process. If a signal is not detected, the acquisition manager searches the next cell. Once all the cells are exhausted the next GPS satellite is searched and the process is repeated.

5.2 Detection Threshold

Acquisition is a two-dimensional (code phase and Doppler) search process whereby the search range is decided by a priori knowledge of the satellite positions. If this information is not available then a sky search has to be performed. The Doppler range should be carefully chosen to include the frequency uncertainty resulting from satellite motion, user dynamics and the receiver clock offset. A Doppler bin is defined as 2/(3T), where T is the signal integration time or dwell time per cell in seconds [Tsui and Bao, 2000]. The dwell time should be longer to acquire weak signals. However, the actual signal strength received depends upon the signal environment and is not known until the SV signal is

acquired. The SV signal power decreases under foliage condition, urban canyon and indoor environments.

The search pattern is usually in the code phase direction from 1 to 1023 at a constant Doppler bin. In the Doppler search direction, the search pattern is typically from the mean value of the Doppler uncertainty and then symmetrically one Doppler bin at a time on either side of the mean Doppler value until the 3-sigma Doppler uncertainty has been searched [Tsui and Lin, 2001]. The integrate dump module integrates the in-phase (I) and the quadrature (Q) signals over the dwell time for each cell. Then the envelope $\sqrt{I^2+Q^2}$ is computed and compared to a threshold to determine the presence of the SV signal. The signal detection is a statistical process because each cell contains noise with or without the signal [Kaplan, 1996]. Each case has its own probability density function (PDF) which is shown in Figure 5.2.

The PDF for the noise without the signal has a zero mean while the PDF for the noise with the signal has a non-zero mean. The detection threshold is usually based on an acceptable false detection probability. If the envelope obtained from $\sqrt{I^2+Q^2}$ is above the detection threshold the signal is present otherwise it is deemed as noise. Figure 5.2 illustrates the four outcomes from a single trial process with two being right and two being wrong. The detection threshold can be properly computed knowing both PDFs of the envelopes and it depends upon the single trial probability of detection (P_d) and single trial probability of false alarm (P_{fd}) defined in Equations (5.1) and (5.2).

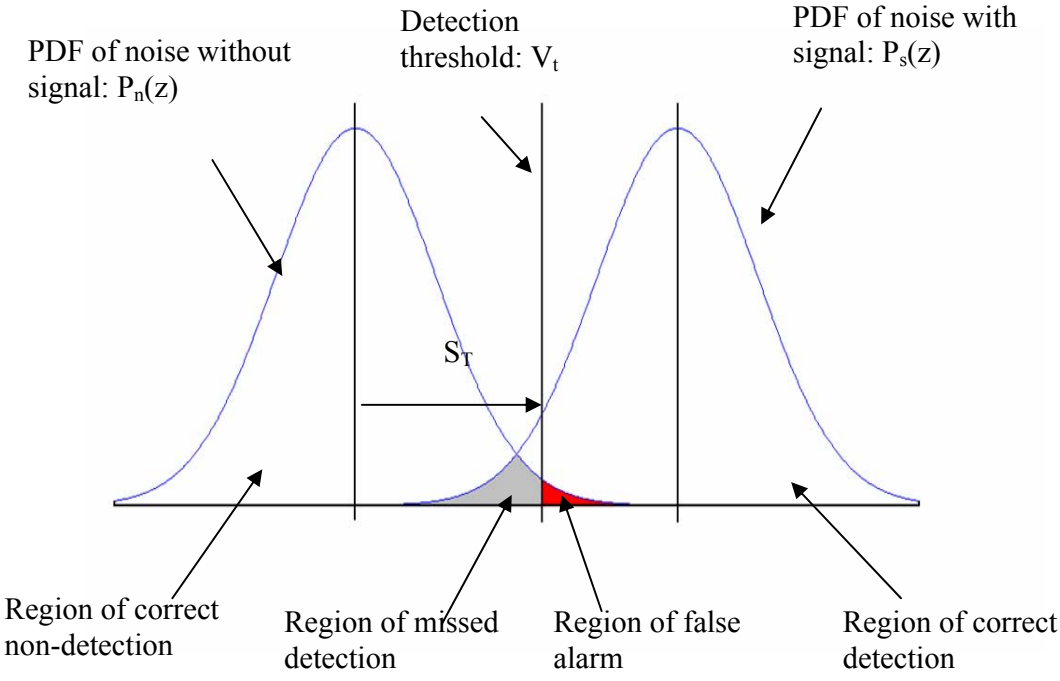

Figure 5.2: PDF of noise and signal

$$P_d = \int_{V_t}^{\infty} P_S dz \qquad 5.1$$

$$P_{fd} = \int_{V_t}^{\infty} P_n dz \qquad 5.2$$

where

$P_s(z)$ is the PDF of the envelope in the presence of the signal, and

$P_n(z)$ is the PDF of the envelope in the absence of the signal.

The I and Q signals have a Gaussian distribution which causes the envelope formed by $\sqrt{I^2 + Q^2}$ to have a Ricean distribution defined in Equation (5.3).

$$P_S(z) = \frac{z}{\sigma_n^2} e^{\frac{-(z+A^2)}{2\sigma_n^2}} I_o\left(\frac{zA}{\sigma_n^2}\right) \text{ for } z \geq 0;\ P_s(z) = 0 \text{ otherwise} \qquad 5.3$$

where

z is the random variable,

σ_n is the RMS noise,

A is the RMS signal amplitude, and

$Io\left(\frac{zA}{\sigma_n^2}\right)$ is the modified Bessel function of zero order.

Equation (5.3) can be expressed in terms of the predetection SNR (s/n) as given in Equation (5.4).

$$P_S(z) = \frac{z}{\sigma_n^2} e^{-\left(\frac{z^2}{2\sigma_n^2}+s/n\right)} I_o\left(\frac{z\sqrt{2s/n}}{\sigma_n}\right) \qquad 5.4$$

where

s/n is the predetection SNR = $A^2/2\sigma_n^2$ (power ratio) = $10^{(S/N)/10}$,

S/N is the predetection SNR in dB = C/No + 10log T (dB),

C/No is the carrier to noise power density ratio in dB, and

T is the search dwell time = predetection integration time.

The PDF for the envelope without the signal present can be obtained by setting the signal amplitude (A) to zero in Equation (5.3). This yields a Rayleigh distribution as defined in Equation (5.5).

$$P_n(z) = \frac{z}{\sigma_n^2} e^{-\left(\frac{z^2}{2\sigma_n^2}\right)} \quad 5.5$$

Equation (5.6) is obtained by integrating the results of substituting Equation (5.5) into Equation (5.2).

$$P_{fd} = e^{-\left(\frac{V_t^2}{2\sigma_n^2}\right)} \quad 5.6$$

Equation (5.6) is rearranged to obtain an expression for the detection threshold (V_t) in terms of the single trail probability of false alarm and measured 1-sigma noise power as in Equation (5.7) [Kaplan, 1996].

$$V_t = \sigma_n \sqrt{-2 \ln P_{fd}} \quad 5.7$$

The 1-sigma noise power was found to be insufficient to prevent false locks for the software receiver implemented by the PLAN group. Hence, a 3-sigma noise power along with a standard value of 10% for the false probability detection was used during the analysis.

5.3 Acquisition Schemes Comparison

Different acquisition methods were discussed in Section 3.3. Time domain correlation, circular convolution and modified circular convolution were implemented in software to analyze the acquisition process. Time domain correlation performs a sequential cell by cell search and is time consuming for the software receiver implementation compared to other two methods. Hence only circular convolution and modified circular convolution

methods are compared in this section. Time domain correlation is preferred for a hardware correlator because of its simplicity.

5.3.1 Details of Data Set Collected and Processing Methodology

Digitized IF data is required to perform software acquisition and can be obtained by tapping data from a GPS RF front-end or by simulating the GPS signal in software and quantizing it. A GPS RF front-end data logger (Signal Tap) was used to collect the data which gives the advantage of using real GPS signals for analysis instead of simulating them in the software with different models. The Signal Tap is a GPS RF front-end data logger from Accord Software & Systems Pvt. Ltd. which allows logging of the digitized IF data at various sampling frequencies for different durations [Shashidhar, 2003]. It has different IF bandwidths and a suitable one should be chosen depending upon the application. Higher bandwidths provide a precise and accurate GPS solution but increase the computational burden. The GPS data was collected using a NovAtel 600 antenna located on the rooftop of the CCIT building. Figure 5.3 shows the setup for data collection and the details of the data sets are given in Table 5.1. Four different sampling frequencies (4, 7, 9 and 12 MHz) were selected for collecting the data sets. These sampling frequencies were chosen at random to verify the proper functioning of acquisition methods. A detailed analysis of the sampling frequency is presented in Section 5.4. Each data set was logged for a duration of one second using the Signal Tap and a laptop. Ten data sets were collected for each sampling frequency and thus a total of 40 data sets were collected.

Table 5.1: Real GPS signal scenario parameters

Parameter	Value
User position	Latitude: 51°4.45' N Longitude: 114°8.06' W Altitude: 1118 m
Time	20:00 Oct. 14, 2003 GMT
Visible PRNs	1,13,16,2,20,24,27,3
GPS signal frequency	L1 frequency
Navigation data	ON
Doppler	N/A
Signal Power used	N/A

NovAtel GPS antenna with LNA of +26 dB

Signal Tap

Laptop

Figure 5.3: Setup for collecting data from GPS satellites

A GPS simulator (STR 6560) was also used to collect single satellite and multiple satellite data to verify the acquisition schemes. The single channel simulator in the STR 6560 allows configuration of the PRN number and the Doppler of the satellite as well as to enable/disable the navigation data on the simulated signal. The signal power and

Doppler can be varied during the simulation run. This simulator mode is useful to verify the GPS acquisition process since the acquisition results (the acquired PRN and Doppler) can be directly compared with the simulator settings. Figure 5.4 shows the setup for collecting data using the GPS simulator with the scenario parameters described in the Table 5.2.

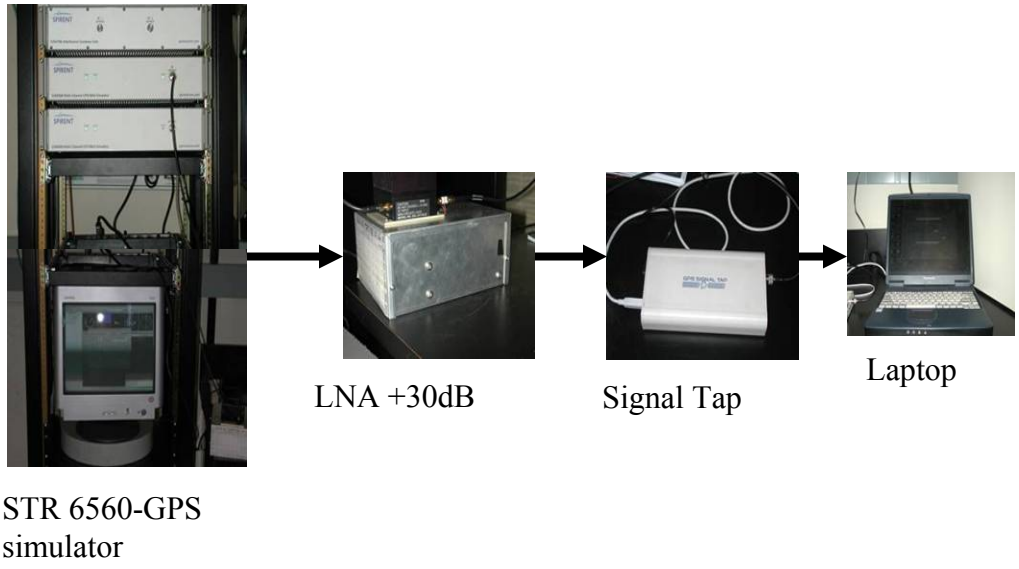

Figure 5.4: Setup for collecting data from GPS simulator

The Doppler was varied over the Doppler search range in steps of 1 KHz to ensure successful acquisition for all possible Doppler frequencies. A total of 600 (10 Doppler frequencies, 3 power levels, 4 sampling frequencies and 5 samples per configuration) data sets were collected using the Signal Tap. The STR 6560 was used in normal mode to collect multiple satellite data sets. In the multiple satellite scenario the signal strength can be varied during simulation and the navigation data can be switched off before running the simulation. The Doppler of the satellite cannot be configured as desired. The setup for multiple satellites scenario is shown in Figure 5.4 with scenario details presented in

Table 5.3. The signal strength and sampling frequency were varied to collect 120 data sets of one second duration each.

Table 5.2: Simulator configuration for single satellite data sets

Parameter	Value
User Position	N/A
Time	17:00 Oct. 14, 2003 GMT
PRN	3
GPS signal frequency	L1 frequency
Navigation data	ON
Doppler	Fixed for a particular data set Varied from ± 5 KHz in range of 1 KHz
Signal Power	-120, -125 and –130 dBm

Table 5.3: Simulator configuration for multiple satellite data sets

Parameter	Value
User position	Latitude: 51°4.45’ N Longitude: 114°8.06’ W Altitude: 1118 m
Time	18:00 Oct. 14, 2003 GMT
Visible PRNs	1,13,16,2,20,24,27,3
GPS signal frequency	L1 frequency
Navigation data	ON
Doppler	N/A
Signal Power used	-120 -125 and –130 dBm

A software receiver was developed during this research to analyze the interference effects. Two different acquisition schemes were used to analyze the performance of acquisition and then combined to improve the acquisition performance. Circular convolution scheme was then selected to analyze RFI effects on the acquisition process. Different RF signals were used to determine the variation of noise power and SNR (discussed in Chapter 6). These analyses determine the additional noise power introduced by interference signals. This information was then incorporated in the software receiver. The acquisition process was modified to determine the noise present in the incoming signal to indicate the presence of interference. If the noise power is more than due to thermal noise, it indicates presence of interference. A coherent integration of 4/8 ms was used to determine the additional noise introduced which allows determining the type of interference present. A proper predetection integration time depending upon the interference type was used to acquire the signal. The predetection integration time was chosen depending upon the additional noise present since the thermal cross-correlation noise is constant. The interference analysis and predetection integration time required to acquire the signal with interference are discussed in Chapter 6.

A combination of the MEX (C code compiled in Matlab) and Matlab code was used to reduce the processing times. Table 5.4 lists the acquisition parameters used to perform the acquisition on the collected data sets.

Table 5.4: Acquisition parameters used during analysis

Parameter	Values for single satellite data set	Values for multiple satellite data set and real GPS signal data sets
Intermediate Frequency (IF)	15.42 MHz (Signal Tap)	15.42 MHz (Signal Tap)
Sampling Frequency (SF)	4, 7, 9 and 12 MHz depending on data set	4, 7, 9 and 12 MHz depending on data set
Start value of Doppler search	-5 KHz	-7 KHz
End value of Doppler search	+5 KHz	+7 KHz
Coherent integration time	8 ms	8 ms
Non-coherent integration time	16 ms	16 ms
False detection probability	5%	5%
Number of PRNs to be searched	32	32
List of PRNs to be searched	1 to 32 (3*)	1 to 32 (1*,13*,16*,2*,20*,24*,27*,3*)

*-indicates the PRNs which are present in the data set.

The Signal Tap IF is at 15.42 MHz which was used to generate the local replica carrier signal. Different sampling frequencies were used to ensure proper functioning of the acquisition process. The Doppler search range had to be increased to ±7 KHz for multiple satellite data sets to ensure acquisition of all visible satellites. The oscillator on the Signal Tap has an offset of 2 KHz from the reference frequency which requires the Doppler

range to be increased to ±7 KHz. The acquisition manager uses the specified parameters to determine the Doppler bin using the coherent integration time. The detection threshold is computed as explained in Section 5.2. The PDF of the noise is determined using correlation values from all cells searched by the acquisition process. The 3-sigma of the noise power computed along with a false detection probability of 10% was used to compute the detection threshold.

5.3.2 Single Satellite Results

Acquisition was performed on all the single satellite data sets using both schemes to be verified. The acquisition results from all the data sets were analyzed in terms of the mean processing time, the acquisition gain and the memory required. The results from all the data sets were averaged to obtain an estimate of the above mentioned parameters. The single satellite results were verified with the simulator settings and were found to acquire at the correct Doppler. There were no false locks for the remaining 31 PRNs.

5.3.2.1 Mean Processing Time

The processing time was calculated using the time taken by the PC to perform the desired task. The PC used for the analysis was the Intel Pentium 4 processor operating at 2.0 GHz speed and Matlab version 6.5 was used to code the acquisition algorithms. The processing times for all Doppler bins for an 8 ms coherent integration period at different sampling frequencies are shown in Table 5.5.

Table 5.5: Processing times for 8 ms coherent integration period

Acquisition scheme	Sampling frequency (time in seconds)			
	4 MHz	7 MHz	9 MHz	12 MHz
Circular convolution	10.00	12.93	15.76	19.33
Modified circular convolution	8.96	11.47	14.27	16.90

The modified circular convolution scheme takes less time than the circular convolution scheme because it uses a half of the GPS spectrum. This reduces the number of the FFT points and thus the FFT processing time. FFT is the most time consuming operation in a software receiver. The FFT and IFFT were performed in Matlab and hence the processing times are in the order of seconds. The processing time increases with an increase in the sampling frequency since the number of samples (i.e. FFT points) is more at higher sampling frequencies for the same duration of time. The processing time also depends on the Doppler search range used for acquisition and increases linearly with an increase in the Doppler range as represented in Table 5.6.

Table 5.6: Processing time for different Doppler range

Doppler search range	Acquisition schemes (time in seconds)							
	Sampling frequency							
	Circular convolution				Modified circular convolution			
	4 MHz	7 MHz	9 MHz	12 MHz	4 MHz	7 MHz	9 MHz	12 MHz
10 KHz	10.00	12.93	15.76	19.33	8.96	11.47	14.27	16.90
14 KHz	14.42	27.01	38.13	50.01	11.70	22.17	34.42	40.82
20 KHz	20.10	38.00	55.00	73.72	16.12	32.06	46.16	61.12

The Doppler search range increases with an inaccurate receiver clock and high user dynamics. It can be reduced with knowledge of the satellite positions, an approximate GPS time and an approximate user position. Almanac and ephemeris data along with the

GPS time can be used to compute the satellite positions. The user position in conjunction with the satellite position is used to compute an approximate code phase and Doppler for that satellite. The acquisition manager uses this information to reduce the search range and acquisition time.

5.3.2.2 Processing Gain

Acquisition gain is an important factor to determine satellite acquisition. It was computed as a ratio of the correlation peak against the detection threshold. The acquisition schemes should provide as high gain as possible to acquire weak signals. The gains obtained for the two schemes at different signal strengths and sampling frequencies are shown in Table 5.7.

Table 5.7: Processing gain for 8 ms coherent integration period

Signal power level	Acquisition schemes (gain in dB)							
	Circular convolution				Modified circular convolution			
	Sampling frequency (MHz)				Sampling frequency (MHz)			
	4	7	9	12	4	7	9	12
-120 dBm	21.08	23.03	23.11	23.20	19.84	22.28	22.31	22.16
-125 dBm	16.62	19.62	19.62	19.62	15.75	18.75	18.75	18.75
-130 dBm	10.33	13.33	13.33	13.33	9.56	12.56	12.56	12.56

The gain is nearly the same for different sampling frequencies except for the 4 MHz sampling frequency. A sampling frequency of 4 MHz causes an aliasing effect which introduces a signal loss and results in lower gain. The sampling frequency effect is studied in detail in Section 5.4. Acquisition gain from the modified circular convolution scheme is about 1-1.5 dB lower than the circular convolution method. This is due to the

use of half the input signal spectrum to reduce the processing time. The GPS signal information contained in the other half of the GPS spectrum is lost which results in a lower gain. Thus the reduction in the processing time is at the cost of lower gain.

5.3.2.3 Memory Requirements

One important criterion for choosing the acquisition scheme to implement in an embedded system is the amount of memory required. Memory usage should be as minimal as possible to implement the algorithm across the microprocessors and a DSP where available memory is a constraint. Memory requirements were analyzed at two stages in both acquisition schemes. The first stage is the FFT stage wherein the FFT of the incoming signal and a local signal is taken. The memory locations needed for this stage at different sampling frequencies are given in Table 5.8. The next stage is the IFFT stage wherein the inverse FFT is taken of the signal resulting from convolution of the two spectrums. The memory locations needed for this stage at the different sampling frequencies are given in Table 5.9.

Table 5.8: Memory required for 1 ms coherent integration period at FFT stage of acquisition schemes

Acquisition scheme	**Number of memory locations**			
	Sampling frequency			
	4 MHz	**7 MHz**	**9 MHz**	**12 MHz**
Circular convolution	4000	7000	9000	12000
Modified circular convolution	4000	7000	9000	12000

Table 5.9: Memory required for 1 ms coherent integration period at IFFT stage of acquisition schemes

Acquisition scheme	Number of memory locations			
	Sampling frequency			
	4 MHz	7 MHz	9 MHz	12 MHz
Circular convolution	4000	7000	9000	12000
Modified circular convolution	2000	3500	4500	6000

These memory requirements were obtained when each sample was stored in a separate memory location. These samples can be packed in bytes to reduce the memory requirements by a factor of eight. The memory required increases linearly with an increase in the coherent integration time. A higher sampling frequency requires more memory as the number of samples is more at higher frequencies for the same duration of time. Hence the coherent integration time and the sampling frequency should be chosen depending upon available system resources.

5.3.2.3.1 Acquisition Plots

Figure 5.5 shows the autocorrelation plots (first eight) and the cross-correlation plots (last two) for the two acquisition schemes at different sampling frequencies (SF) and signal power levels.

Circular convolution

Autocorrelation plot, SF =12 MHz

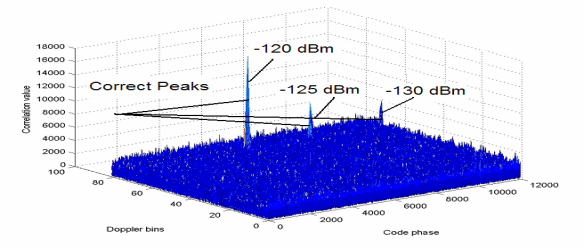

Modified circular convolution

Autocorrelation plot, SF = 12 MHz

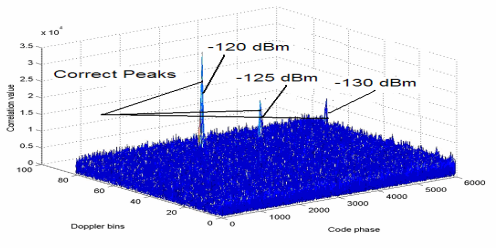

Autocorrelation plot, SF =9 MHz

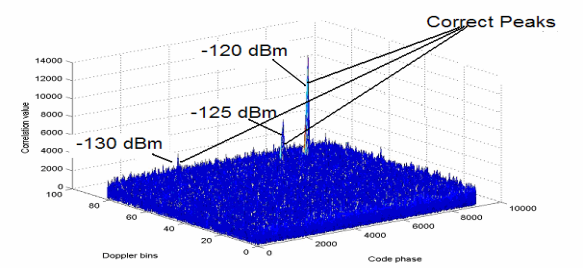

Autocorrelation plot, SF =9 MHz

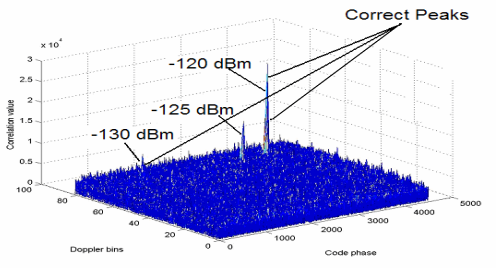

Autocorrelation plot, SF =7 MHz

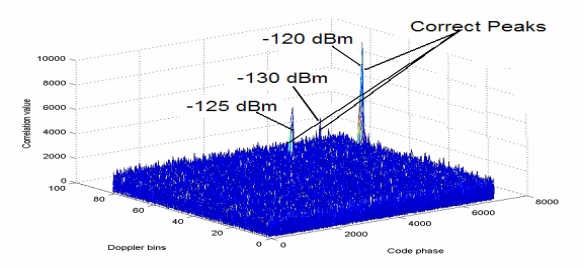

Autocorrelation plot, SF =7 MHz

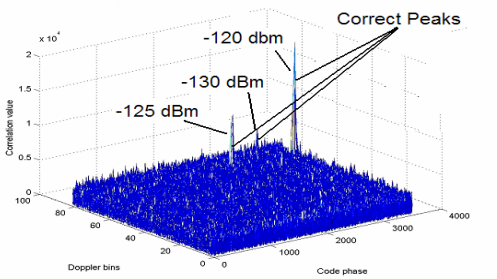

Autocorrelation plot, SF =4 MHz

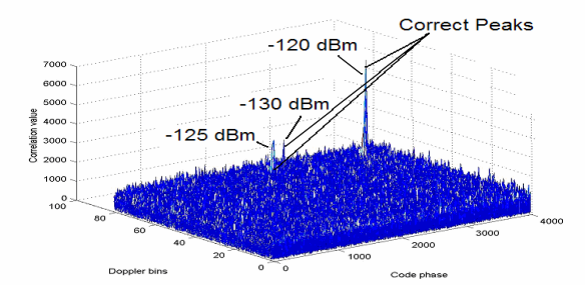

Autocorrelation plot, SF =4 MHz

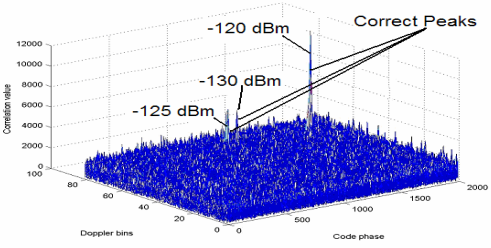

Cross-correlation plot, SF =12 MHz

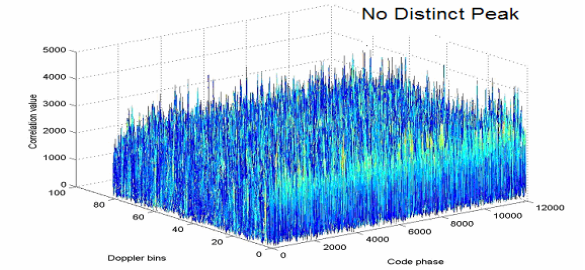

Cross-correlation plot, SF =12 MHz

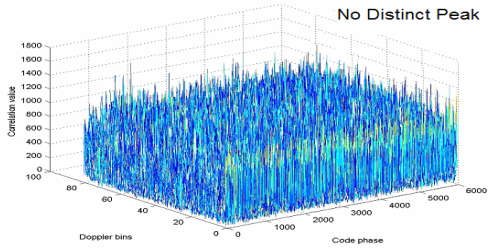

Figure 5.5: Correlation plots for two different acquisition schemes

The plots show that a correlation peak is generated when the phase of the PRN codes match during autocorrelation. Cross-correlation does not yield a peak as observed in the correlation plots. This correlation property of the GPS PRN codes allows proper acquisition of the GPS signal. The signal peak decreases with a decrease in the GPS signal strength which leads to a cross correlation problem for weak signal acquisition.

5.3.3 Multiple Satellite Results

Acquisition was performed on the multiple satellite data sets using both the schemes. An acquisition search was performed on all the PRN numbers (1 to 32) and all visible satellites were acquired with no false locks. The Doppler range had to be increased to ±7 KHz due to the oscillator clock offset in the Signal Tap. The processing times for one satellite at different sampling frequencies are given in Table 5.5 and they increase linearly with an increase in the number of satellites searched sequentially. The power level for all visible satellites was kept within ±1 dB of the signal strengths analyzed. The processing gain obtained for the acquired satellites is the same as given in Table 5.7 for different power levels. The memory requirements increase linearly with the number of satellites processed simultaneously. In the case of sequential processing of the satellites, the memory requirement is that of single satellite. The acquisition (correlation) plots at different power levels at a sampling frequency of 12 MHz are shown in Figure 5.6.

Circular convolution

Autocorrelation plot for -120 dBm

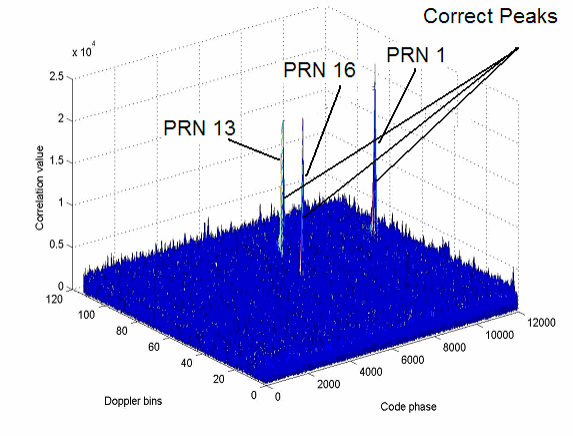

Modified circular convolution

Autocorrelation plot for -120 dBm

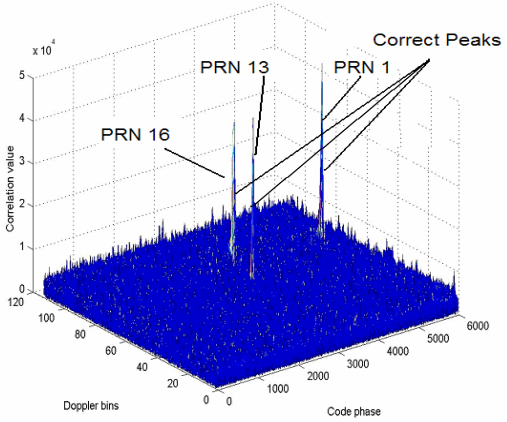

Autocorrelation plot for -125 dBm

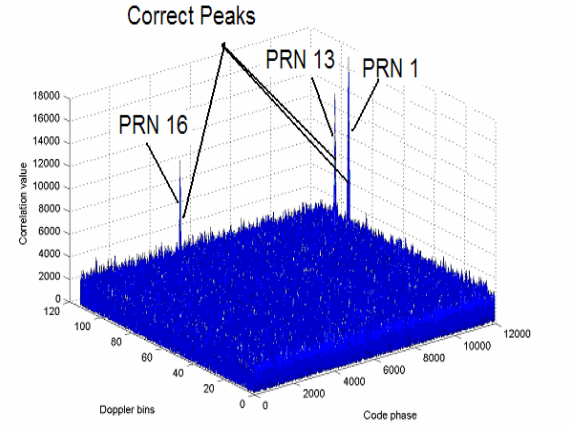

Autocorrelation plot for -125 dBm

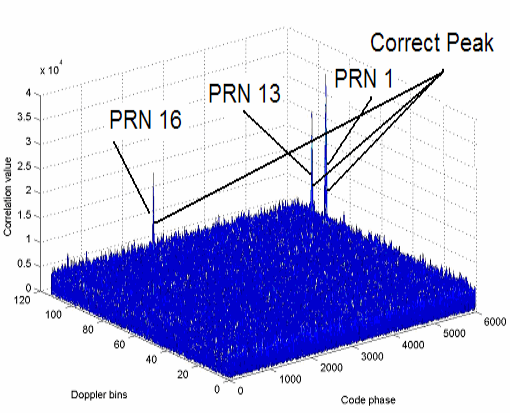

Autocorrelation plot for -130 dBm

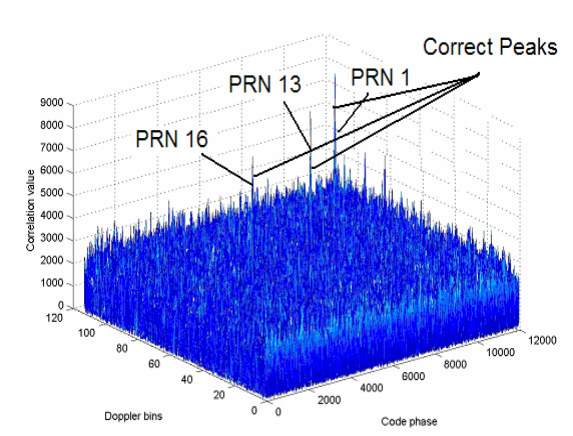

Autocorrelation plot for -130 dBm

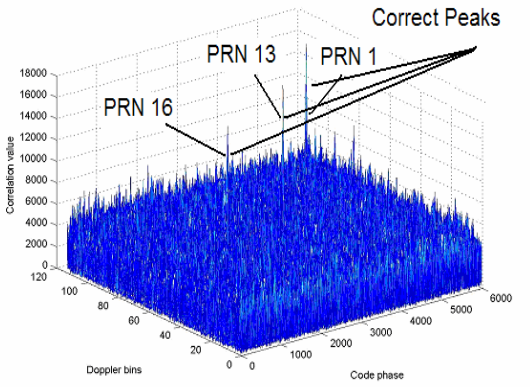

Figure 5.6: Multiple satellite acquisition

5.3.4 Real GPS Signal Results

The software receiver developed as a part of this research was used to acquire the signals present in the data sets logged from the GPS antenna. All PRN numbers (1 to 32) were searched and the visible satellites were acquired with no false locks. The acquisition plots for different sampling frequencies are shown in Figure 5.7.

Circular convolution
Autocorrelation plot, SF = 12 MHz

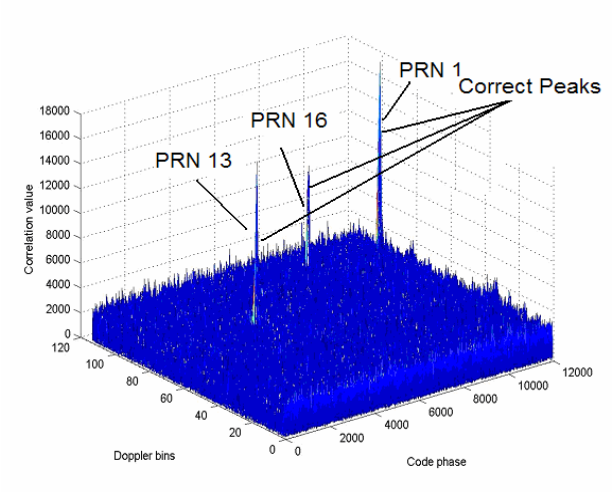

Modified circular convolution
Autocorrelation plot, SF = 9 MHz

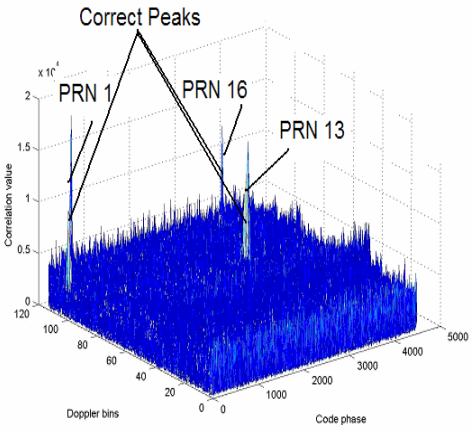

Autocorrelation plot, SF = 7 MHz

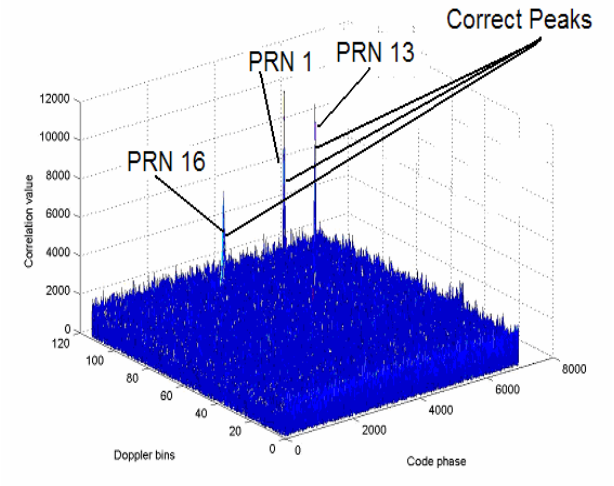

Autocorrelation plot, SF = 4 MHz

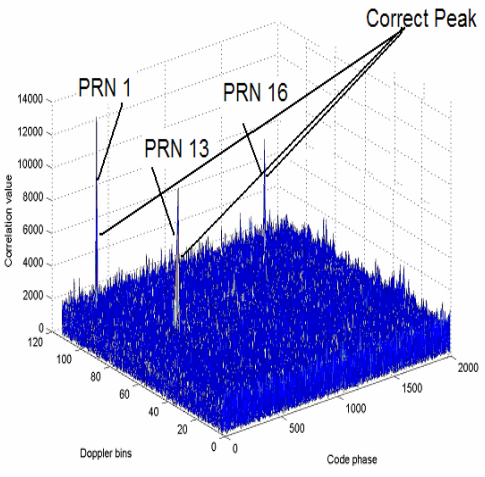

Figure 5.7: Acquisition with real GPS signal

These results verify the two GPS acquisition schemes. The circular convolution scheme provides a better gain but at the cost of processing time and memory. The modified circular convolution scheme can be used to reduce acquisition time and memory requirements but the gain is less than that for circular convolution scheme. An intelligent acquisition scheme will be to first use the modified circular convolution scheme to acquire the signals with good signal strength in a less amount of time and later switch to the circular convolution scheme to acquire the signals with low signal strength. This was implemented in the software receiver and found to be effective in reducing processing time.

5.4 Sampling Frequency

The analog GPS signal has to be converted to a digital signal to process it using a DSP. An analog signal is continuous while a digital signal is discrete in both time and amplitude. Sampling is used to convert a signal from the continuous time domain to the discrete time domain. The value of the signal is measured at certain intervals in time and each measurement is referred to as a sample. The rate at which the samples are measured is called as the sampling frequency. When the continuous analog signal is sampled at a frequency, F, the resulting discrete signal has more frequency components than did the analog signal [Zawistowski and Shah, 2001]. After sampling, the frequency components of the analog signal are obtained at their original position and also centred on ± F, ±2F, etc.

The sampling frequency should be selected according to the Shannon's sampling theorem and the Nyquist criteria. Shannon's sampling theorem states that a signal can be exactly reproduced if it is sampled at a frequency F, where F is greater than twice the maximum frequency in the signal [Peterson et al., 1995]. This frequency is called as the Nyquist frequency (or rate) [Zawistowski and Shah, 2001]. When the sampling rate is less than the Nyquist rate, the reconstructed signal exhibits a phenomenon called aliasing. Aliasing is the presence of the unwanted signal components (not present in the original analog signal) in the reconstructed signal. Also, some of the frequencies in the original signal may be lost in the reconstructed signal [Agilent Technologies, 2003]. Aliasing occurs because signal frequencies fold around half the sampling frequency for lower sampling frequency and hence aliasing is often referred to as the frequency fold effect [Zawistowski and Shah, 2001].

Figure 5.8 shows an analog signal, x(t), that can be viewed as a continuous function of time. This signal can be represented as a discrete time signal by using the values of x(t) at intervals of nTs to form x[n] as shown in Figure 5.8. The samples from the function x(t) are grabbed at regular intervals of time, Ts, called the sampling period. The sampling effects on a sinusoidal signal of frequency B Hz that results from the use of different sampling frequencies (Fs) are shown in Figure 5.9.

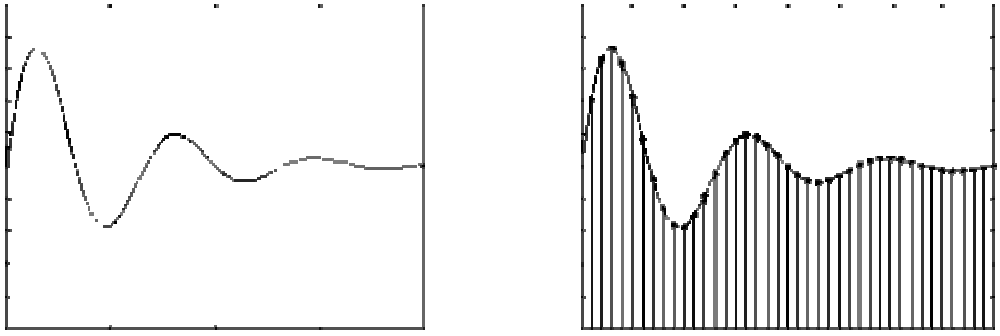

Analog Signal Sampled Signal

Figure 5.8: Original and sampled signal [Zawistowski and Shah, 2001]

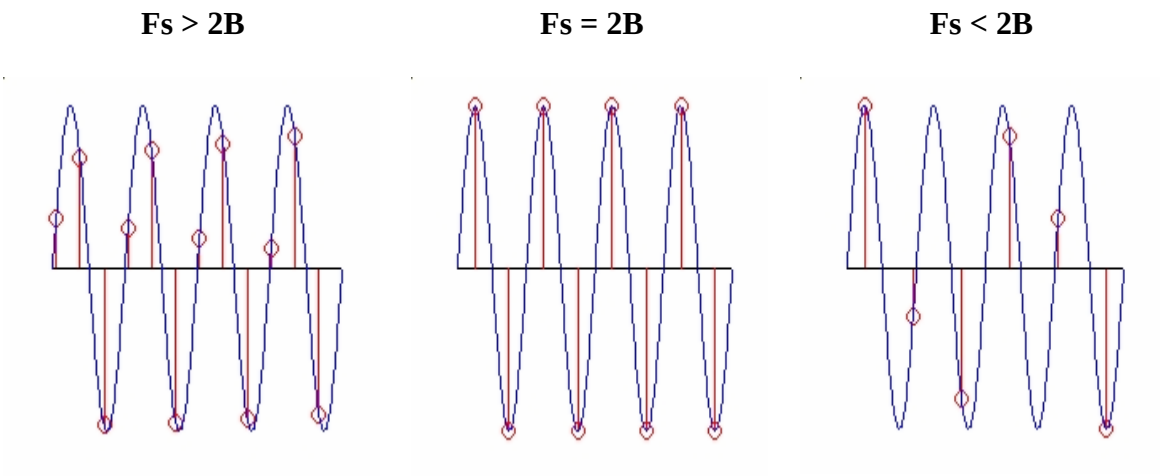

Figure 5.9: Different sampling frequency effects

Sampling results in a spectrum which repeats every Fs Hz. The spectrum will overlap with each other when the frequency (Fs) is less than twice the signal bandwidth (B). Hence a frequency greater than twice the bandwidth will cause no interference among the spectrums and the signal can be recovered by filtering the signals beyond the original spectrum. An aliasing effect is caused by the overlapping of the sampled spectrum [Sayed, 2004]. When this occurs, the original spectrum is distorted and is not possible to

reconstruct the original signal. Two signals are said to alias when the difference of their frequencies falls in the frequency range of interest [Agilent Technologies, 2003]. This difference frequency is always generated during the sampling process. Aliasing is not always bad and is called mixing or heterodyning in analog electronics. It is commonly used for tuning household radios, TVs and other communication products.

The aliasing problem can be avoided using an LPF to remove frequencies beyond the desired range. An anti-aliasing filter is usually built into the analog interface chips and codecs (which convert analog input signals into digital form for processing by a DSP) [Agilent Technologies, 2003]. The filter can be constructed using either analog or digital circuits. The digital filter has less noise and drift problems compared to analog filters.

The sampling frequency accuracy affects signal reconstruction and data processing. The down conversion process introduces a small error in the output frequency due to the inaccuracy of the sampling frequency [Tsui and Bao, 2000]. The output frequency (f_o) resulting from sampling a signal with the frequency (f_i) by a frequency (f_s) is given by Equation (5.8).

$$f_o = f_i - n\frac{f_s}{2} \quad \text{and} \quad f_o < \frac{f_i}{2} \qquad 5.8$$

where

n is an integer.

For example, if the IF frequency is at 15.5 MHz and the sampling frequency is at 5 MHz, the output frequency will be at 0.5 MHz using the Equation (5.8) and the integer n will have a value of six. If there is an error in the sampling frequency of +100 Hz, the output

frequency will be at 0.4997 MHz. Thus an error of 300 Hz will be introduced which is three times the error in the sampling frequency because n=6. This error will affect the Doppler search range of the acquisition process. This error will be large when a single stage down conversion is performed in the RF front-end. For example, if a sampling frequency of 5 MHz is used to down convert the L1 (1575.42 MHz) signal, the output frequency will be at 0.42 MHz with n=630 from Equation (5.8). An error of 100 Hz in the sampling frequency will down convert the signal to 0.4515 MHz introducing an error of 31.5 KHz (because n = 630). This error will cause the Doppler search range to be insufficient to cover all frequencies. This frequency error will have a severe impact on the acquisition process [Tsui and Bao, 2000].

The sampling frequency effect on the acquisition process is analyzed in Section 5.4. This entails analyzing the aliasing effect of the signal for a particular sampling frequency and determining the signal interference due to the effect.

5.4.1 Data Sets Collected and Processing Methodology

Single satellite data sets were collected from the STR 6560 for analysis. The Signal Tap was used to collect the digitized IF data from the simulator. The sampling frequency effect on the GPS signal of one satellite is the same for all the remaining satellites since the GPS frequency is the same for all satellites. The selection of the sampling frequency should consider the IF bandwidth of the RF front-end. Bandwidths of 2 and 8 MHz were used to collect the data sets. The STR 6560 was used in single channel mode with

constant Doppler. The signal strength was maintained constant throughout the entire range of sampling frequencies. The data sets configurations are listed in Table 5.10.

Table 5.10: Data set configuration for different bandwidths

Parameter	Value
PRN	1
GPS signal frequency	L1 frequency
Navigation data	ON
Doppler	Fixed
Sampling frequency	2 to 20 MHz in steps of 1MHz
Signal Power used	-125 and –130 dBm
Duration of data set	1 second
Number of data sets	10 for each sampling frequency

The circular convolution method was used to analyze the effect of sampling frequency. This effect is present in the input data for the acquisition schemes. Hence the effect on one method will be similar for the other methods. The set of acquisition parameters used for analysis is given in Table 5.11.

Table 5.11: Acquisition parameters used during analysis

Parameter	Values for single satellite data set
Intermediate Frequency (IF)	15.42 MHz (Signal Tap)
Sampling Frequency (SF)	2 to 20 MHz depending upon data set
Start value of Doppler search	-5 KHz
End value of Doppler search	+5 KHz
Coherent integration time	8 ms
Non-coherent integration time	16 ms
False detection probability	5%
Number of PRNs to be searched	1
List of PRNs to be searched	1

Table 5.12 lists the sampling frequencies which should theoretically cause the aliasing effect for the two bandwidths under consideration. This was determined using Equation (5.8) with the relation of the sampling frequency being greater than twice the bandwidth of the signal. The spectral inversion occurs when the output frequency obtained from Equation (5.8) is negative [Shashidhar, 2003]. Whenever there is a spectral inversion due to the sampling frequency, the local signal must be generated with the in-phase and quadrature signals interchanged. The detection threshold was computed using the correlation values for all Doppler bins at a particular sampling frequency to compute the noise power, and a false detection probability of 5%.

Table 5.12: Aliasing effect due to different sampling frequencies

Sampling frequency (MHz)	Signal bandwidth (2 MHz)		Signal bandwidth (8 MHz)	
	Aliasing present	Spectral inversion	Aliasing present	Spectral inversion
2	Yes	Yes	Yes	Yes
3	Yes	No	Yes	No
4	Yes	Yes	Yes	Yes
5	Yes	No	Yes	No
6	Yes	Yes	Yes	Yes
7	No	No	Yes	No
8	Yes	Yes	Yes	Yes
9	No	Yes	Yes	Yes
10	Yes	No	Yes	No
11	No	No	Yes	No
12	No	No	Yes	No
13	No	No	Yes	No
14	No	No	Yes	No
15	Yes	No	Yes	No
16	Yes	Yes	Yes	Yes
17	No	Yes	Yes	Yes
18	No	Yes	Yes	Yes
19	No	Yes	Yes	Yes
20	No	Yes	No	Yes

5.4.2 Results

Acquisition was performed on all the data sets collected and the results were verified with the simulator settings. The results obtained were analyzed to determine the acquisition success percentage, the correct acquisition probability and the acquisition gain.

5.4.2.1 Acquisition Success Percentage

The acquisition percentage was determined from the number of times the satellite was acquired at each sampling frequency, irrespective of whether the Doppler was correct or not. Satellite acquisition indicates a correlation peak was obtained above the detection threshold. The acquisition percentages for two different bandwidths are tabulated in Table 5.13.

The results show that a higher sampling frequency is required for wider bandwidths to acquire the signal. The signal is acquired for all sampling frequencies with a 2 MHz bandwidth at -125 dBm while it fails for some frequencies at -130 dBm. The signal with an 8 MHz bandwidth can be acquired 100% of the time for sampling frequencies above 16 MHz at -125 dBm. Aliasing effects cause a significant signal loss which is evident from the acquisition percentage at -125 and -130 dBm especially for the 8 MHz bandwidth. It causes an overlap of the high frequency components of the signal over the low frequency components resulting in the high frequency noise being present in the reconstructed signal. This noise increases the detection threshold and causes signal distortion decreasing the acquisition percentage at lower sampling frequencies. There was

acquisition success at sampling frequencies of 6 and 14 MHz for an 8 MHz bandwidth at signal strength of -130 dBm. These were false locks resulting from aliasing effect as indicated in next section.

Table 5.13: Acquisition percentage for different sampling frequencies at different signal strength and signal bandwidth

Sampling frequency (MHz)	Signal bandwidth (2 MHz)		Signal bandwidth (8 MHz)	
	-125 dBm	-130 dBm	-125 dBm	-130 dBm
2	100%	0%	0%	0%
3	100%	0%	0%	0%
4	100%	100%	0%	0%
5	100%	66%	0%	0%
6	100%	66%	0%	33%
7	100%	100%	0%	0%
8	100%	100%	0%	0%
9	100%	100%	0%	0%
10	100%	66%	0%	0%
11	100%	100%	0%	0%
12	100%	100%	66%	0%
13	100%	100%	33%	0%
14	100%	100%	33%	33%
15	100%	100%	0%	0%
16	100%	100%	100%	0%
17	100%	100%	100%	66%
18	100%	100%	100%	33%
19	100%	100%	100%	33%
20	100%	100%	100%	33%

5.4.2.2 Correct Acquisition Percentage

Section 5.4.2.1 presented the results for the acquisition success irrespective of the correctness of the Doppler acquired. The results were further analyzed to determine if the acquired peak was at the correct Doppler, which was obtained from the simulator settings. An analysis was done to determine the correctness of the correlation peak irrespective of whether the peak was above the detection threshold. The detection threshold can be reduced by increasing the false detection probability or by taking a lesser percentage of the noise power into consideration. The results are tabulated in Table 5.14. To obtain the percentage of the correct Doppler being above the detection threshold, the results from Tables 5.13 and 5.14 needs to be multiplied.

The acquisition peak is at the correct Doppler for all the sampling frequencies at a 2 MHz bandwidth with -125 dBm power level. This decreases for the sampling frequencies below 6 MHz when the signal strength is reduced by 5 dB. This is due to the decrease in the signal gain and thus the aliasing effect is more visible at lower signal strengths. A strong signal will have a high autocorrelation peak which can tolerate more noise resulting from the aliasing effect. Thus stronger signals are less affected by the signal distortion during sampling.

Table 5.14: Percentage of correct acquisition for different sampling frequencies at different signal strength and signal bandwidth

Sampling frequency (MHz)	Signal bandwidth (2 MHz)		Signal bandwidth (8 MHz)	
	-125 dBm	-130 dBm	-125 dBm	-130 dBm
2	100%	0%	0%	0%
3	100%	33%	0%	0%
4	100%	100%	0%	0%
5	100%	67%	0%	0%
6	100%	100%	0%	0%
7	100%	100%	0%	0%
8	100%	100%	0%	0%
9	100%	100%	33%	0%
10	100%	100%	67%	0%
11	100%	100%	33%	0%
12	100%	100%	67%	0%
13	100%	100%	67%	0%
14	100%	100%	33%	0%
15	100%	100%	0%	0%
16	100%	100%	100%	0%
17	100%	100%	100%	67%
18	100%	100%	100%	67%
19	100%	100%	100%	33%
20	100%	100%	100%	67%

The results for a bandwidth of 8 MHz indicate that acquisition is possible for a sampling frequency above 9 MHz at -125 dBm and above 16 MHz at -130 dBm. A wider bandwidth introduces more noise into the system. This reduces the acquisition success at lower sampling frequencies which have a signal loss due to the aliasing effect. Thus a

wider bandwidth requires a higher sampling frequency to avoid the aliasing effect and to acquire the signal.

5.4.2.3 Acquisition Gain

Acquisition gain can be used to determine the signal loss due to the aliasing effect. Aliasing causes a frequency overlap resulting in high frequency noise being added with the noise in the desired spectrum which increases the noise power and reduces the gain. The gains for different sampling frequencies are shown in Table 5.15. The acquisition gain (Table 5.15) is compared against the aliasing effect at different sampling frequencies (Table 5.13) which indicates that for sampling frequencies that cause aliasing, a loss of 2-3 dB is introduced. A bandwidth of 8 MHz has less gain than for the 2 MHz bandwidth case since the amount of noise contained in the 8 MHz bandwidth is greater. Thus increasing the bandwidth increase the noise power which makes acquisition more difficult at low signal strengths.

Table 5.15: Acquisition gain for different sampling frequencies at different signal strength and signal bandwidth

Sampling frequency (MHz)	Acquisition gain (dB)			
	Signal bandwidth (2 MHz)		Signal bandwidth (8 MHz)	
	-125 dBm	-130 dBm	-125 dBm	-130 dBm
2	7.35	0.00	0.00	0.00
3	7.80	3.03	0.00	0.00
4	8.36	5.29	0.00	0.00
5	8.36	5.41	2.35	0.00
6	8.36	5.31	0.00	0.00
7	10.01	5.01	0.00	0.00
8	9.29	5.24	0.00	0.00
9	9.30	5.66	4.21	0.00
10	7.85	5.11	3.90	0.00
11	10.81	5.66	2.43	0.00
12	10.26	5.59	5.46	2.92
13	10.19	5.53	4.13	0.00
14	9.18	6.77	5.57	4.56
15	7.67	5.19	0.00	0.00
16	9.17	5.81	6.03	0.00
17	10.10	6.28	5.63	5.44
18	10.28	6.35	7.76	5.52
19	10.31	6.62	7.09	5.07
20	9.55	5.69	6.46	4.39

Thus the sampling frequency selection is important in the correlator design. It should be chosen properly depending upon the IF bandwidth to avoid aliasing effects and to reduce processing power and memory requirements.

5.5 Predetection Integration Time

The predetection integration time plays an important role in signal detection by determining the achievable gain. It should be optimally chosen to achieve the desired acquisition sensitivity with the available processing power. The predetection integration time is a combination of the coherent and non-coherent integration times [Kaplan, 1996]. The coherent integration time performs an algebraic sum of the signal while the non-coherent integration does an absolute sum of the signal. Thus the amount of noise in the coherent integration time is less than that of the non-coherent integration time. The Doppler bin size is the inverse of the coherent integration time. A longer coherent integration time means a smaller Doppler bin size which increases the number of the Doppler bins to be searched.

The coherent integration time is limited by two factors-navigation data bit transition and the Doppler effect on the C/A-code. A navigation data bit transition will spread the spectrum causing the output to be no longer a CW signal. This spectrum spreading will reduce the acquisition gain and distort the acquisition peak. For example, if 10 ms of data is used for acquisition and there is a phase transition at 5 ms, the width of the spectrum spread is about $(2/5 \times 10^{-3}) = 400$ Hz [Tsui and Bao, 2000]. This peak can be detected to allow proper acquisition but it suppresses the carrier frequency. The maximum coherent integration time can be 10 ms when the navigation data bit transition instant is not known. This is because the data bit transition will be absent in either one of the two

adjacent 10 ms data sets [Tsui and Bao, 2000]. Thus two consecutive 10 ms data sets should be used to perform acquisition to ensure there is no navigation data bit transition.

The Doppler effect on the C/A-code also puts a constraint on the coherent integration time. If a perfect correlation peak is 1, then the correlation peak decreases to 0.5 when a C/A code is off by half a chip. The C/A-code Doppler is 1540 (L1 frequency/C/A-code frequency) times lower than the Doppler on the L1 frequency. A Doppler of ±10 KHz in the L1 frequency introduces a C/A-code Doppler of 6.4 Hz. This Doppler is important during acquisition and tracking of the C/A-code. It takes about 78 ms for two frequencies different by 6.4 Hz to change by half a chip [Tsui and Bao, 2000]. This limit on the data length is longer than the 10 ms limit imposed by the navigation data bit transition. Hence 10 ms is the maximum coherent integration time possible without knowledge of the data bit transition.

A method of processing the data beyond 10 ms is through non-coherent integration. Non-coherent integration sums up the results across the coherent integration period. This increases the signal strength by a factor of 2 and noise by $\sqrt{2}$. It also increases the SNR by $\sqrt{2}$ or 1.5 dB. This improvement is less compared to the coherent integration method but requires fewer operations. Non-coherent integration is not affected by the navigation data bit transition since the correlation results of the coherent integration time are squared before summation.

The predetection integration time should be carefully chosen to avoid false locks. The GPS Gold (C/A) codes were selected to have the best cross-correlation properties possible among the set of the PRN sequences obtained using two 10-bit shift registers [Spilker and Parkinson, 1996]. These Gold codes have a cross-correlation tolerance of 21-24 dB among each other [Kaplan, 1996]. The GPS signal level difference between a satellite at the horizon and at a higher elevation can be up to 16 dB due to transmitted power difference, multipath, low atmospheric loss, and antenna gain variation [Kaplan, 1996]. Thus only a 5 dB signal difference can cause cross-correlation. Signal fading due to foliage, urban canyon conditions or indoor environments reduce the signal level by more than 5-10 dB [MacGougan, 2003]. This difference in the power level will prevent acquisition of the weak signals and reduce the satellite availability. Weak signals will have autocorrelation peaks close to the cross-correlation peaks of the strong signals. Thus, there is a strong possibility of the cross-correlation peaks exceeding the autocorrelation peaks for the weak signal when multiple correlations are done. The acquisition process will detect these cross-correlation peaks as the signal peaks resulting in false acquisition. Hence the detection threshold should be optimally chosen to avoid false locks which can be achieved by selecting a proper value of the false detection probability.

5.5.1 Data Sets Collected and Processing Methodology

The STR 6560 was used in single channel mode and the digitized IF data was logged using the Signal Tap. The effect of the predetection integration period on a single satellite

has a similar effect on the other satellites. An aliasing free sampling frequency was chosen to collect the data at different signal strengths listed in Table 5.16.

Table 5.16: Data set configuration

Parameter	Value
User Position	N/A
Time	12:00 Oct. 20, 2003 GMT
PRN	1
GPS signal frequency	L1 frequency
Navigation data	First ON and then OFF
Doppler	Fixed
Sampling frequency	7 MHz
Signal Power used	–130, -135 and –140 dBm
Duration of data set	2 s
Number of data sets	10 for each signal strength and data on/off

Two acquisition methods (circular convolution and modified circular convolution) were used to analyze the effect of the predetection integration time. The coherent integration time was varied from 1 to 100 ms to determine the acquisition gain possible and to analyze the effect of the navigation data bit transition and the Doppler. Non-coherent integration factor was varied from 1 to 50 using a 2 ms coherent integration time. Acquisition parameters used during the analysis are listed in Table 5.17. Ten trials were performed for each integration time using both acquisition schemes.

Table 5.17: Acquisition parameters used during analysis

Parameter	Values for Single satellite data set
Intermediate Frequency (IF)	15.42 MHz (Signal Tap)
Sampling Frequency (SF)	7 MHz
Start value of code delay search	N/A
End value of code delay search	N/A
Start value of Doppler search	-3 KHz
End value of Doppler search	+3 KHz
Coherent integration time	1–100 ms
Non-coherent integration time	2–100 ms for 2 ms coherent integration time
False detection probability	5%
Number of PRNs to be searched	1
List of PRNs to be searched	1

5.5.2 Results

The results were analyzed to determine the acquisition gain at different signal strengths for both the acquisition schemes. The navigation data bit transition effects on the coherent and non-coherent integration times, and the effect of false detection probability, are also studied.

5.5.2.1 Coherent Integration Time

The acquisition gain is calculated as the ratio of the correlation peak at the correct Doppler to the detection threshold. Detection threshold computation depends on the false

detection probability. A lower value of the probability increases the threshold making it difficult to acquire the satellite. The gain obtained for different coherent integration times using both methods at -130 dBm is given in Figure 5.10.

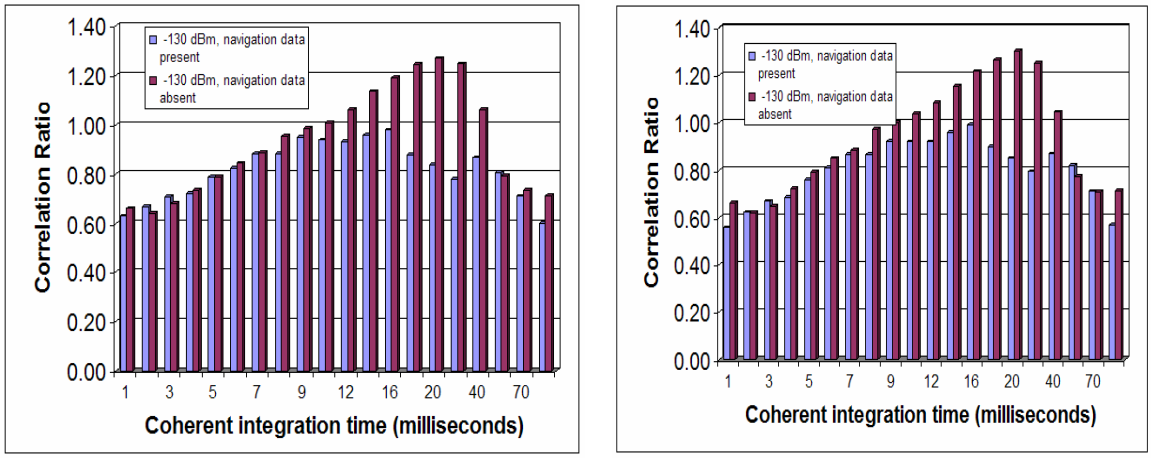

a) Circular convolution **b) Modified circular convolution**

Figure 5.10: Acquisition gain for different coherent integration time

The gain increases with an increase in the coherent integration time. This is because more signals are accumulated for longer coherent integration times. The acquisition peak decreases for lower signal strengths while the noise remains the same. This causes problems for weak signal acquisition.

The acquisition gain increases when the navigation data bits are absent because the navigation data bit transition introduces a loss in the acquisition gain. When the navigation data is absent only the Doppler affects the acquisition peak. Thus a reduction in the gain above the coherent integration of 10 ms is due to the Doppler. The effect of the navigation data bits is shown in Table 5.18. The signal peak is higher for circular convolution compared to the modified circular convolution approach. Thus circular convolution provides more gain which allows for weak signal acquisition. Modified

circular convolution provides less gain since it uses only half of the GPS spectrum for correlation. This causes a signal loss of about 1-1.5 dB over the different signal levels. The results indicate that a coherent integration time of 8-10 ms is sufficient to acquire a signal strength of -130 dBm. However to acquire signal strength of -135 dBm, the coherent integration time has to be increased beyond 30 ms. This is not possible for unaided acquisition wherein the knowledge of the navigation data bit value and transition instant is unknown. The cross-correlation peaks have comparable power to the autocorrelation peaks below -135 dBm. The noise power in the acquisition process remains the same irrespective of the GPS signal strength. This causes the gain to decrease for lower signal strengths because the GPS signal peak has less power while the noise remains the same. This effect is the same for both acquisition methods.

Acquisition time is an important parameter to determine the TTFF for the receiver and should be as low as possible. The time taken for performing coherent integration using both the methods for a 6 KHz Doppler search range is shown in Figure 5.11.

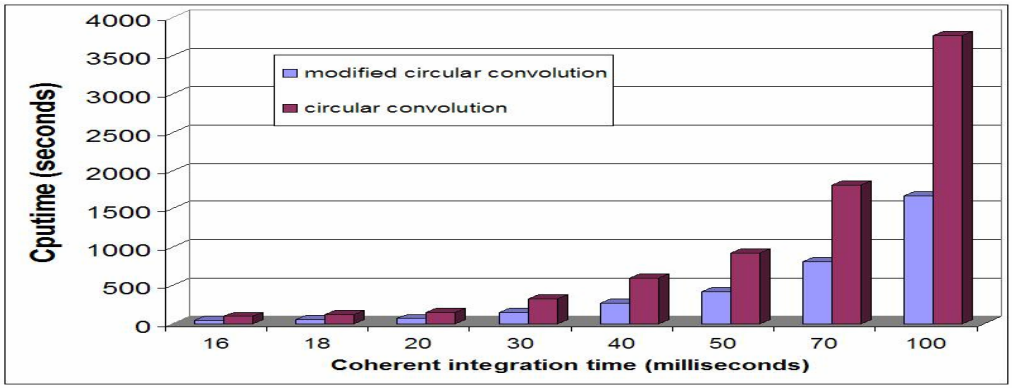

Figure 5.11: Time taken for 1 PRN at different coherent integration time using circular convolution and modified circular convolution methods

The time required increases linearly with an increase in the coherent integration time. This is due to an increase in the number of FFT points for longer coherent integration times. An increase in the number of FFT points increases the processing time and the processing power required. Modified circular convolution method requires about 50% less time than the circular convolution method. This is due to the 50% decrease in the number of IFFT points used in modified circular convolution compared to circular convolution. FFT and IFFT are the most time consuming operations for both of these methods. Hence a reduction in the number of the FFT/IFFT points directly reduces the processing time. Weak signal acquisition requires a longer coherent integration time which increases the search time. Hence a trade off between the acquisition search time and the acquisition gain is always required before selecting the coherent integration time.

5.5.2.2 Non-Coherent Integration Time

Non-coherent integration involves squaring and summing the signals across coherent integration periods. The coherent integration period was kept at 2 ms and the non-coherent integration factor was varied to analyze its effect. The processing time for non-coherent integration is a direct multiple of the non-coherent integration factor and the time required to perform coherent integration. An advantage of using non-coherent integration is that the predetection integration time can be extended beyond 20 ms without any effect from the navigation data bit transition. A disadvantage is that the noise power increases as the signal and noise are squared before summation. Acquisition gains for different non-coherent integration factors using both the methods are given in Figure 5.12. Acquisition gain increases with an increase in the non-coherent integration factor.

There is no difference in gain between the data sets with and without the navigation data present. This confirms that non-coherent integration is unaffected by navigation data transitions. The increase in the noise power during non-coherent integration results in a lower gain compared to coherent integration. The noise power increases because of the squaring loss introduced during squaring of the correlation values in non-coherent integration. However non-coherent integration is advantageous in unaided acquisition. The circular convolution method provides more gain compared to the modified circular convolution method due to the use of the entire signal present in the GPS spectrum.

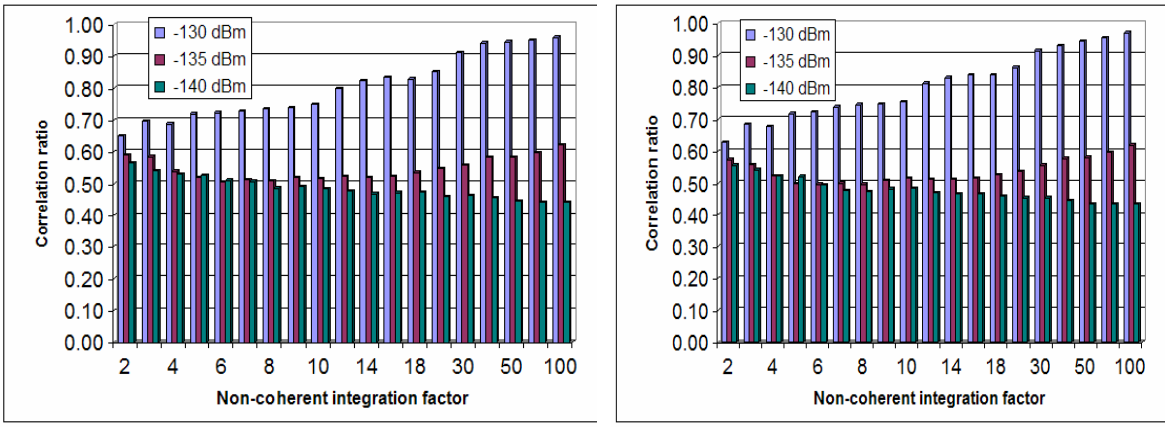

a) Circular convolution **b) Modified circular convolution**

Figure 5.12: Acquisition gain for non-coherent integration time

The noise power variance during non-coherent integration follows the Chi-square distribution which decreases the noise power at higher non-coherent integration and increases the SNR of the signal. The noise power from coherent integration is Gaussian in nature which is squared during non-coherent integration resulting in Chi-square distribution. The non-coherent integration reduces noise variance and provides a gain for signal acquisition.

5.5.2.3 False Detection Probability

The false detection probability plays an important role in determining the detection threshold. It is a scaling factor for the noise power to prevent false acquisition. It also depends upon the amount of noise power considered for the threshold. If 1-sigma of noise power is considered, then either the false detection probability factor should be high or the false detection probability should be close to zero. The gains obtained for different the false detection probabilities using the circular convolution at -130 dBm are shown in Figure 5.13.

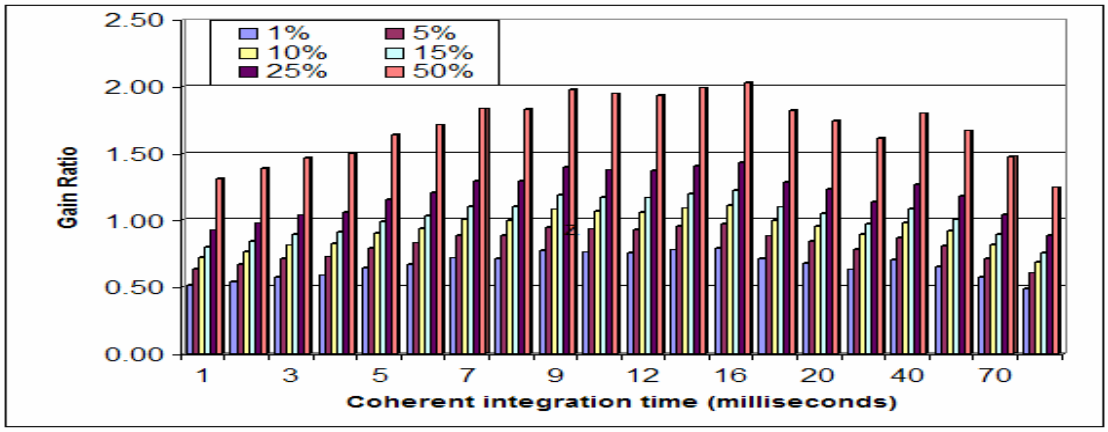

Figure 5.13: Gain for different false detection probabilities at -130 dBm for different coherent integration time using circular convolution

The gain increases with an increase in the false detection probability. Thus for the same coherent integration time, a correlation peak for the weak signal can exceed the threshold at a higher false detection probability but the same is true for the cross-correlation peaks. Hence the false detection probability cannot be kept higher when false lock avoidance is important. A value of 5 to 10 % is usually used to ensure that false locks do not occur while at the same time the threshold is not stringent. The results are similar for the

modified circular convolution. This is because the false detection probability affects the detection threshold and not the correlation process. The correlation process determines the signal peak obtained which varies for different acquisition methods. However the computation of the detection threshold is independent of the correlation process (i.e. acquisition method) even though it uses the correlation values to compute the noise power. Thus the false detection probability is independent of the acquisition methods and should be chosen optimally.

CHAPTER 6: RFI EFFECT ON GPS SIGNAL ACQUISITION

This chapter discusses different types of RFI and their effects on GPS signal acquisition. The results of various RFI signals on the GPS acquisition process are also explained.

6.1 RFI Signals

Different interference signals (CW, swept CW, AM, FM, broadband noise and pulse signals) were analyzed as a part of this research. The interference effect of each signal on the GPS spectrum is studied and analyzed for different predetection integration periods.

A receiver can acquire satellites only when the SNR is above a certain threshold. In the presence of jamming, the J/S ratio varies greatly which influences the probability of GPS signal acquisition. Satellite availability is dependent upon the constellation geometry, the performance of jamming mitigation, and the receiver acquisition time [Behre et al., 2002]. The spread spectrum concept is used in GPS to minimize the effect of interference signals whereby the interference signal is spread during correlation which decreases the interference signal power thereby providing some RFI mitigation. However, a high power interference signal will have sufficient power to distort the correlation peak or give rise to the correlation peak at incorrect estimates. If the interference is exactly at the same frequency and phase with the GPS signal, it can suppress the desired GPS signal and capture the receiver [Macabiau et al., 2001]. The interference effect depends on the details of the receiver design, especially the front-end bandwidth and the early-late

spacing in the discriminator. It has a different effect on the code tracking accuracy than on other aspects of a GPS receiver.

If the interference signal is Gaussian in nature, then it simply adds to the Gaussian thermal noise and increases the noise power in the receiver. This will affect weak signal acquisition since the noise power has increased. The detection threshold needs to be set higher to accommodate the increase in the noise power and to avoid false locks. A sinusoidal interference can be a CW, narrowband or a wide band signal like an FM signal and will a have severe impact on the receiver performance [Kaplan, 1996]. Hardware interference mitigation techniques try to filter the interference signal or provide zero gain for the interference signal. However, the interference signal can bypass these interference detectors and affect the GPS correlator. The RFI effect on code correlation reduces the C/No for all GPS signals [Spilker and Parkinson, 1996]. A C/No below the tracking threshold causes loss of lock and reduces the ability to navigate. If it is below the acquisition threshold it prevents acquisition or reacquisition of the satellites and reduces the GPS availability.

Acquisition is a weak link for RFI in the signal processing section of a GPS receiver. Acquisition uses only one correlator per acquisition search cell to acquire the signal while the tracking process has three or more correlators tracking the same signal. The acquisition threshold in a GPS receiver is about 10 dB higher than the tracking threshold. Thus a GPS receiver may be able to track weak signals but not acquire them. Hence the power required to jam the acquisition process is lower compared to that required to jam

the tracking process. Mitigating RFI during acquisition is advantageous as it prevents time wastage for the tracking process or navigation process to detect the presence of interference. Also, when there is a false acquisition (due to interference or any other reason), there is a considerable time delay before the tracking process can detect it. The measurements generated during this period will be erroneous and will severely degrade the navigation solution. However, the RFI effect on the acquisition process should be known before it can be mitigated. This research analyses the effect of RFI signals on the acquisition process in terms of the noise power and acquisition success percentage.

6.2 Data Collection Setup

The Signal Tap (RF front end data logger) with an IF bandwidth of 2 MHz was used to collect digitized IF samples. It filters any signal beyond the 2 MHz and hence the interference signal range is limited to 2 MHz. The Agilent signal generator (E 4431B) was used to generate the various interference signals and it is capable of generating a variety of signals such as CW, swept wave, AM, FM, pulsed signals and broadband noise. The signal strength can be varied from -135 to 50 dBm for all signals [Spirent Communications, 2003]. A CW signal can be generated in the 1 to 3 GHz frequency range which allows testing of in-band and out-of-band CW interference (CWI). A swept CW signal is generated as a sequence of CW signals. It is required to specify the start and stop frequencies for the swept CW, the number of points in the range, and dwell time at each point to generate a swept signal [Spirent Communications, 2003]. For example, a swept CW range from 1.5 to 2.5 GHz with 10 points and dwell time of 1 ms will consist

of CW frequencies from 1.5 to 2.5 GHz in steps of 0.1 GHz ((2.5-1.5)/10) and each frequency will be present for 1 ms.

Modulated signals (AM and FM) are used for communications and broadcast services. The Agilent signal generator generates the modulated and pulse signal for different configurations. For example, pulse interference can be generated for different duty cycles and pulse durations. The Agilent signal generator generates a pulse signal with an on/off ratio of about 80 dB [Spirent Communications, 2003]. This is less than the 164 dB specified by the FAA for GPS receivers in aviation applications but is good enough to test pulse interference for automotive and personal GPS receivers [RTCA, 2001]. High power pulse interference will cause saturation of the AGC and ADC. It saturates and introduces a jitter in the tracking loops. Broadband noise is a type of intentional interference signal and it is Gaussian in nature and similar to the GPS correlation noise. Broadband noise is characterized by the bandwidth of the signal which determines the amount of noise introduced in the GPS signal.

A GPS simulator (GSS 6560) capable of generating the L1 C/A-code signals under various scenarios was used to generate the GPS signals. Different users (stationary, automotive, aviation, etc) under various environments can be simulated. The GPS signals and interference signals are combined using an interference combiner (GSS 4766). The interference combiner introduces a loss while combining the input signals. This loss was measured and found to be around 8-10 dB for each channel. This was taken into account to obtain the desired signal strength at the output of the interference combiner. The GPS

simulator was used in single channel mode to avoid additional interference from the other PRN codes. Thus, only the effect of the RFI signals on the GPS acquisition process can be determined. The data collection setup is shown in Figure 6.1. An aliasing-free sampling frequency was chosen and ten data sets were collected for each interference scenario along with a clean GPS signal as a reference.

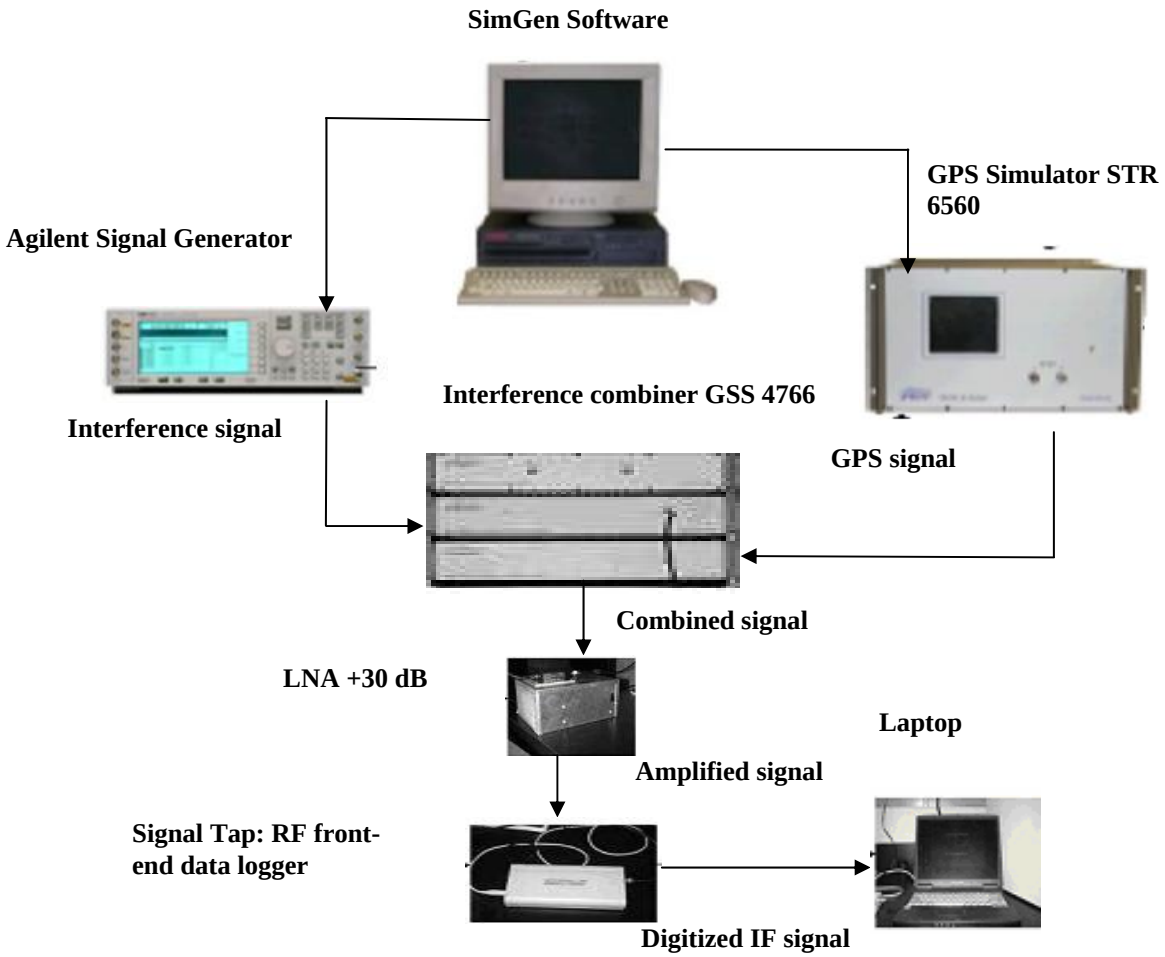

Figure 6.1: Data collection setup

6.3 Processing Methodology

Acquisition gain is an important parameter for RFI mitigation. An acquisition scheme should provide more gain to provide better tolerance to the RFI signals. The circular convolution method provides more gain among the acquisition schemes discussed in Section 3.3. Hence it was used to determine the possible interference tolerance in GPS acquisition. The acquisition parameters used during the analysis are given in Table 6.1.

Table 6.1: Acquisition parameters used during analysis

Parameter	Values
Intermediate Frequency (IF)	15.42 MHz (Signal Tap)
Sampling Frequency (SF)	7 MHz
Start value of Doppler search	-5 KHz
End value of Doppler search	+5 KHz
Coherent integration time	1, 4,5, 8, 10, 15, 20 ms
Non-coherent integration factor	1, 2, 3, 5
False detection probability	10%
Number of PRNs to be searched	1
List of PRNs to be searched	21

The Doppler search range was limited to ±5 KHz to account for the satellite motion and clock offset. Doppler variation over the data set duration (one second) is minimal for static condition. The coherent integration time was varied from 1 to 20 ms to determine a suitable period for acquisition. The non-coherent integration factor was varied from 1 to 5

for every coherent integration period to determine its effect. Acquisition was performed for different predetection integration times using each data set. The correlation value from all the acquisition cells was used to compute the noise power and to determine the detection threshold. The results from the clean GPS signal data set gives the reference values for the code phase and Doppler, which were used to compare the results from the interference data sets.

6.4 Results

The correlation values obtained for different predetection integration periods are used to analyze the interference effects. The correlation gain obtained for each predetection integration period is averaged over all the data sets. This gives the correlation gain over different initial interference conditions. The interference results are categorized into three sections namely noise power analysis, SNR analysis and acquisition success percentage.

Noise power analysis determines the variation of the noise power in the acquisition process for different RFI signals. The correlation noise without the interference signal is Gaussian in nature. The noise averages out for longer coherent integration times. However, with an interference signal present, the resulting correlation noise may not be Gaussian. The noise power variation under various interference conditions will give an indication of the amount and nature of noise introduced.

An SNR analysis compares the correct signal peak with the noise power under various interference conditions. It determines the interference power required to prevent signal

acquisition. The GPS signal strength is kept the same under all interference scenarios. Thus the signal peak power will be the same even though the noise varies for different interference conditions.

Acquisition success percentage determines the percentage of times the correlation peak is obtained at the correct Doppler under different interference conditions. It gives an indication of the interference tolerance possible when the noise power in the acquisition process is reduced. The detection threshold was computed using the 3-sigma value of the correlation noise power and a false detection probability of 10%. Different values for these parameters can be used to reduce the detection threshold. The correct Doppler is determined from the clean GPS signal and used to determine the acquisition success. An interference signal can distort the GPS signal resulting in the correlation peak being obtained at the incorrect Doppler. The maximum interference power required to distort the GPS signal and to make cross-correlation peaks higher than the autocorrelation peak is determined.

6.5 Continuous Wave Interference

CWI can be a pure tone frequency or a narrow modulated signal like an AM/FM signal. A pure tone frequency is considered for CWI analysis in this case. A CW signal within the IF bandwidth is difficult to isolate using the RF filters and the CWI effects on the GPS signal before and after correlation are shown in Figure 6.2. The correlation process during acquisition de-spreads the GPS signal to obtain the signal peak and spreads the CW signal. This causes a decrease in the CW power and reduces the effect of the CWI.

However, for high power CWI, the de-spread signal will have sufficient power to distort the GPS signal peak which causes problems during acquisition. CWI was analyzed in the narrow in-band region of the GPS signal spectrum (limited to the acquisition Doppler search range). The various CWI scenarios analyzed are listed in Table 6.2.

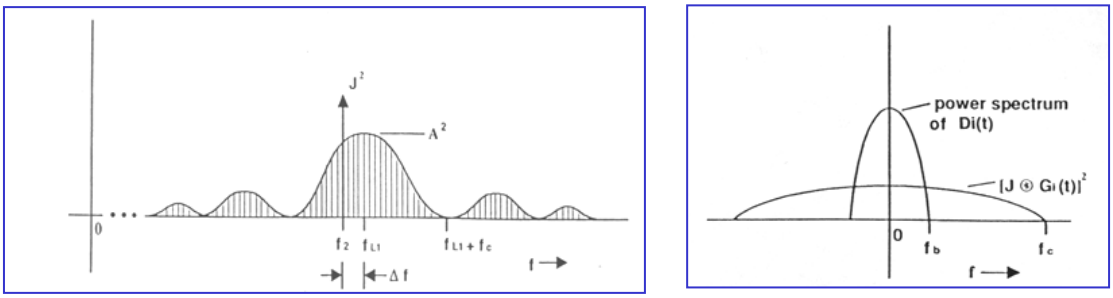

Figure 6.2: CW interference effect on GPS signal spectrum [Heppe and Ward, 2003]

Table 6.2: CW interference configuration

Parameter	Value
User position	Latitude: 51°4.45' N Longitude: 114°8.06' W Altitude: 1118 m
Time	05 Nov, 2003 01:00:00 GMT
PRN	21
GPS signal frequency	L1 frequency
Doppler	N/A
Signal Power used	-130 dBm
Interference frequency	L1 ±5 KHz in steps of 1 KHz
Interference power	-135 to -100 dBm in steps of 5 dB

6.5.1 Results

CWI results are discussed for different interference conditions under adaptive predetection integration.

6.5.1.1 Noise Power Analysis

The noise power variation determines the effect of the interference signal on the detection threshold. The detection threshold is an important parameter in the GPS acquisition which indicates the amount of noise present and is computed as explained in Section 5.2. The signal power was varied from -135 to -100 dBm for each CWI frequency with the GPS signal strength was kept at -130 dBm. The noise power was computed for different interference frequencies and power levels. The noise power obtained at -135 dBm was taken as a reference and the noise power ratio for different power levels was calculated. The noise power ratio for 10 ms coherent integration time at different CWI frequencies are shown in Figure 6.3.

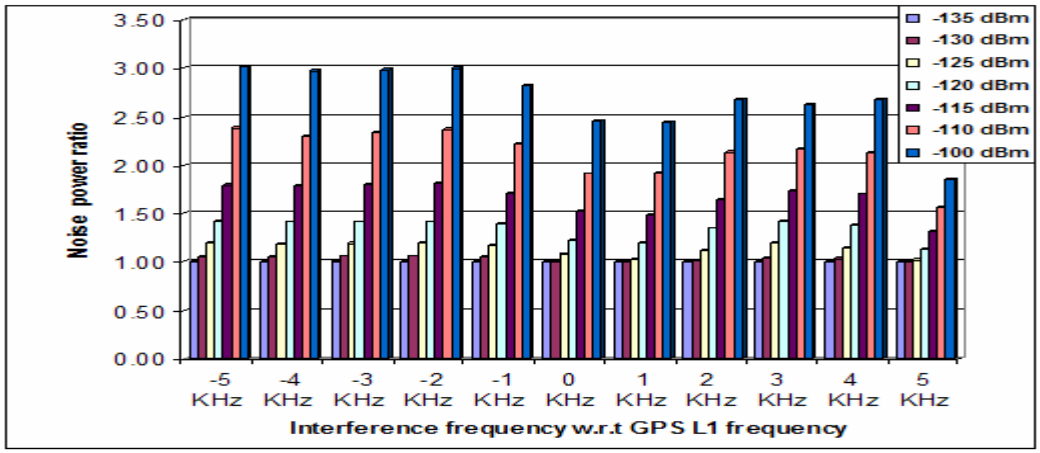

Figure 6.3: Noise power ratios for different interference frequencies at 10 ms coherent integration time and non-coherent integration factor of 1

The noise power increases with an increase in the interference power which is due to more interference power present in the GPS signal. The amount of increase is similar for various CW signals analyzed as shown in the Figure 6.3. The CWI signals in close proximity to the correct GPS Doppler have less noise compared to those away from it. This is because the de-spread CW power adds up with the signal peak when the CWI signal is close to the GPS Doppler and hence contributes less to the noise power. For an L1-5 KHz CWI frequency, the noise power increases by 300% for a 35 dB increase in the interference power. Thus CWI introduces a large amount of noise power. The increase in the noise power with interference power decreases the possibility of successful acquisition since the signal power level is constant while the noise power level has increased.

The effects of the predetection integration time on a particular interference frequency at different interference power levels were analyzed. A coherent integration time should be longer to acquire noisy signals as it allows the noise to average out and thus increases the signal peak. The noise power obtained for the clean GPS signal at each coherent integration time is considered as a reference. It increases with an increase in the coherent integration time. Thus the noise resulting from the CWI is non-Gaussian in nature and accumulates for longer coherent integration times. It increases by 200% for a 1 ms coherent integration time and an increase in interference power by 30 dB. For the same increase in the interference power, the noise power increases by 400% for a 20 ms coherent integration time. An increase in the noise power makes acquisition more difficult for lower coherent integration periods. The noise power variation for different

interference frequencies considered is similar with a similar increase in the noise power for all frequencies within ±5 KHz range of the GPS L1 frequency.

Non-coherent integration is used in combination with a coherent integration period to increase the signal level. However, the noise power level accumulates across the coherent integration period. The results indicate an increase in the noise power with an increase in the non-coherent integration factor. An increase in the interference power by 35 dB for a non-coherent integration factor of five increases the noise power by 1000%. The results are the same for other CWI frequencies tested. Thus CWI causes an increase in the noise power with an increase in the coherent integration time, non-coherent integration factor and interference power. The CWI results in non-Gaussian noise which increases with time and power.

The CWI effect on the positive side of the L1 spectrum is analyzed for different integration times and power levels. The noise power obtained at -135 dBm for a 1 ms coherent integration period is considered as a reference for each CWI frequency. An increase by a factor of 14-17 in the noise power is observed for a 35 dB increase in the interference power and a predetection integration time of 100 ms. This is an enormous increase in the noise power making signal acquisition nearly impossible. The amount of increase in the noise power is nearly the same for all frequencies analyzed and thus any frequency can jam the signal.

Similarly, the CWI effect on the negative side of the L1 spectrum was also analyzed for different integration times and power levels. The noise power obtained at -135 dBm from a 1 ms coherent integration period was taken as a reference for each CWI frequency. An increase by a factor of 14-18 in the noise power is observed for a 35 dB increase in the interference power and a predetection integration time of 100 ms. This is nearly the same as observed for the CWI frequencies on the positive side of the L1 spectrum. Thus the interference frequency on either side of the L1 spectrum will affect the acquisition process in a similar manner.

6.5.1.2 SNR Analysis

In Section 6.5.1.1, the noise power variation over different frequencies and power levels is discussed. After analyzing the amount of noise power variation with the interference frequency, integration time and power level, the SNR analysis is presented in this section. A correlation peak has to exceed the detection threshold for the acquisition process to declare the signal as acquired. There is a possibility (due to the large amount of noise at higher interference power levels) of the acquisition peak being obtained at a different Doppler other than the correct Doppler. False acquisition will occur when the cross-correlation peak exceeds the noise power. This also has to be avoided during acquisition otherwise it will introduce large errors in the navigation solution.

The SNR is an important factor to monitor during the acquisition process. The correct Doppler was determined from the clean GPS signal. This information was used to determine the correlation peak at the correct Doppler for all the interference signals. The

signal peak obtained at the correct Doppler was then compared with the noise power values for different conditions. The SNRs for different interference frequencies at a coherent integration of 10 ms are shown in Figure 6.4.

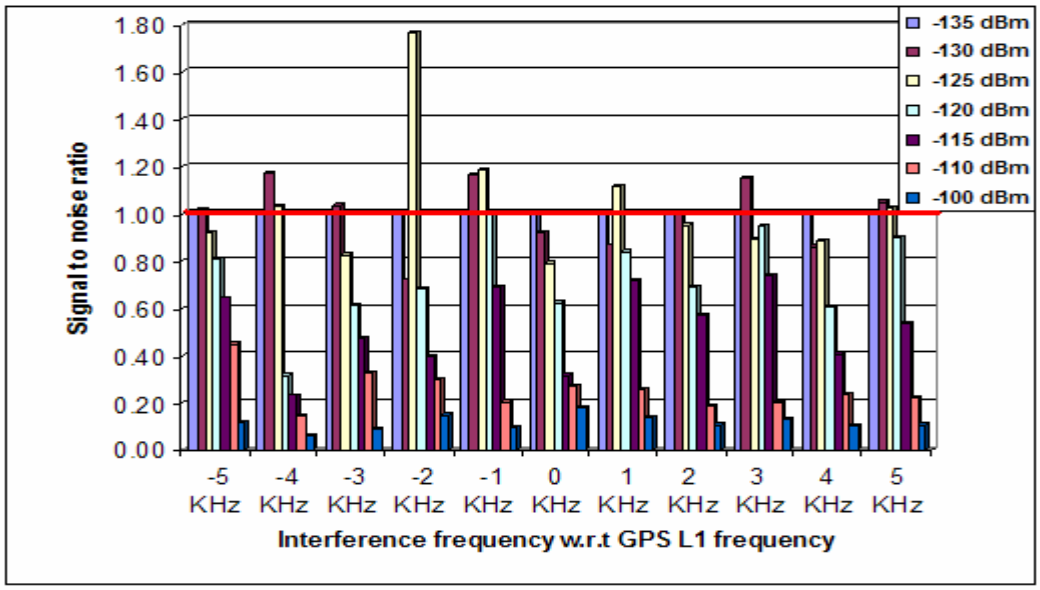

Figure 6.4: SNRs for different interference frequencies at 10 ms coherent integration period

An SNR above one indicates successful signal acquisition. The results in the Figure 6.4 indicate that the acquisition peak and the correct peak are the same until an interference power level of -120 dBm is reached. The acquisition peak is at the correct Doppler for an interference power of -115 dBm but the SNR is below one and hence the signal is not acquired. However, for an interference power level above -115 dBm, the correlation peak is different from the signal peak which might lead to false acquisition. The SNR is very high for the L1-2 KHz CWI frequency case at -125 dBm. This is because for that particular scenario, the Doppler coincided with the CWI frequency. Thus the interference peak added with the GPS signal peak increasing its power. An interference power of 15 dB higher than the GPS signal power decreases the SNR below one and prevents

acquisition. The SNR increases with an increase in the coherent integration time. This is because more signal is considered for correlation at longer coherent integration times. The SNR is close to one for coherent integration times beyond 5 ms. An interference power of 10 dB more than the GPS signal power is strong enough to reduce the SNR below one for a coherent integration time less than 10 ms. This is because of the enormous noise introduced by the CW signals. Non-coherent integration can be used to increase the signal power across coherent integration periods. The SNR increases with an increase in the non-coherent integration factor thereby increasing the tolerance to CWI. An additional 5 dB tolerance to the CWI signal is provided by increasing the non-coherent integration factor to five.

6.5.1.3 Acquisition Success Percentage

The SNR analysis indicated that GPS acquisition is possible up to an interference power of 10-15 dB greater than the GPS signal power. The percentage of time the acquisition peak is obtained at the correct Doppler is determined irrespective of whether the SNR is above one. This will give an indication of the interference power required to jam the acquisition process. The acquisition success percentages for different interference frequencies with a coherent integration time of 10 ms are shown in Figure 6.5. The results indicate that the correlation peak is obtained correctly for a 10 dB relative interference power for all the CWI frequencies analyzed. CWI frequencies close to the correct Doppler has better tolerance than the CWI frequencies away from it. This is due to the de-spread interference signal adding to the signal peak to increase its power and providing further tolerance to interference.

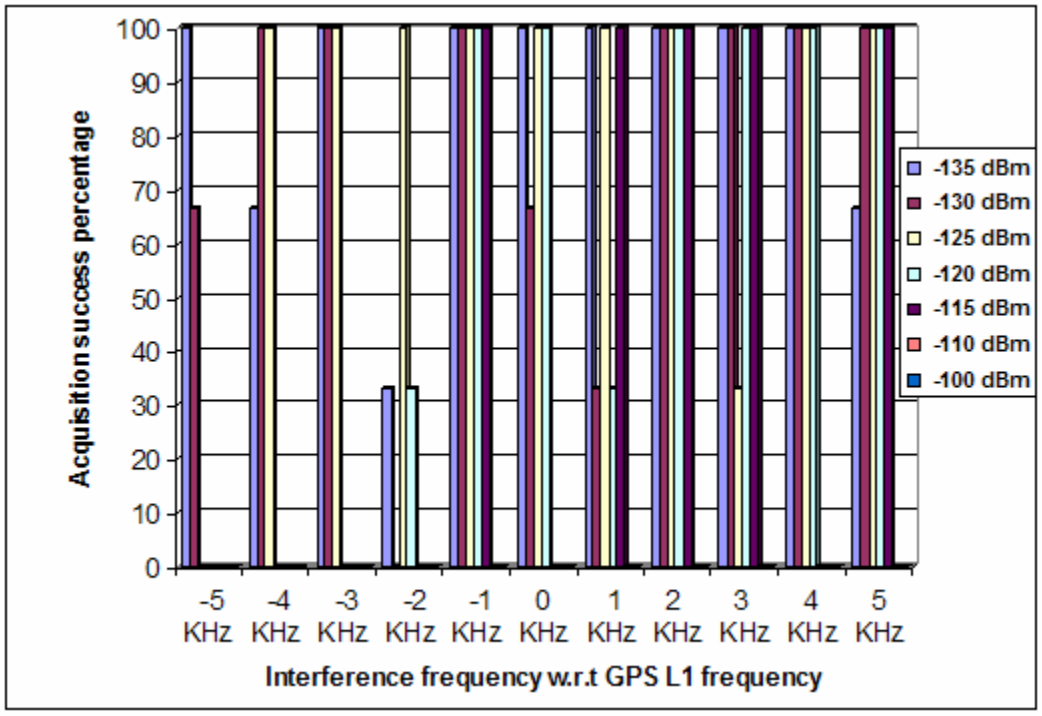

Figure 6.5: Acquisition success percentage for different interference frequencies for a 10 ms coherent integration time and a non-coherent factor of 1

A coherent integration time of 20 ms gives a correct acquisition peak for +15 dB relative interference power. A shorter coherent integration time gives a lower acquisition success percentage. This indicates that the incorrect correlation peak is higher than the signal peak for most of the time which will lead to false acquisition. The acquisition success percentage increases with an increase in the non-coherent integration factor. The acquisition process is jammed for a +20 dB relative interference power. The CWI analysis indicates that the GPS signal can be successfully jammed with 15-20 dB more interference power than the GPS signal power. The spectrum gets distorted causing the cross-correlation peaks to be higher than the signal peak which increases the possibility of false detection.

6.5.1.4 Acquisition Plots

The acquisition plots for an L1 + 3 KHz interference frequency and a 40 ms predetection integration at different interference powers are shown in Figure 6.6. These plots give an indication of the CWI effects on acquisition. The correlation of local C/A-code signal and RFI signal during correlation de-spreads the RFI signal over the C/A-code bandwidth and causes a sinc effect on the cross correlation signals. This is the reason the cross-correlation values for a particular Doppler frequency increase compared to other frequencies. This effect for CWI signals is similar for other narrow modulated signals analyzed in this research. The increase in cross-correlation peaks with an increase in the interference power masks the correct peak and causes acquisition failure.

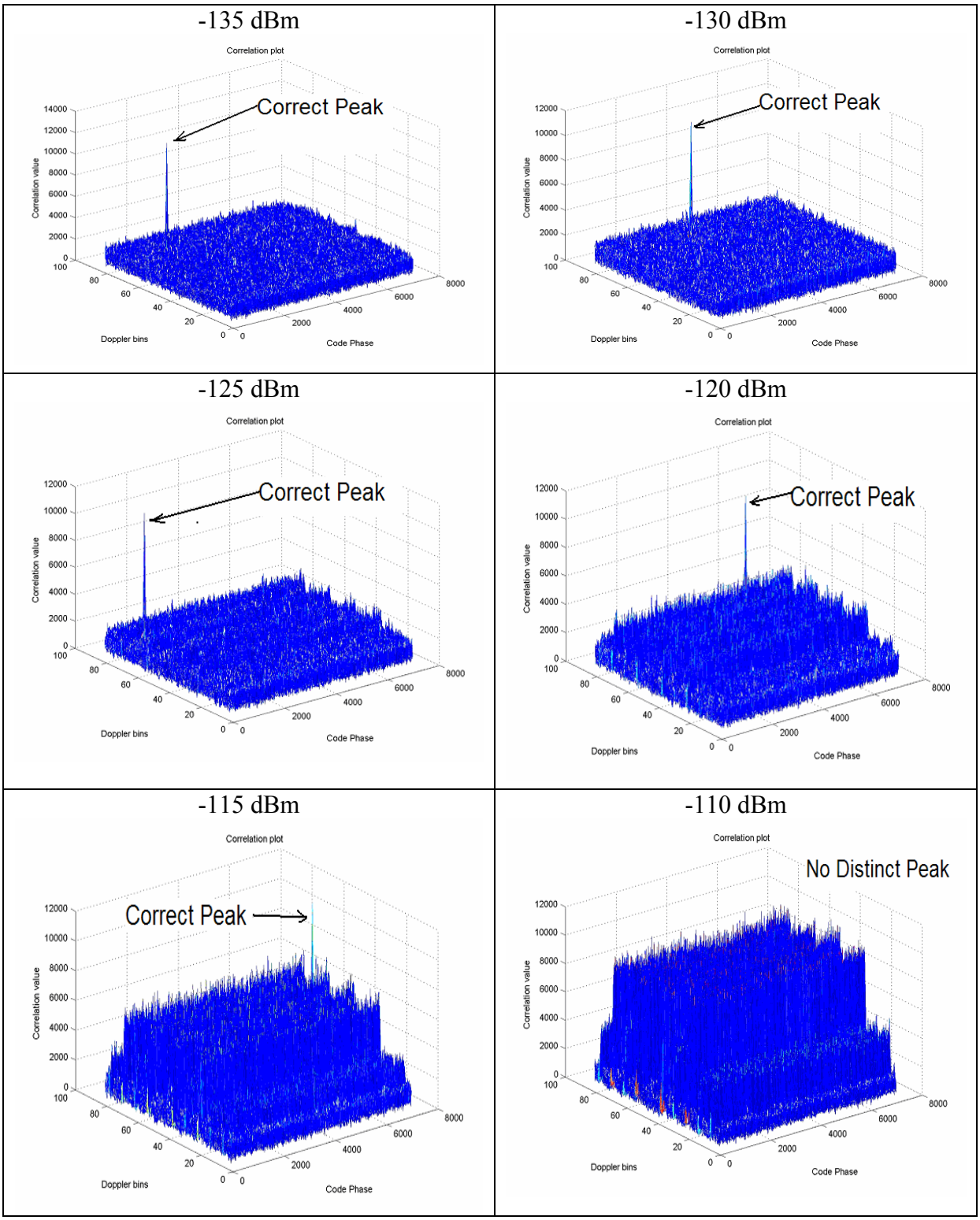

Figure 6.6: Correlation plots for the CWI at different interference power levels

6.6 Swept CW Interference

A Swept CW signal is a sinusoidal signal whose frequency is continuously varied (not in steps) over the desired range. The Agilent signal generator generates the swept signal in a different manner as explained in Section 6.2. It generates the signal as a collection of CW signals over the desired frequency range. Table 6.3 gives the different scenarios tested for swept CWI.

Table 6.3: Swept CW interference configuration

Parameter	Value
User position	Latitude: 51°4.45' N Longitude: 114°8.06' W Altitude: 1118 m
Time	05 Nov, 2003 01:00:00 GMT
PRN	21
GPS signal frequency	L1 frequency
Doppler	N/A
Signal Power used	-130 dBm
Swept frequency range	0.02, 0.1 and 1 MHz centred at L1
Number of points	10, 20 and 50
Dwell times	1 and 2 ms
Interference power	-130 to -100 in steps of 5 dB

Swept CWI can be more damaging than the pure tone CWI because it can cover multiple Doppler frequencies and affect more than one receiver channel at the same time. The swept CW power has to be higher compared to the pure tone frequency to have the same effect. The signal frequency varies continuously this requires more time and power to jam

the acquisition process compared to the pure tone CW signal. RF filters can be used to limit the sweep range but cannot isolate the interference signals. Swept interference effects depend upon the sweep range and the dwell time at each sweep frequency.

6.6.1 Results

Swept CWI results are discussed for different interference conditions under an adaptive predetection integration effect.

6.6.1.1 Noise Power Analysis

The noise power obtained for the clean (reference) signal is compared against the noise power obtained for an interference power of -130 dBm. It determines the additional noise introduced in the acquisition process at the GPS signal power. The noise power ratios for different coherent integration times at different swept frequency ranges with different numbers of points and dwell times are given in Tables 6.4 and 6.5.

Table 6.4: Noise power ratio for different coherent integration times for different swept frequencies at interference power of -130 dBm

Swept frequency range	**Noise power ratio with clean signal as reference**						
	Number of points = 10, dwell time = 1ms						
	1 ms	4 ms	5 ms	8 ms	10 ms	15 ms	20 ms
20 KHz	0.99	1.03	1.05	1.09	1.10	1.17	1.15
100 KHz	0.99	1.03	1.05	1.07	1.08	1.13	1.11
1 MHz	0.99	1.03	1.05	1.07	1.09	1.14	1.12

Table 6.5: Noise power ratio for different coherent integration times for different swept frequencies at interference power of -130 dBm

Swept frequency range	Noise power ratio with clean signal as reference						
	Number of points = 50, dwell time = 1ms						
	1 ms	4 ms	5 ms	8 ms	10 ms	15 ms	20 ms
20 KHz	0.99	1.01	1.03	1.05	1.05	1.11	1.08
100 KHz	0.99	1.00	1.01	1.02	1.04	1.07	1.03
1 MHz	1.00	1.02	1.03	1.05	1.06	1.11	1.08

A longer coherent integration time accumulates more interference signal and thus increases the noise power. The noise power increases by 4-5% with an increase in the coherent integration time from 1 to 20 ms. A 12-15% increase in the noise power is observed for different sweep ranges with 10 points and dwell time of 1 ms. Thus even an interference power of -130 dBm introduces a considerable amount of noise. The noise power obtained for an interference power of -130 dBm is considered as the reference for further analysis. The increase in the noise power depends upon the frequencies present in the signal considered during the predetection interval.

The noise power ratios for different dwell times and numbers of points for a swept frequency range of 100 KHz and a 10 ms coherent integration time are shown in Figure 6.7. The noise power increases with an increase in the interference power which is due to the high power induced by the interference signal. The increase in the noise power is nearly the same for 20 and 50 points with different dwell times. The noise power increase is more for the 20 KHz range compared to the 100 KHz range. It increases by 67-120% for 10 ms coherent integration for the 20 KHz range as compared to 61-80% for the

100 KHz range with a 30 dB increase in the interference power. A similar trend is observed for a 20 ms coherent integration. This is because a smaller sweep range will have more signals in the predetection bandwidth of the acquisition process. Thus more interference is present during correlation which increases the noise power. The noise power nearly doubles for 10 ms coherent integration with a 30 dB increase in the interference power which makes signal detection nearly impossible. A dwell time of 2 ms has a 10% additional noise compared to the dwell time of 1 ms.

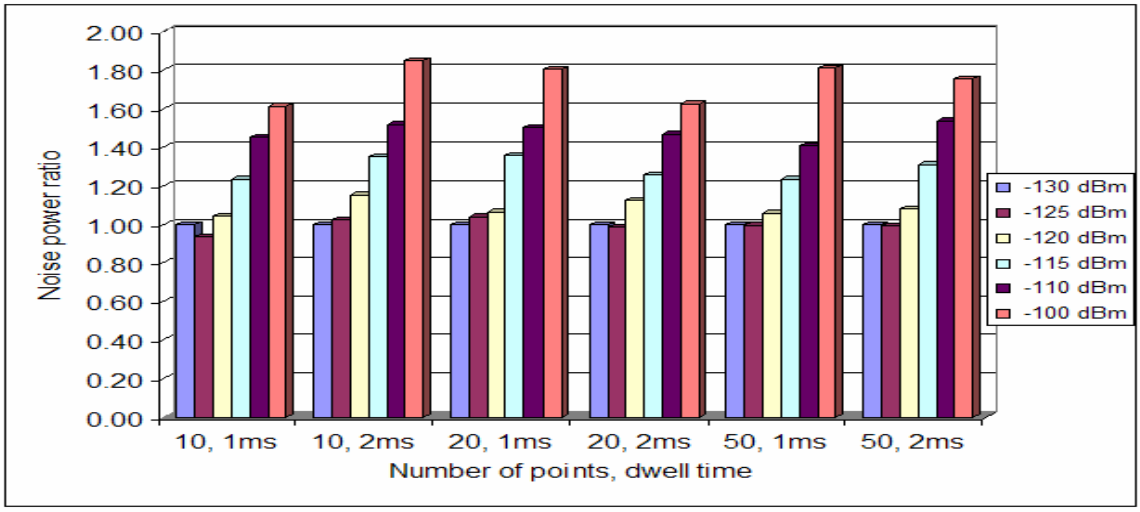

Figure 6.7: Noise power ratios for swept frequency range of 100 KHz for 10 ms coherent integration time and non-coherent integration factor of 1

The coherent integration time should be longer to integrate more GPS signal and allow the noise to average out. However, with the interference signal present, a longer coherent integration time allows more interference frequencies to be included in the correlation data. This causes an increase in the noise power which distorts the signal spectrum. Noise power increases by a negligible amount for a 10 dB increase in the interference power for all coherent integration times. It increases for higher dwell time which is because the swept signal appears as a pure tone signal for a larger dwell time. The noise power

increases by the same amount for different numbers of points. For a 30 dB increase in the interference power, the noise power increases by 40% and 100% for 1 ms and 20 ms coherent integration times, respectively. Longer coherent integration increases the signal power and hence there is a greater possibility of the signal peak being higher than the noise power even with a 100% increase in the noise power.

The non-coherent integration was varied from 1 to 5 to determine its effect on the noise power. It increases by 400% for a non-coherent integration factor of five at an interference power of -130 dBm. The increase in the noise power follows the same pattern for different dwell times but increases at a higher rate for higher dwell times. The noise power increases by a factor of 7-8 for a non-coherent integration factor of five and a 30 dB increase in the interference power. This is an enormous increase and requires the signal power to increase by a large amount to exceed the noise power. The noise power increases by 2-3% for an increase in the number of points from 10 to 50.

The noise power increases similarly for different swept frequency ranges at different dwell times and different non-coherent integration factors. It increases most for the 20 KHz range while for the 100 KHz and 1 MHz cases, the increase in noise power is nearly the same. A 750-800% increase in the noise power is observed for predetection integration of 100 ms and a 30 dB increase in the interference power. This makes GPS signal acquisition nearly impossible.

6.6.1.2 SNR Analysis

The GPS acquisition algorithm uses the correlation properties of the GPS PRN codes to determine the signal peak. The clean or reference signal was used to determine the signal peak for the interference results which were compared against the detection threshold. The SNR analysis for different numbers of points and dwell times for the 1 MHz frequency range with a 10 ms coherent integration period is shown in Figure 6.8.

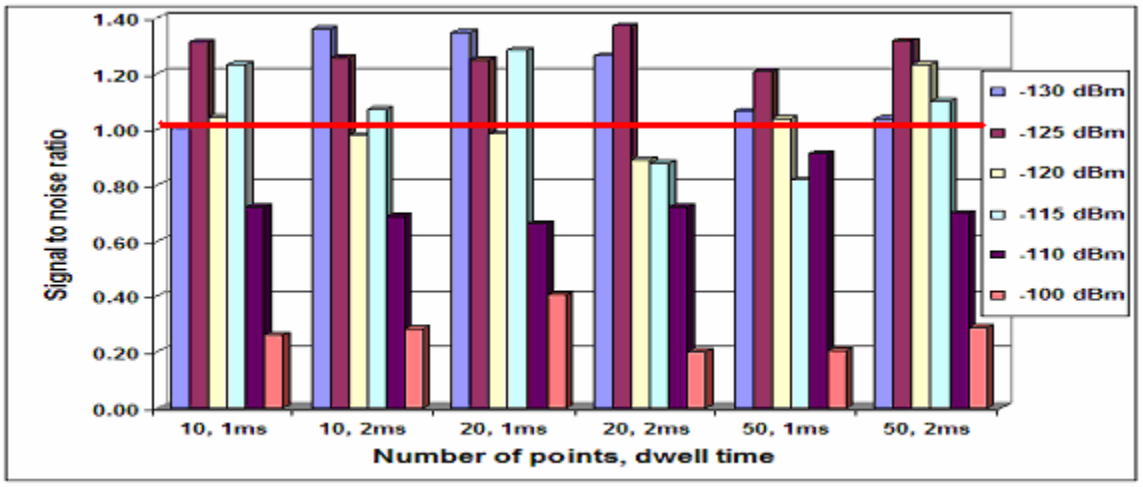

Figure 6.8: SNRs for swept frequency range of 1 MHz for 10 ms coherent integration time and non-coherent integration factor of 1

The acquisition process is able to tolerate a 10-15 dB increase in interference signal power as shown in the Figure 6.8. The SNR reduces with an increase in the number of points and the dwell time. This is due to the presence of more spurious frequency components in the signal considered for the correlation. The SNR is found to decrease for a smaller frequency range. A larger frequency range will result in some of the frequency components being outside the predetection bandwidth. Thus there are less interference effects resulting in a high SNR. A coherent integration time of 10 ms is sufficient to

tolerate 10 dB of relative interference signal for a 20 KHz range and 15 dB of relative interference signal for ranges above 100 KHz.

The SNR increases with an increase in the coherent integration time and is able to tolerate more interference signals. The maximum unaided coherent integration period can tolerate 15 dB relative interference power. This reduces with an increase in the number of points and dwell time. However, with an increase in the frequency range, the tolerance is improved by about 5 dB. Non-coherent integration is used to extend the integration time beyond the navigation data bit duration. The interference tolerance is increased at a higher non-coherent integration factor. Coherent integration of 5 ms is insufficient to acquire the signal for +10 dB relative interference power. Coherent integration of 10 ms and 20 ms extend the relative interference tolerance to 10 and 15 dB, respectively. The results are the same for different numbers of points in the swept frequency range. The SNR decreases considerably beyond a 20 dB relative interference power and the signal peaks get buried in the noise. The results obtained for 100 KHz and 1 MHz swept frequency ranges are similar to those for the 20 KHz range.

6.6.1.3 Acquisition Success Percentage

Section 6.6.1.2 showed an analysis of the SNR for different swept frequency ranges and predetection integration times. A relative interference power of +20 dB is sufficient to reduce the SNR below one. The peak obtained by the acquisition process is analyzed to determine whether it is at the correct Doppler. The acquisition success percentages for the

swept frequency range of 1 MHz at different numbers of points and dwell times with a coherent integration time of 10 ms are shown in Figure 6.9.

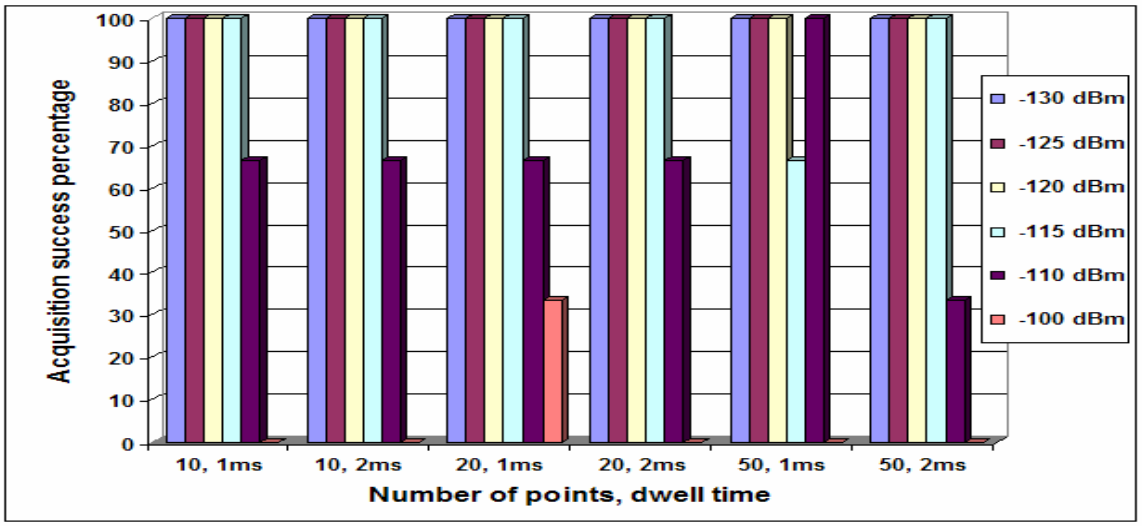

Figure 6.9: Acquisition success percentage for swept frequency range of 1 MHz for 10 ms coherent integration time and non-coherent integration factor of 1

A 100% success is obtained for 15 dB (-115 dBm) relative interference power which drops to about 70% for 20 dB (-110 dBm) relative interference power. For sweep ranges below 100 KHz, the success percentage drops to 70% for 15 dB relative interference power. This is because the higher sweep range will have some signals outside the predetection bandwidth which reduces the interference in the correlated signal. Thus, a smaller frequency range is more damaging and will cause the GPS receiver to jam at a low power. The acquisition success percentage is found to decrease with an increase in the number of frequency points in the sweep range. The interference tolerance decreases by 5-10 dB when the number of frequency points is varied from 10 to 50. The dwell time of each frequency point also has an effect on the GPS signal spectrum. A longer dwell time causes the swept interference to behave like a pure tone CWI and jams the receiver at lower signal strengths.

The acquisition success percentage increases with an increase in the coherent integration time. A coherent integration time of 1 ms is not sufficient enough to obtain correct results. A coherent integration time of 5 ms can tolerate about 10 dB relative interference while a 15 ms coherent integration time can tolerate 15 dB relative interference power for a 20 KHz sweep range. A coherent integration time above 15 ms can tolerate up to 20 dB relative interference power for sweep frequency ranges above 100 KHz. The correct peak is obtained 30% of the time for 10 dwell points with +30 dB relative interference power and a 100 ms predetection integration time. However with an increase in the number of points from 10 to 20 or 50, the correct peak cannot be obtained for +30 dB relative interference power. Thus the success percentage decreases with an increase in the number of points and a lower sweep range. This is because a higher number of points ensures more spurious interference signals are present during the correlation which distorts the GPS signal spectrum.

6.6.1.4 Acquisition Plots

The correlation plots for a swept frequency range of 100 KHz with 10 points and a dwell time of 1 ms at different interference powers are shown in Figure 6.10. The correlation plots indicate that the cross-correlation peaks at higher interference powers bury the signal peak into the noise which prevents acquisition.

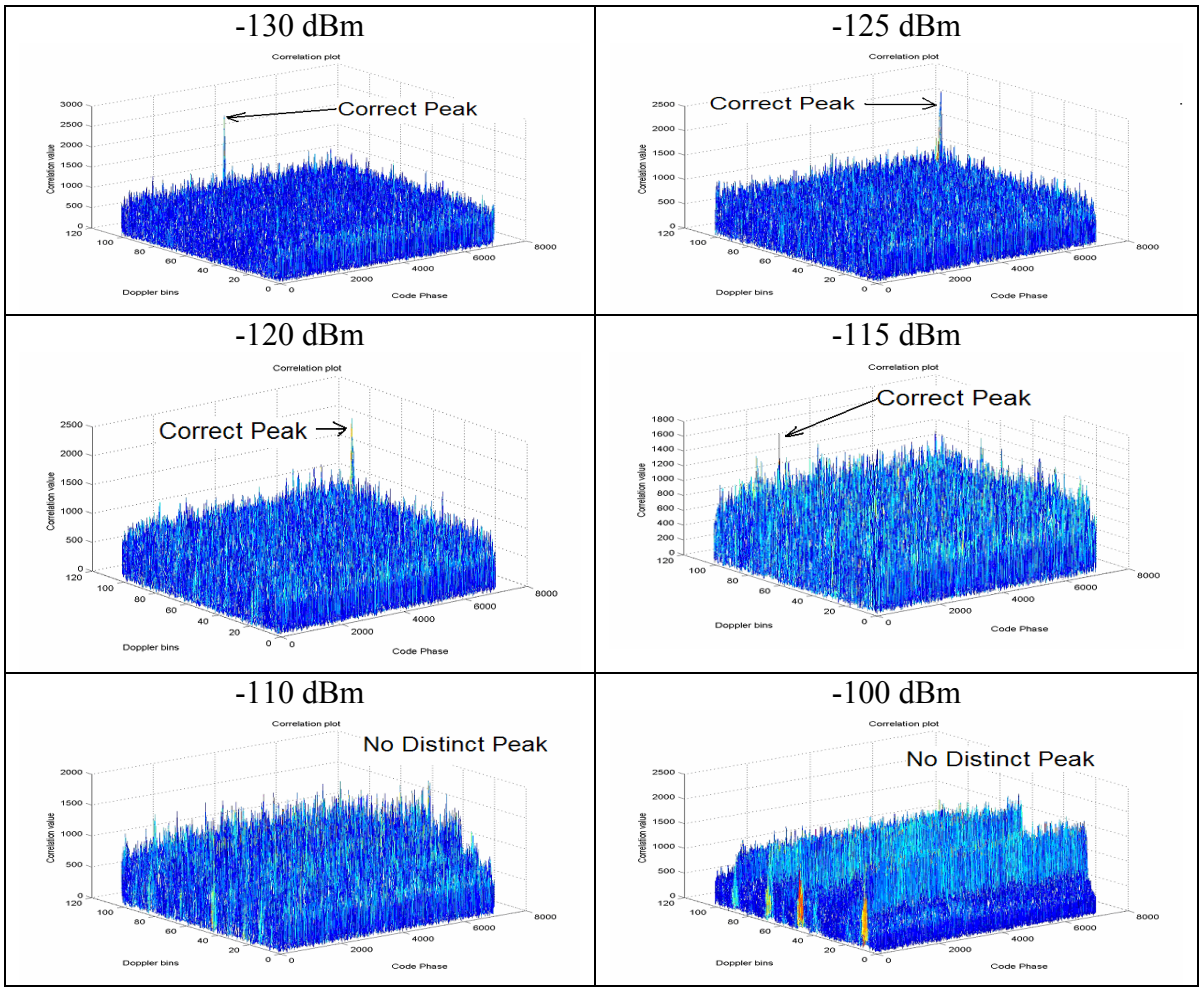

Figure 6.10: Correlation plots of Swept CWI for different interference power levels

6.7 Broadband Noise

Broadband interference is a wideband Gaussian interference signal that is usually generated by an intentional noise jammer [Spilker and Parkinson, 1996]. A broadband interference signal is similar to GPS correlation noise and was generated using the noise function of the Agilent signal generator. It adds to the GPS correlation noise to increase the noise in its bandwidth and the effect on the GPS C/A-code spectrum is shown in Figure 6.11. The resulting spectrum is similar to the C/A-code spectrum but with more

noise present. Noise bandwidth determines the amount of noise introduced in the GPS signal. A broadband signal is very difficult to detect and isolate using filters or to nullify using the antenna [Spilker and Parkinson, 1996].

Table 6.6 lists the broadband noise scenarios tested during the analysis. The total noise power introduced by broadband noise is determined by its bandwidth and interference power. For example, a broadband noise of 50 KHz bandwidth and an interference power of -130 dBm introduces a total power of 50 KHz * -130 dBm.

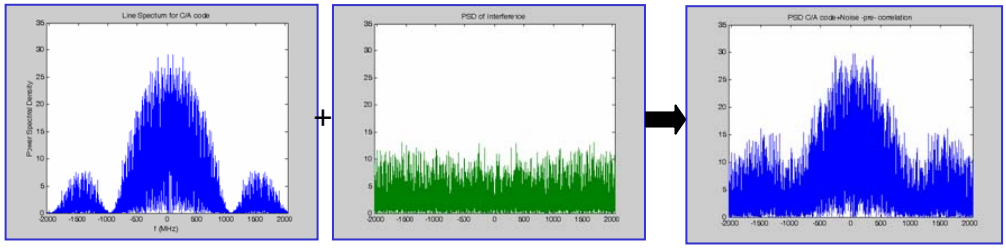

CA Code spectrum **Broadband noise** **Resulting spectrum**

Figure 6.11: Broadband noise effect on GPS C/A code spectrum

Table 6.6: Broadband noise interference configuration

Parameter	Value
User position	Latitude: 51°4.45' N Longitude: 114°8.06' W Altitude: 1118 m
Time	05 Nov, 2003 01:00:00 GMT
PRN	21
GPS signal frequency	L1 frequency
Doppler	N/A
Signal Power used	-130 dBm
Noise bandwidth	0.05, 0.1, 0.5, 1, 2 MHz
Interference power	-130, -125,-120,-110, -90 and -70 dBm

6.7.1 Results

Broadband noise interference is analyzed for different noise bandwidths using adaptive predetection integration.

6.7.1.1 Noise Power Analysis

Noise power is analyzed for different bandwidths and predetection integration periods for different interference powers. Figure 6.12 shows the noise power ratios for different bandwidths for a 10 ms coherent integration time. The noise power at an interference power of -130 dBm was taken as a reference. It increases by 17% with an increase in the interference power level by 60 dB. The Gaussian nature of broadband noise causes a lower increase in noise power compared to CWI.

Different coherent integration times were tested to determine their effect on the noise power at different interference bandwidths. The noise power obtained for each coherent integration time at an interference power of -130 dBm was taken as a reference. It increases by 35% for a 1 ms, and 3% for 20 ms, coherent integration time for a 100 KHz bandwidth with a 60 dB increase in the interference power. The increase in the coherent integration period causes the noise to average which reduces the noise power for higher coherent integration times.

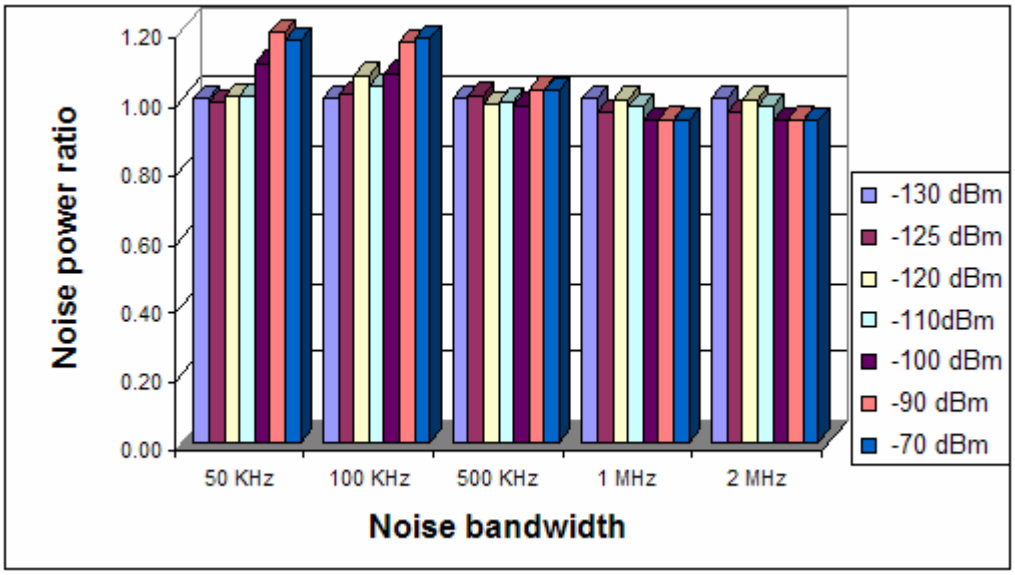

Figure 6.12: Noise power ratios for different noise bandwidths at a 10 ms coherent integration time

Non-coherent integration sums the signal across coherent integration periods. The summing of the signal causes the noise to add up and increase the noise level. A non-coherent integration factor of five increases the noise power level by 400% for 60 dB relative interference power.

6.7.1.2 SNR Analysis

The signal peak obtained at the correct Doppler for different interference conditions was determined and compared against the noise power level to analyze the SNR under different conditions. The SNRs for different interference bandwidths at a coherent integration time of 10 ms are shown in Figure 6.13.

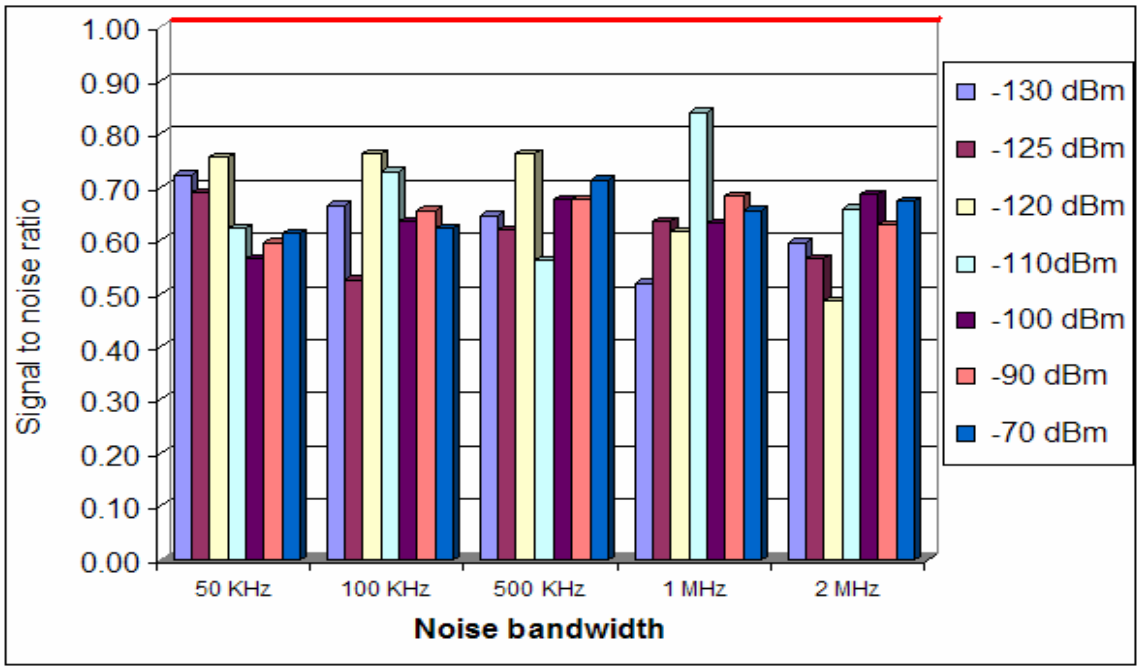

Figure 6.13: SNRs for different noise bandwidths at a 10 ms coherent integration time

The SNR decreases with an increase in interference power level because of the increase in the noise power level with the signal level remaining the same. A longer coherent integration period accumulates more signal and allows the noise to average out thereby increasing the SNR. The false detection probability can be increased to reduce the detection threshold which increases the SNR but also allows for false acquisition.

The SNR increases with an increase in the coherent integration time. It is close to one for an integration time above 8 ms at an interference power level of -130 dBm. The signal peak gets buried in the noise for a higher interference power level. The results obtained for a 2 MHz bandwidth are similar to the results for a 100 KHz bandwidth. Thus, for an increase in the interference power by 10-15 dB, the signal peak falls below the noise power level which prevents signal acquisition. Different coherent integration times

provide similar results for different interference bandwidths. A higher bandwidth introduces more noise in the acquisition process which reduces the SNR. Thus, the higher the bandwidth the lesser the interference power required to jam the signal. The results indicate that the SNR increases with an increase in the non-coherent integration factor. However, non-coherent integration does not boost the SNR above one.

6.7.1.3 Acquisition Success Percentage

The previous section analyzed the SNR, wherein the signal value obtained at the correct Doppler was considered. However, with interference signal there is a possibility of the correlation peak being greater than the peak at the correct Doppler. This section analyses whether the correlation peak obtained is the correct one. The success percentage indicates the influence of the interference signals on signal distortion in the GPS spectrum. The acquisition success percentages for different interference bandwidth are shown in Figure 6.14.

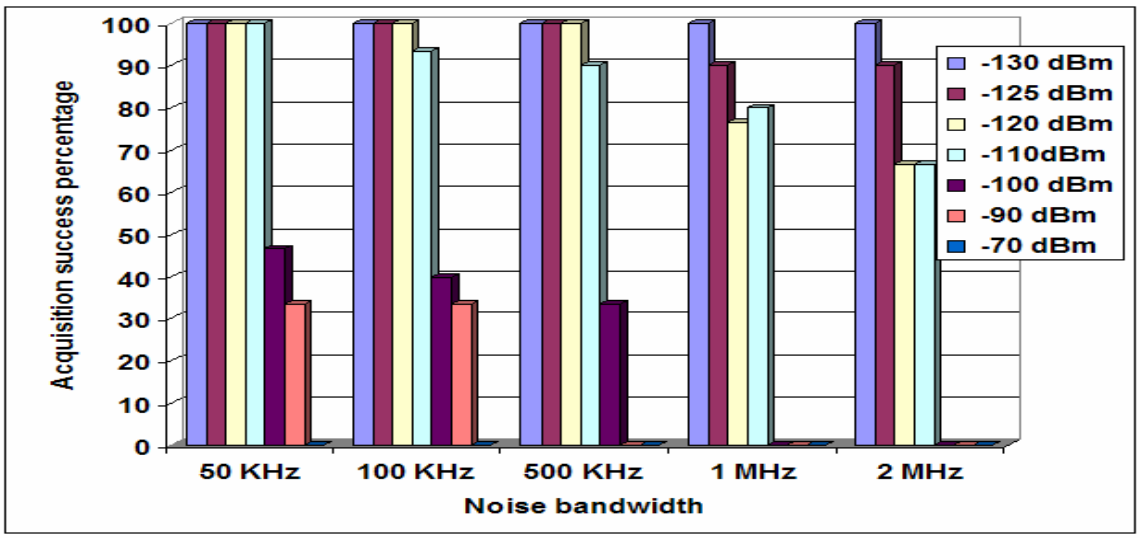

Figure 6.14: Acquisition success percentage for different noise bandwidths for 8 ms coherent integration time

The results indicate that the success percentage decreases as the bandwidth becomes higher. This is due to the high noise introduced in the acquisition process by wider bandwidths. Longer coherent integration can tolerate more interference power. An interference power of +30 dB higher than the GPS signal power reduces the acquisition success percentage to zero.

6.7.1.4 Acquisition Plots

The correlation plots for predetection integration times of 50 ms for a 2 MHz interference bandwidth at different interference power levels are shown in Figure 6.15. These plots indicate the increase in the cross-correlation peaks with an increase in the interference power. A cross-correlation peak increases the noise power and buries the signal peak.

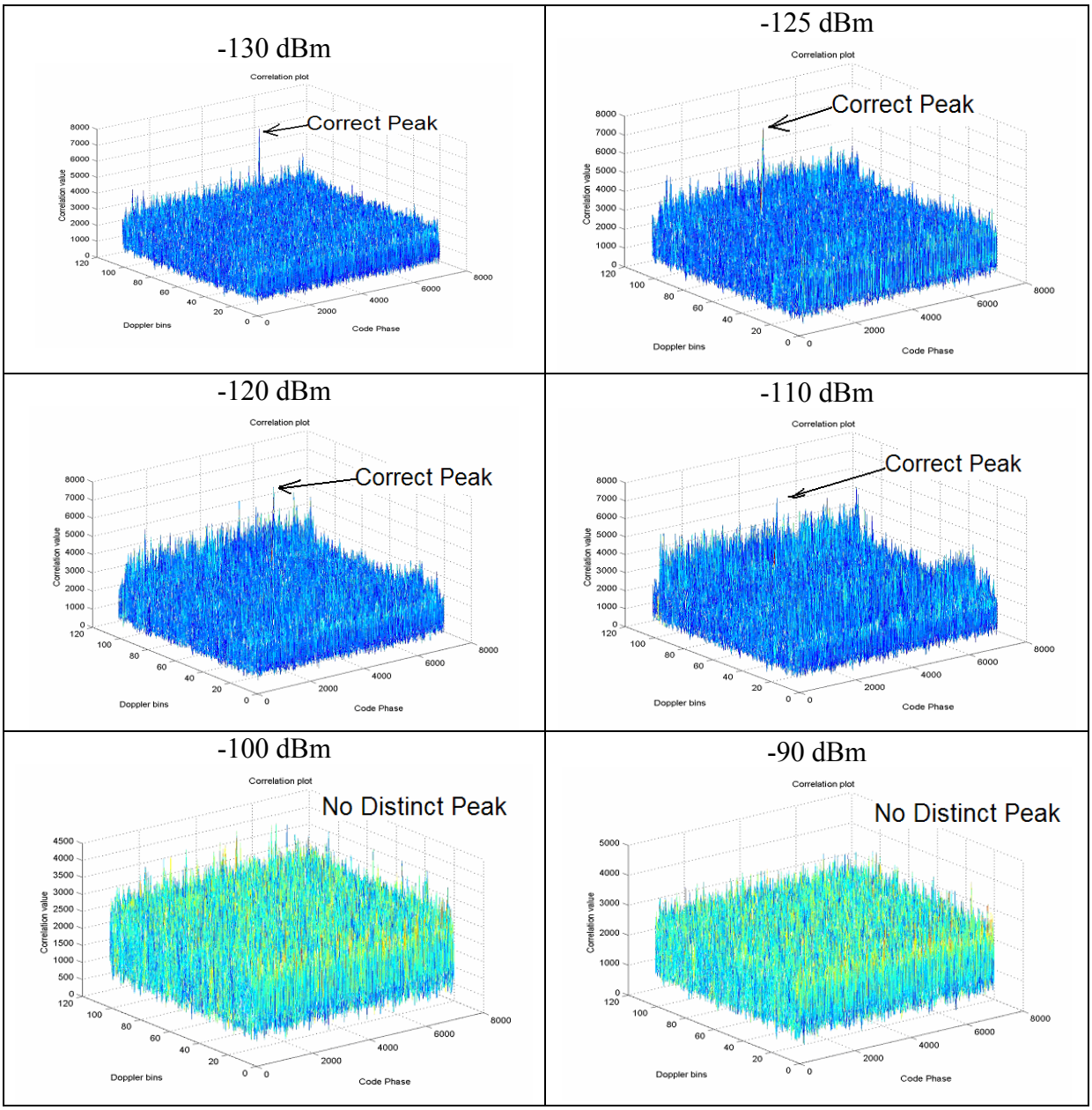

Figure 6.15: Correlation plots for broadband noise at different power levels

6.8 Pulsed Interference

Pulse interference was analyzed for different pulse durations and duty cycles at various power levels. Pulse signals can cause problems to the hardware components in the GPS

receiver when it exceeds their power specifications and hence it was tested in the low power range to prevent any damage to the Signal Tap. The Signal Tap RF front-end has a power specification of +10 dBm [Shashidhar, 2003]; hence the interference power was limited to -40 dBm before the LNA. A GPS receiver should use an RF power limiter to protect the hardware components from the pulse interference. A pulse signal above -60 dBm can cause problems to some hardware components of a GPS receiver. High power pulse interference is expected to cause saturation of the ADC and correlator loops. The Agilent signal generator is capable of generating pulse signals with duration of 1 μs to 1 ms. Different pulse interference data sets collected are given in Table 6.7.

Table 6.7: Pulsed interference scenarios

Parameter	Value
User position	Latitude: 51°4.45' N Longitude: 114°8.06' W Altitude: 1118 m
Time	30 Nov, 2003 04:00:00 GMT
Visible PRNs	21
GPS signal frequency	L1 frequency
Doppler	N/A
Signal Power used	-130 dBm
Pulse duration	125, 250, 500 and 1000 μs
Pulse duty cycle	10%, 25% ,50% and 90%
Pulse power level	-130, -100, -70 and -40 dBm

6.8.1 Results

Pulse interference is analyzed for different pulse durations and duty cycles for adaptive predetection integration.

6.8.1.1 Noise Power Analysis

The noise power variation gives an indication about the nature of the noise introduced. The effect of pulse interference on the noise power for a pulse duration of 125 μs is shown in Figure 6.16.

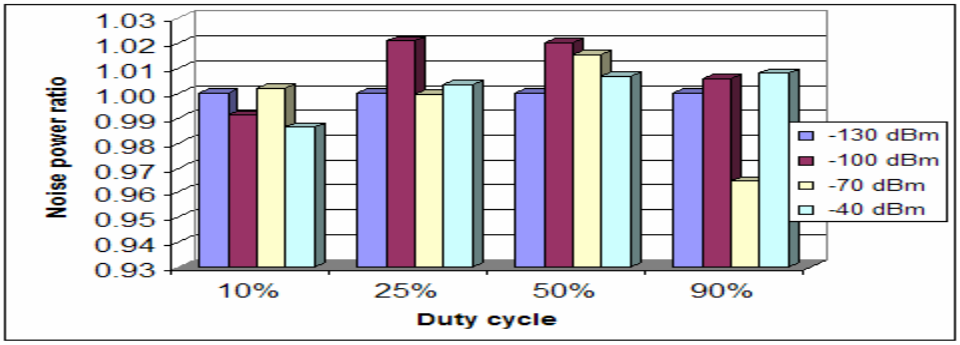

Figure 6.16: Noise power ratios for different duty cycle for 125 μs pulse duration at coherent integration of 10 ms with non-coherent integration factor of 1

The noise power variation is minimal for different pulse durations and the duty cycles. A low power pulse signal has negligible effect on the noise in the acquisition process. The noise power for duty cycle of 90% at -70 dBm power level shows about 3-4% less increase in noise compared to reference signal. This is because of Gaussian nature of noise. Thus the pulse duration, duty cycle or the interference power level does not affect the noise power in acquisition. This is because the local C/A-code signal spreads the pulse signal during correlation which decreases its power significantly and hence does not contribute to the noise power. Noise power variation is negligible for low power pulse interference at different durations and duty cycles. However, the low power pulse signals can still affect the hardware components of the GPS receiver.

6.8.1.2 SNR Analysis

The SNR was analyzed to determine the pulse interference effect on the signal peak. The correlation peak obtained at the correct Doppler was considered in determining the SNR. The SNRs for different duty cycles at 125 μs pulse duration for a 10 ms coherent integration period are shown in Figure 6.17. The SNR is greater than one for all the pulse signals analyzed. The increase in the interference power has no effect on the SNR allowing the acquisition process to acquire the GPS signal at the correct peak. Thus the GPS signal is easily acquired in the presence of low power pulse interference irrespective of the pulse duration and duty cycle.

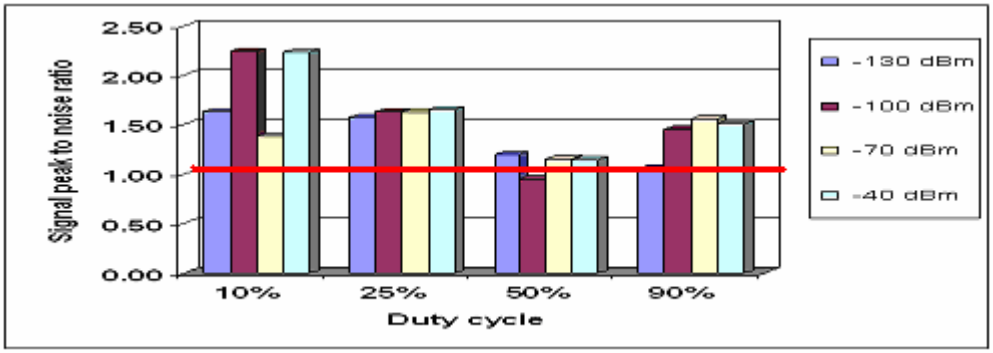

Figure 6.17: SNRs for different duty cycle for 125 μs pulse duration at coherent integration of 10 ms with non-coherent integration factor of 1

6.8.1.3 Acquisition Success Percentage

Section 6.8.1.2 analyzed the effect of the pulsed interference on the SNR. In this section, the percentage of times, the acquisition peak is obtained at the correct Doppler is analyzed. The acquisition peak is always at the correct peak irrespective of the duty cycle. Thus the duty cycle variation has no effect on the GPS acquisition process.

Coherent integration of 10 ms is sufficient to acquire the signal at the correct peak at all times irrespective of the pulse duration and the duty cycle. For a 1 ms coherent integration period, the acquisition success is close to 30% and hence a coherent integration time of 4 ms or higher is suggested. The acquisition success percentage decreases from 100% to 70% with an increase in the pulse duration (to 1 ms) for a 5 ms coherent integration period. Low power pulse interference does not affect the acquisition success for a coherent integration period above 8 ms.

6.8.1.4 Acquisition Plots

The correlation plots for the different pulse interference power levels for a pulse duration of 250 μs, and duty cycle of 50%, are shown in Figure 6.18. The noise power is nearly the same for different interference power levels which allows successful acquisition.

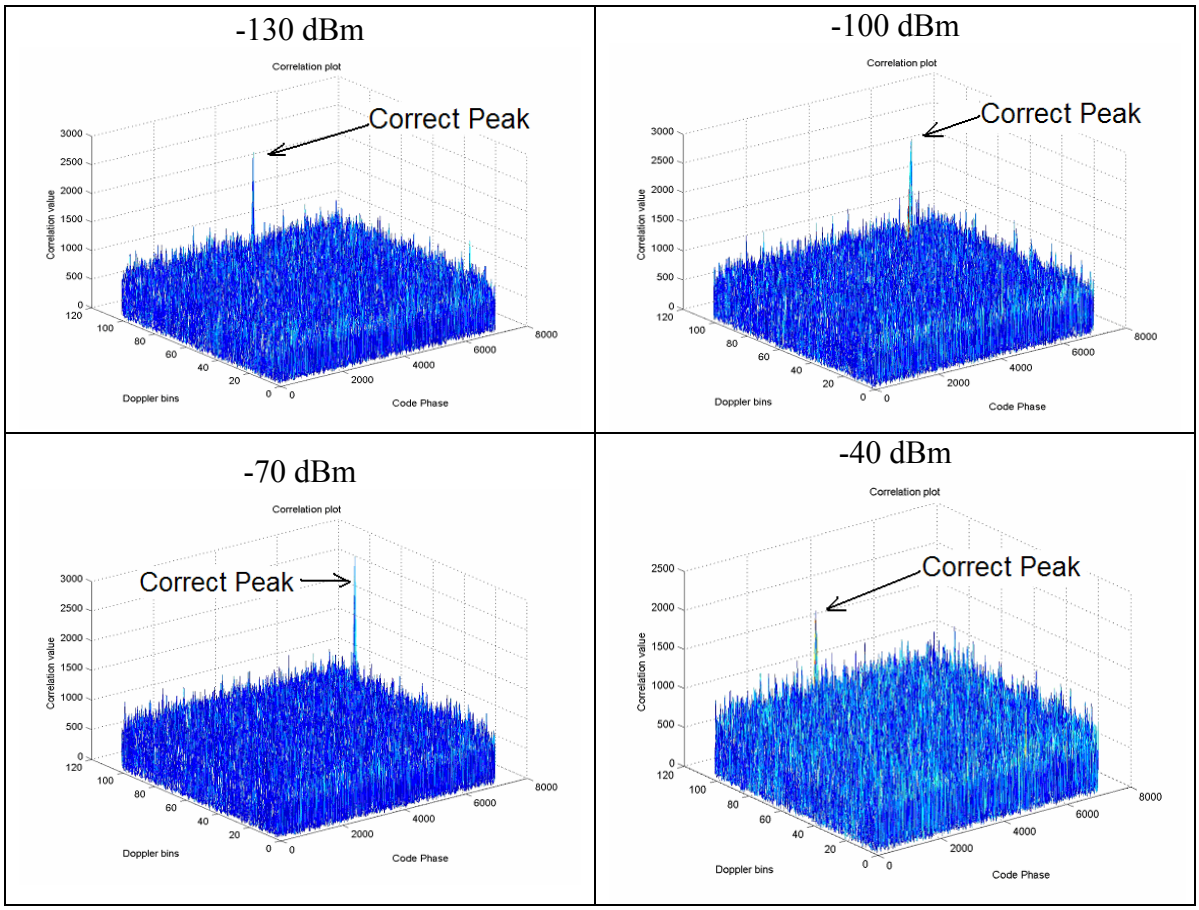

Figure 6.18: Correlation plots for different pulse interference powers

6.9 Amplitude Modulated Signals

Amplitude modulation implies the modulation of a coherent carrier wave by mixing it in a nonlinear device with the modulating signal to produce discrete upper and lower sidebands [Sastry, 1997]. These sidebands are the sum and difference frequencies of the carrier and modulating signal. The modulated wave envelope takes the form of the modulating signal. An instantaneous value of the modulated signal is the vector sum of the corresponding instantaneous value of the carrier wave and the modulating signal. The recovery of the modulating signal is by direct detection or by heterodyning [Agilent

Technologies, 2003]. This was the first and simplest type of modulation used for communicating signals from one point to another. AM consists of multiplying a relatively slowly varying signal by a relatively quickly varying periodic signal. The frequency response of the AM signal is equivalent to the frequency response of the slowly varying signal shifted by the frequency of the rapidly changing signal in the positive and negative directions [Sastry, 1997]. In AM, the carrier signal $A\cos(\omega * t)$ has its amplitude, A, modulated in proportion to the modulating signal $m(t)$ to give an AM signal $Am(t)\cos(\omega * t)$. The AM index is defined to be $\beta = \max m(t)$ and the AM signal appears as shown in Figure 6.19.

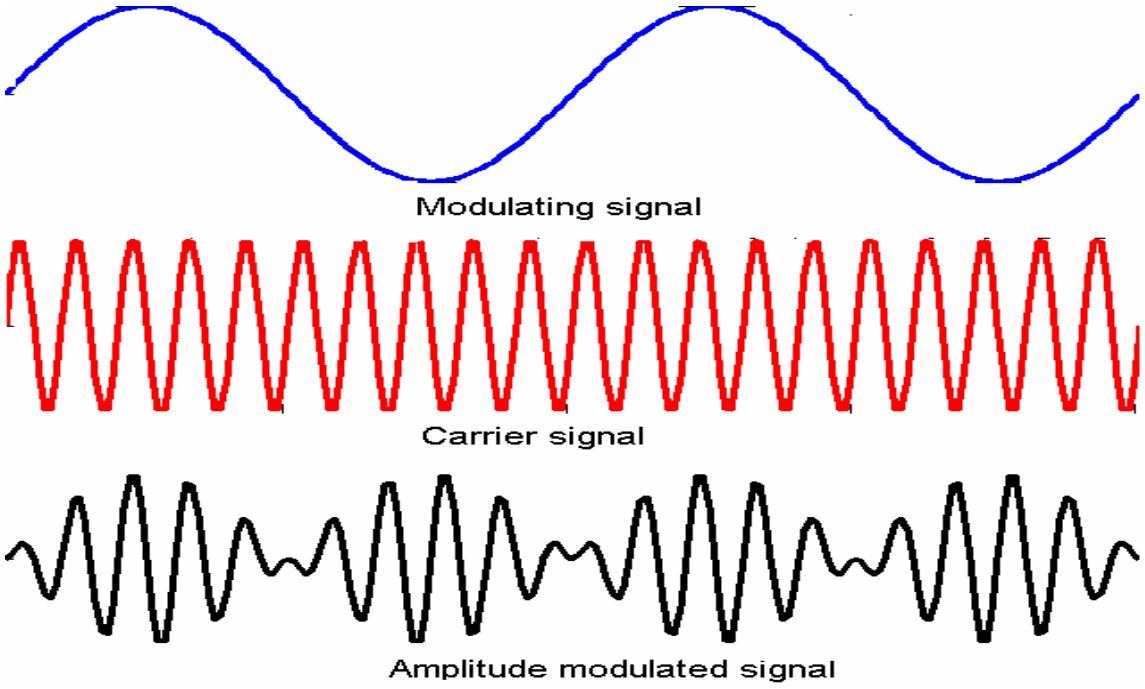

Figure 6.19: AM signal

High order harmonics emissions of the AM broadcast signals fall close to the GPS L1 frequency to cause interference. Analog TV broadcast maximum EIRP limits are higher

than the FM signals and the harmonic orders are lower (2 to 9 for RFI signals within 2 MHz of GPS L1) which will cause more interference [Erlandson and Frazier, 2002]. TV signals use a form of AM modulation for transmission. AM is also used widely for radio communication. AM signals were tested with the carrier frequency kept at the GPS L1 frequency and the modulating frequency was varied from 1 Hz to 50 KHz. The AM index was varied from 10% to 100% and this defines the amount of the modulating signal present in the AM signal. The AM carrier frequency was kept at the GPS L1 frequency which is difficult to isolate using an RF filter. The correlation process spreads the interference signal over the predetection integration bandwidth and decreases the power which reduces the effect of the interference signal. The various AM signals tested for interference are listed in Table 6.8.

Table 6.8: AM interference scenarios parameters

Parameter	Value
User position	Latitude: 51°4.45’ N Longitude: 114°8.06’ W Altitude: 1118 m
Time	30 Nov, 2003 04:00:00 GMT
Visible PRNs	21
GPS signal frequency	L1 frequency
Doppler	N/A
Signal Power used	-130 dBm
AM carrier frequency	L1
AM modulation frequency	0.001,0.01,0.1,1,10,25 and 50 KHz
AM modulation depth	10%, 25%, 50%, 75% and 100%
Interference power	-130, -125,-120,-110,-100 and -90 dBm

6.9.1 Results

AM signals were analyzed for different modulating frequencies, modulation depths, and interference powers. The results are discussed for different interference conditions under adaptive predetection integration.

6.9.1.1 Noise Power Analysis

This section determines the amount of noise introduced by an AM signal. The GPS signal strength was kept at -130 dBm and the noise power obtained at a -130 dBm interference power is considered as a reference. The noise power is computed over different modulating frequencies and modulation depths at different predetection integration periods. The noise power ratios for different modulation depths are shown in Figure 6.20. The noise power increases nearly doubles for a 40 dB increase in the interference power. It increases by 250% for a modulation frequency of 50 KHz at a 100% modulation depth, and a 40 dB increase in the interference power. The noise power increases for higher modulation depths due a larger amount of the modulating signal present at higher modulation depths which increases the interference. The noise power increases by 100% when the complete modulating signal is present. The noise power variation with modulation depth is similar for other modulating frequencies analyzed. The increase in noise power reduces acquisition probability. Noise power variation for different modulating frequencies at a modulation depth of 50% is represented in Figure 6.21.

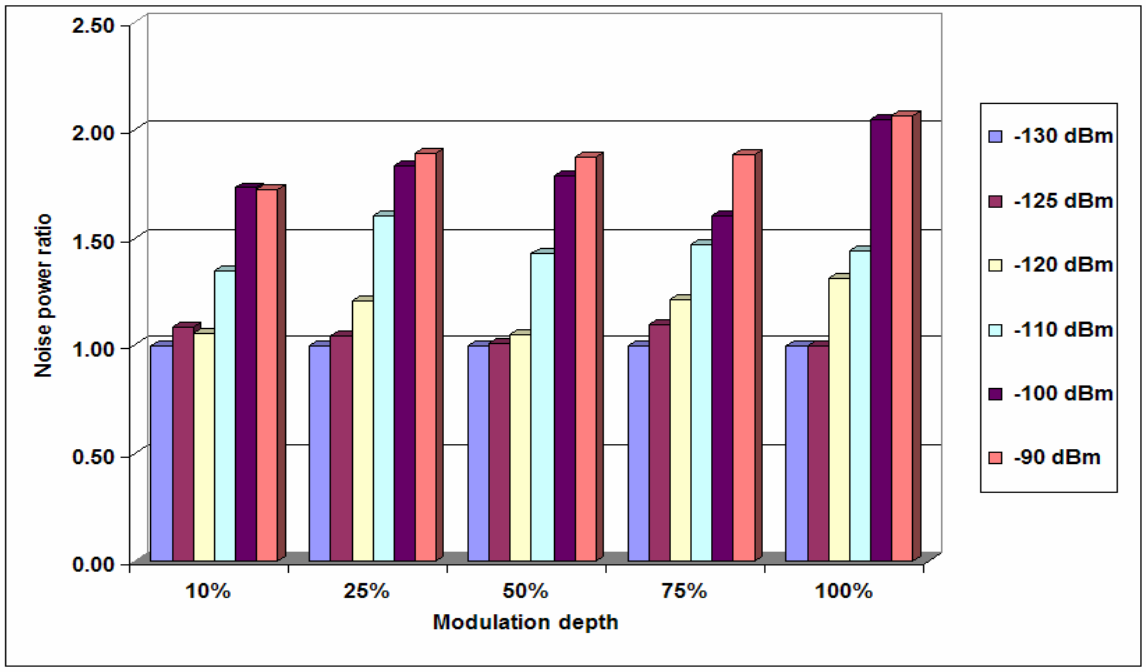

Figure 6.20: Noise power ratios for different modulation depths at frequency of 1 Hz

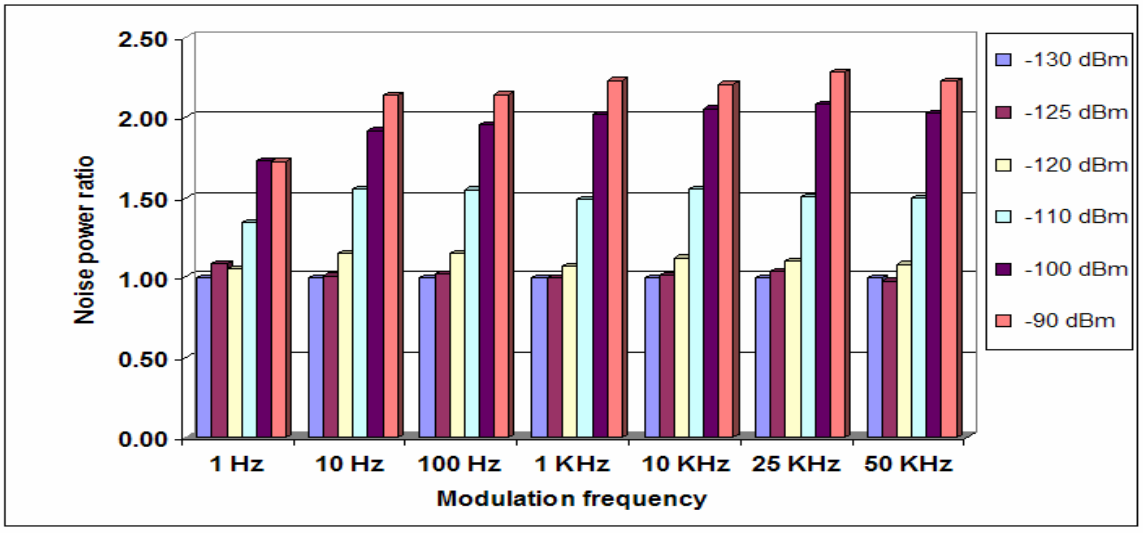

Figure 6.21: Noise power ratios for different modulation frequencies at 50% depth

The noise power increases by 10-15% for +10 dB relative interference power. It increases by 60% with a +20 dB relative interference power and above 100% when the interference power is increased by 40 dB. The noise power for a modulation frequency of 1 Hz and 40 dB relative interference power increases by 70 to 90% when the modulation depth is

varied from 10 to 100%. For the same specifications, the noise power for a modulation frequency of 50 KHz increases from 130 to 140%. Thus, higher modulation frequencies result in more noise. A smaller modulation frequency has a longer modulation period. Thus a lesser amount of the interference signal is present in the predetection integration period which decreases the rate of increase in the noise power.

The de-spread interference signal after correlation results in non-Gaussian noise. Thus the noise increases with an increase in the predetection integration period. The increase in the noise power is found to be consistent across different configurations of the interference signal. This is because a longer coherent integration period accumulates more interference signal. The noise power increases from 70 to 140% for an increase from 20 to 40 dB relative interference power for different modulation depths, modulating frequencies, and coherent integration times. The noise power obtained at a non-coherent integration factor of 1 and an interference power of -130 dBm was taken as the reference to study its variation with non-coherent integration. It increases with an increase in the non-coherent integration factor. This is because both the signal and noise are added during non-coherent integration. Thus the noise power adds up causing an increase in the noise power which increases for higher interference power. It increases by 700% for 40 dB relative interference power and a non-coherent integration factor of five. This enormous increase causes the signal to be buried in the noise and jams the receiver.

6.9.1.2 SNR Analysis

This section analyses the signal peak obtained at the correct Doppler against the noise power under different interference conditions. The SNRs at different modulation depths for a modulation frequency of 1 Hz are shown in Figure 6.22.

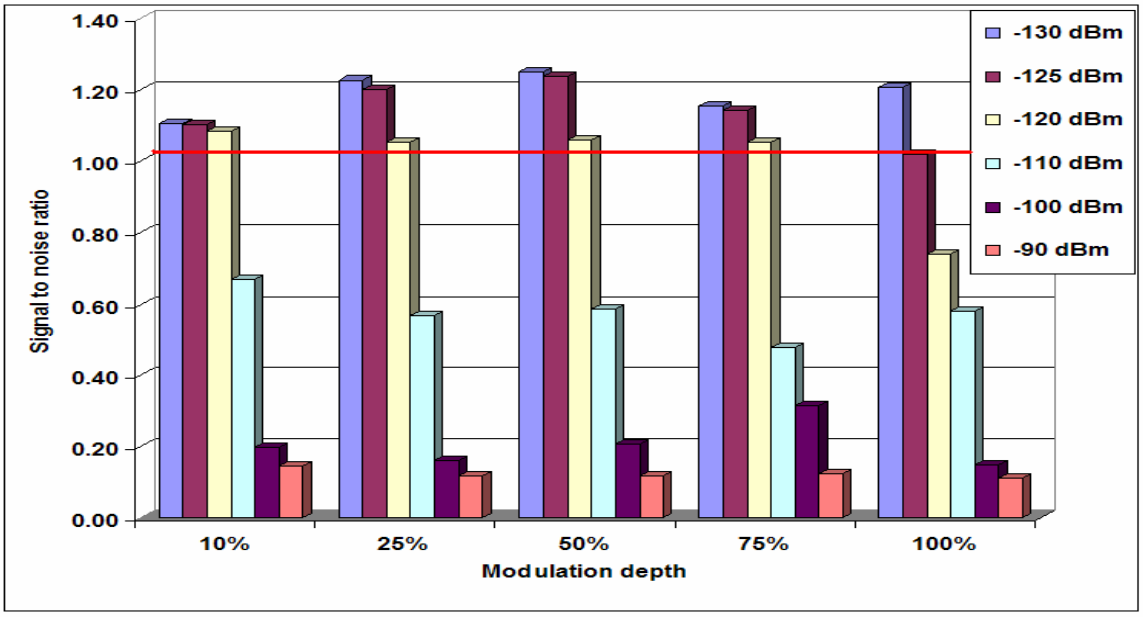

Figure 6.22: SNRs for different modulation depths at modulation frequency of 1 Hz

The SNR decreases with an increase in the modulation depth. This is because a higher modulation depth introduces more interference signal which decreases the SNR. The SNR decreases with an increase in the interference power at different modulation depths. The SNR falls below one for +10 dB relative interference power and reduces drastically with a +30-40 dB increase in the interference power. Its variation for different modulation depths at various interference frequencies is similar. The SNRs for different modulation frequencies at a modulation depth of 10% for a coherent integration time of 10 ms are shown in Figure 6.23.

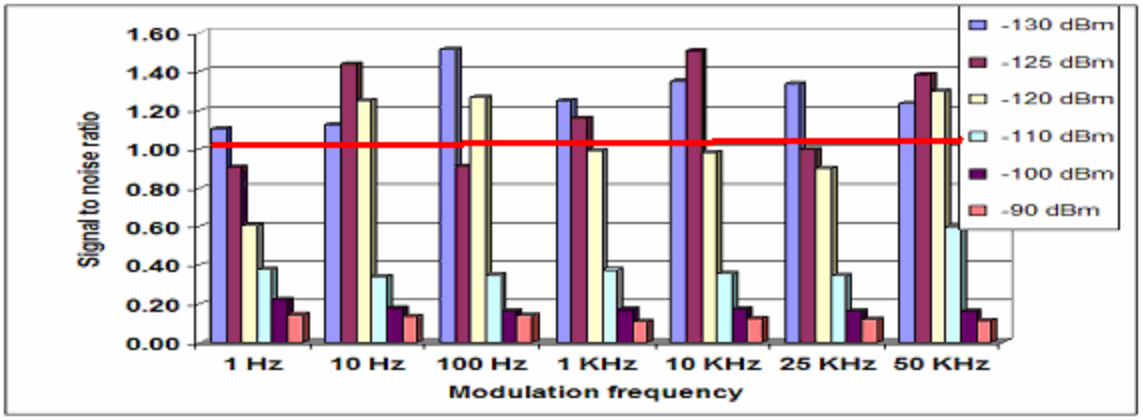

Figure 6.23: SNRs for different modulation frequencies for 10% modulation depth

The amplitude of the autocorrelation signal peak depends on the extent of the correct match in phase and Doppler between the incoming and local signals. The Doppler for the GPS signal with a 10 KHz interference signal matched closely with the replica signal compared to the other interference scenarios. This results in a high SNR as shown in the Figure 6.23. The SNR variation is similar for different modulating frequencies. It goes below one for a +10 dB relative interference power except for modulating frequencies of 10 and 25 KHz. The Doppler closely matches the interference signals with modulating frequencies of 10 KHz and 25 KHz yielding a higher SNR. An interference power of 10 dB more than the GPS signal power reduces the SNR below one for 10-15% of the time. However a relative interference power of +20 dB will reduce the SNR below one and will prevent successful acquisition. A predetection integration of 100 ms can tolerate up to +20 dB relative interference power. A longer coherent integration time accumulates more signal which increases the signal peak. However, it also means more interference signal is present which reduces the SNR.

The GPS signal can be acquired for a coherent integration time above 10 ms. A coherent integration time below 8 ms is not sufficient to acquire the GPS signal even for +5 dB relative interference power. The signal can be acquired if the false detection probability is increased causing a reduction in the detection threshold. A coherent integration of 20 ms is sufficient to tolerate the relative interference power of 10-15 dB. A predetection integration time of 100 ms can withstand a relative interference power of 20 dB. An interference power of 20 dB more than the GPS signal power is sufficient to reduce the SNR below one and prevent GPS signal acquisition.

6.9.1.3 Acquisition Success Percentage

An interference signal can distort the GPS signal resulting in a correlation peak being obtained at an incorrect Doppler. Acquisition success percentages for different modulation depths at a modulating frequency of 1 Hz are shown in Figure 6.24.

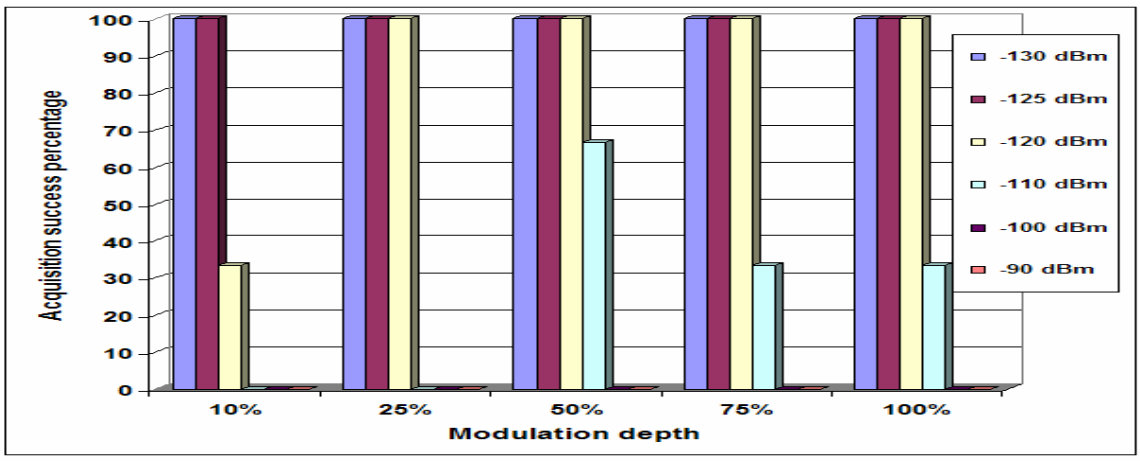

Figure 6.24: Acquisition success percentage for different modulation depths at modulation frequency of 1Hz

The acquisition success increases for higher modulation depths. It is 100% for +10 dB relative interference power and drops to 50% for +20 dB relative interference power. An interference power of 30 dB more than the GPS signal power distorts the GPS signal which results in false acquisition. Acquisition success percentages for different modulation frequencies at a modulation depth of 50% are shown in Figure 6.25. Acquisition success percentage decreases with an increase in the modulation frequency. It is found to be similar for all modulation frequencies until +10 dB relative interference power is reached.

The acquisition success percentage increases for a longer coherent integration time. A coherent integration time of 1 ms is not sufficient to obtain the correct Doppler. The acquisition success percentage is 100% for +10 dB relative interference power at a 20 ms coherent integration but decreases to about 70% for a 4 ms coherent integration period. However, with +20 dB relative interference power the success percentage goes down to zero. A coherent integration time of 8 ms or above provides better tolerance to the AM signals. The acquisition success percentage increases with an increase in the non-coherent integration time. It increases from 30% to 100% with an increase in the non-coherent integration factor from 1 to 5 for +10 dB relative interference power. A predetection integration time of 100 ms is capable of tolerating a 20 dB relative interference power level. An interference power of 20-30 dB more than the GPS signal level is sufficient to jam the acquisition process.

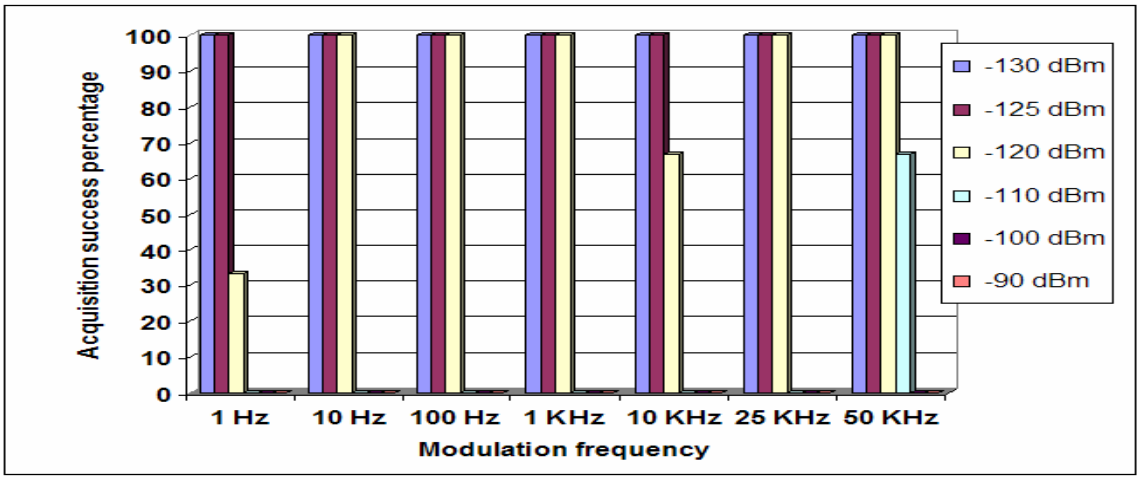

Figure 6.25: Acquisition success percentage for different modulation frequencies at modulation depth of 50%

6.9.1.4 Acquisition Plots

The correlation plots for different AM interference powers with a modulating frequency of 1 Hz and a modulation depth of 10% are shown in Figure 6.27. The cross-correlation peaks increase at higher interference powers which cause false acquisition. The noise induced by the AM signal mask the signal peak which prevents signal acquisition.

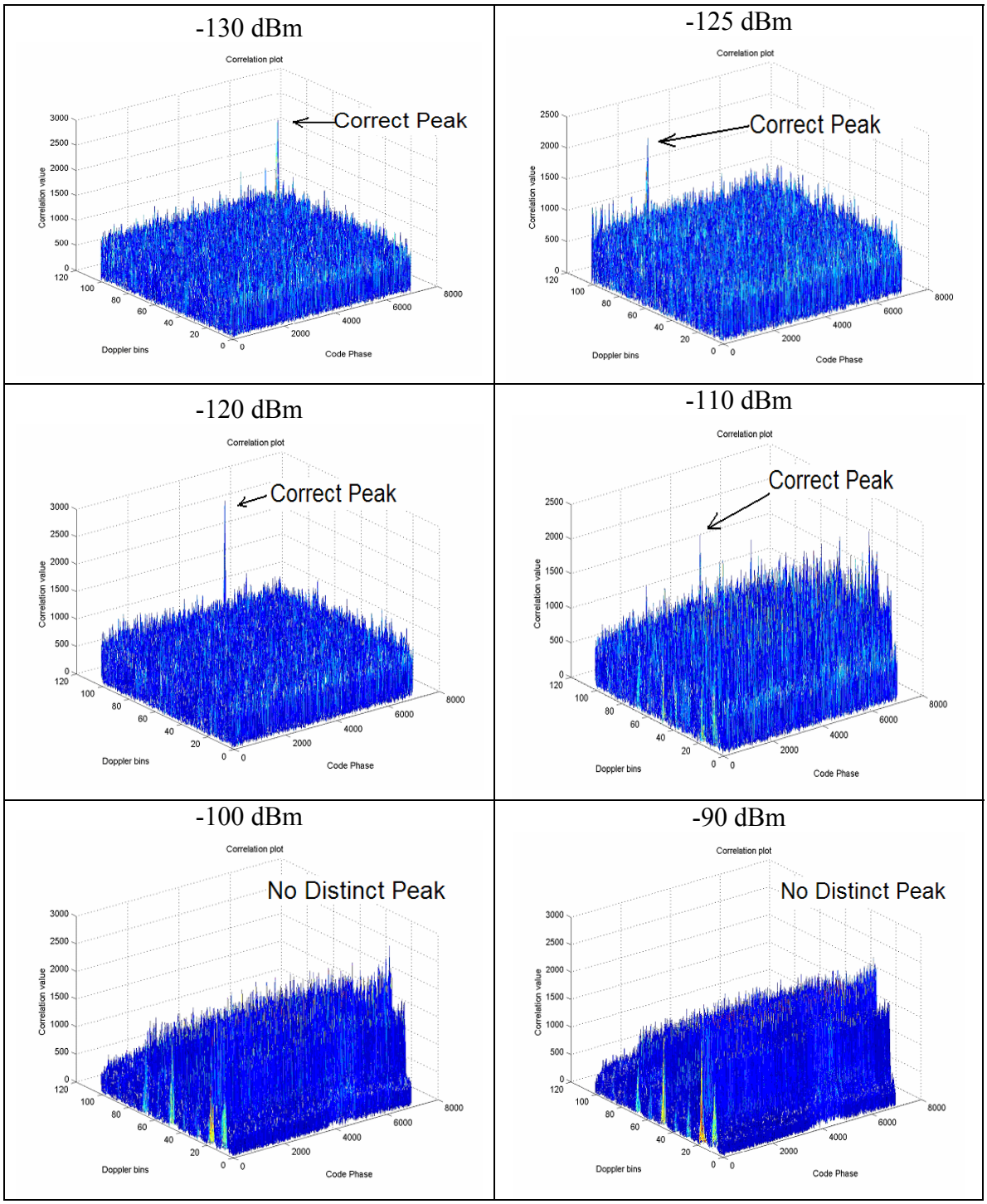

Figure 6.26: Correlation plots for different AM interference powers

6.10 Frequency Modulation Signals

Frequency modulation varies the instantaneous frequency of a carrier signal to depart from its centre frequency by an amount proportional to the instantaneous value of the modulating signal [Sastry, 1997]. It is also called an angle modulation scheme since it was developed from phase modulation. The main advantages of FM over AM are

1. Improved SNR (about 25 dB) with respect to human-made interference
2. Smaller geographical interference between neighbouring stations
3. Less radiated power
4. Well defined service areas for a given transmitter power [Sastry, 1997]

The disadvantages of FM are

1. Higher bandwidth requirement (up to 20 times more than AM)
2. Complicated receiver and transmitter design [Sastry, 1997]

In FM, the frequency of the carrier signal is changed in proportion to the modulating signal $m(t)$. Thus the signal that is transmitted is of the form $A\cos(\omega_c t + \Delta\omega \int_0^t m(t)dt)$.

The signal *m(t)* is normalized so that the maximum of the integral is 1 and $\Delta\omega$ is called the frequency deviation of the FM signal. The modulation index of an FM signal for a modulating signal $m(t) = \cos\omega_m t$ is defined as $\beta = \frac{\Delta\omega}{\omega_m}$ [Sastry, 1997]. An FM signal is represented in Figure 6.27.

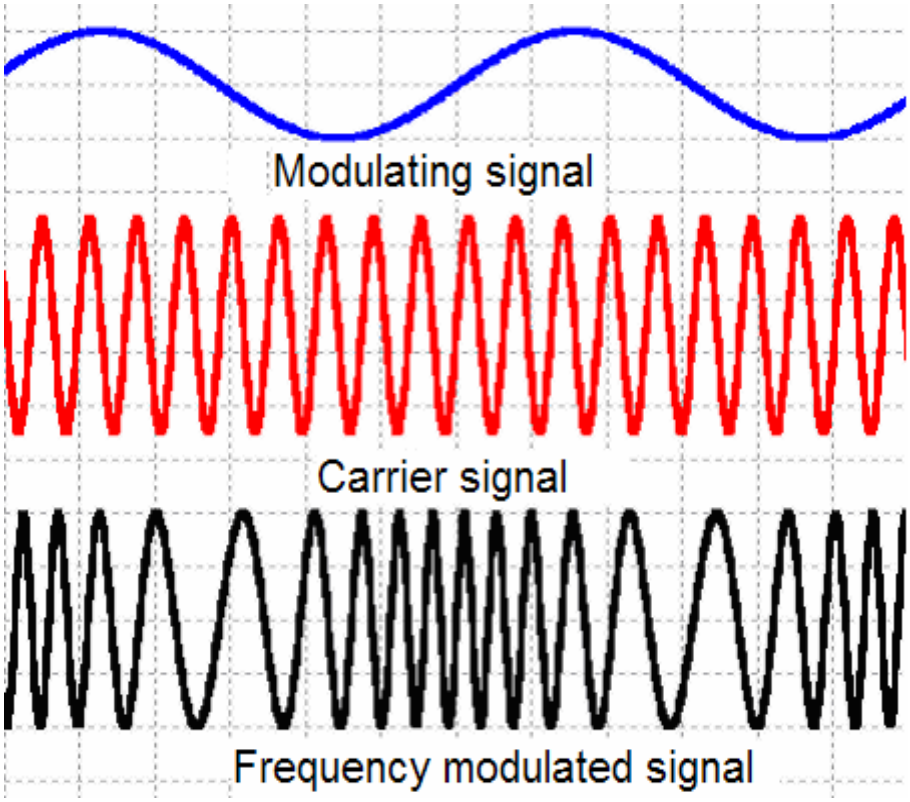

Figure 6.27: FM Signal

An FM wave can be considered as a sum of several CW signals with constant frequencies. It has frequency components at the carrier frequency and at sidebands, spaced above and below the carrier frequency at integer multiples of the modulation frequency [Peterson et al., 1995]. The sidebands should balance the phases and amplitudes in order to add to the carrier wave and to maintain constant amplitude. The upper and lower sidebands of the same order must be matched in amplitude. The odd order sidebands must be exactly out of phase and the even order sidebands must be exactly in-phase to maintain the proper phase.

FM signals are used for radio broadcasts in the 88-108 MHz frequency range and for cellular transmissions at various frequencies listed in Table 6.9. These FM signals use high power for transmission and their high order harmonics fall in the GPS frequency band. These harmonics have considerable power when compared to the GPS signal level and cause interference which needs to be mitigated. The FM carrier frequency was kept at the GPS L1 frequency during the analysis. Different modulating frequencies and frequency deviations were tested for various interference power levels. The FM interference scenarios are listed in Table 6.10.

Table 6.9: Mobile operating frequencies and power levels [Paddan et al., 2003]

GPS jamming frequencies in handset		
Cellular Standard	**Transmit Freq (MHz)**	**Max. Handset output power**
GSM	880-913 and 1710-1785	+33 dBm
IS-95	824-849	+23 dBm
PCS	1850-1910	+24 dBm

Table 6.10: FM interference scenarios

Parameter	**Value**
Time	30 Nov, 2003 04:00:00 GMT
PRN	21
GPS signal frequency	L1 frequency
Signal Power used	-130 dBm
Modulation carrier frequency	L1 frequency
Modulation frequency	0.001, 0.01,0.1,1,10,25 and 50 KHz
Frequency deviation	0.01, 0.1, 1 and 2 MHz
Interference power	-130,-125,-120,-110,-100 and -90 dBm

6.10.1 Results

FM signals were analyzed for different modulating frequencies, frequency deviations and interference powers. The results are discussed for different interference conditions under adaptive predetection integration.

6.10.1.1 Noise Power Analysis

The noise power at a -130 dBm interference power is compared with the noise from the clean GPS signal. This determines the additional noise introduced by an interference signal at the nominal GPS signal strength. Additional noise of 10-12% is introduced for different modulation frequencies and frequency deviations. Modulation frequencies of 1 and 10 Hz introduce more noise compared to the other modulating frequencies analyzed. The amount of noise introduced depends on the predetection bandwidth of the acquisition process. A smaller frequency deviation will result in more interference signal being present in the predetection bandwidth. Thus the noise power increases for a smaller frequency deviation. The noise powers for different frequency deviations at a modulation frequency of 1 Hz for a coherent integration time of 10 ms are shown in Figure 6.28.

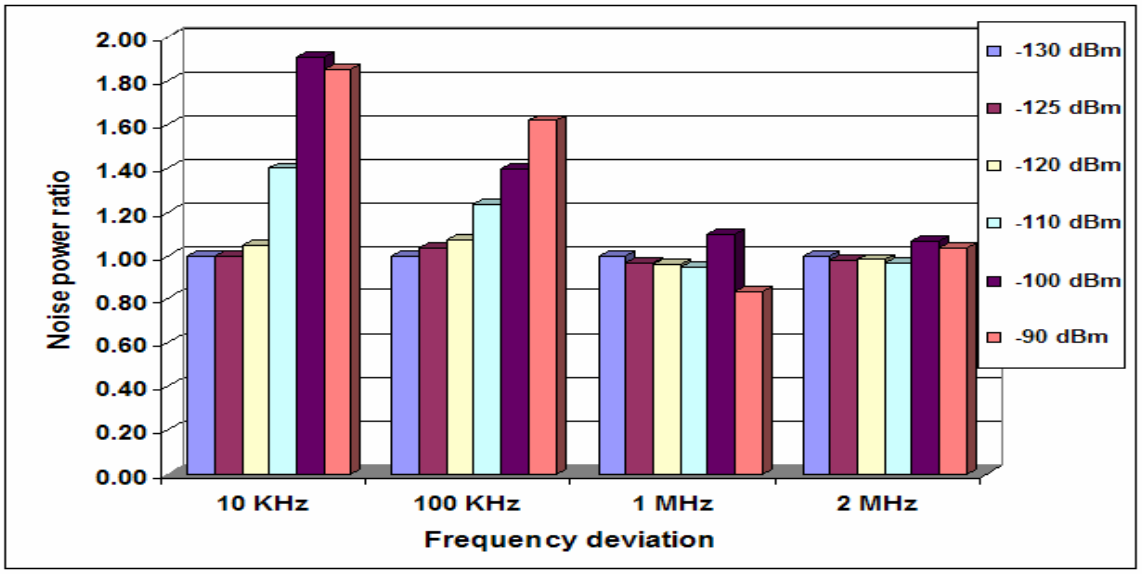

Figure 6.28: Noise power ratios for different frequency deviation at modulating frequency of 1 Hz and coherent integration of 10 ms

A filter can be used to limit the frequency deviation of the FM interference. However, a bandwidth below 2 MHz causes a loss of GPS C/A-code information and degrades the GPS accuracy. Thus it is not possible to reduce the IF bandwidth below 2 MHz. A narrow correlator architecture requires the IF bandwidth to be above 8 MHz which increases the amount of noise present in the incoming signal. The noise power increases by about 60-85% for +40 dB relative interference power for the frequency deviation below 100 KHz. The noise power variation with frequency deviation is similar for the other modulation frequencies.

The modulation frequency in the FM signal decides the rate at which the frequency deviates from the centre frequency. A smaller modulation frequency has less frequency variation and the interference signal appears like a CW frequency. The noise power variation for different modulation frequencies at a frequency deviation of 10 KHz is

shown in Figure 6.29. The noise power increases about 85% for +40 dB relative interference power at modulating frequencies below 1 KHz and a frequency deviation of 10 KHz. The noise power increases by 30-40% for other modulation frequencies. Noise power variation for the different modulation frequencies over various frequency deviations is similar. Thus the noise power increases for a lower frequency deviation and lower modulation frequency.

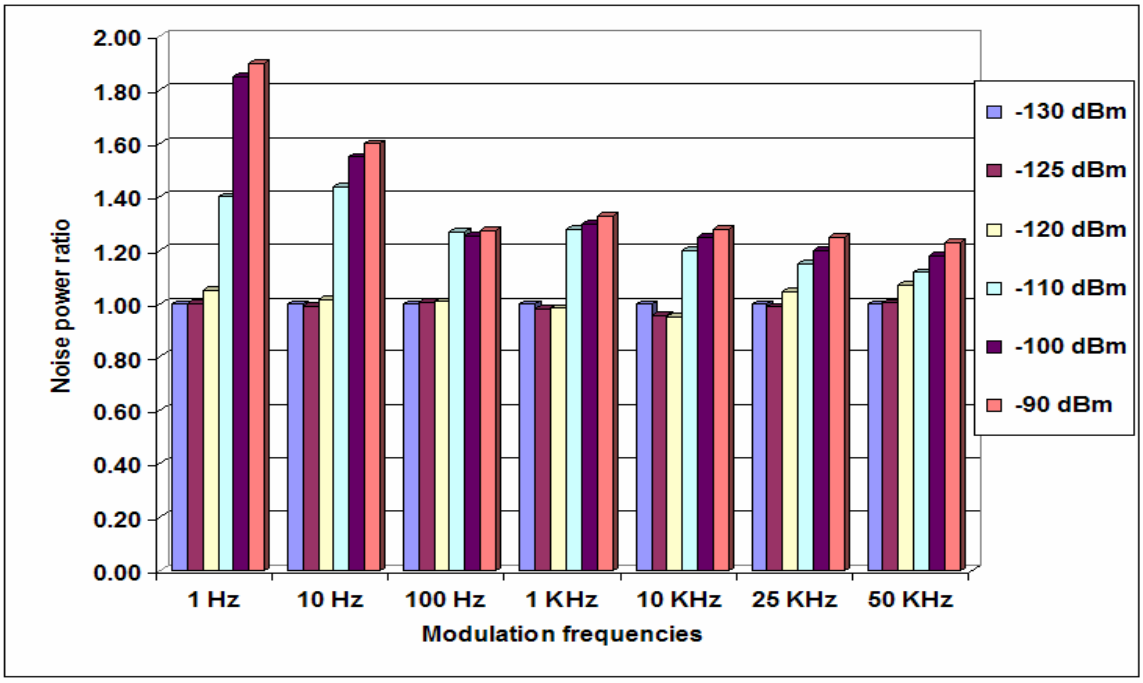

Figure 6.29: Noise power ratios for different modulating frequencies at 10 KHz frequency deviation

The noise power increases with the coherent integration time. Thus the noise is non-Gaussian and hence longer coherent integration is not suitable for reducing the noise in the presence of the FM interference. The amount of increase in the noise power is about 50% for a 1 ms coherent integration period while it is 180% for a 20 ms coherent integration period with +40 dB relative interference power. The amount of increase in the noise power for different modulation frequencies and frequency deviations over different

coherent integration periods is similar. A minimum increase of 20-30% in the noise power is observed for different frequency deviations and modulation frequencies.

Non-coherent integration is usually used to avoid signal loss due to the navigation data bit transition. This allows for using a smaller coherent integration time. The noise power drastically increases for higher non-coherent integration factors. The noise power is found to increase by about 200% for 0 dB and 700% for 40 dB relative interference power for a non-coherent integration factor of five. Thus for FM interference, the noise power is found to increase for smaller frequency deviations, lower modulation frequencies and longer predetection integration times.

6.10.1.2 SNR Analysis

This section determines whether the acquisition was successful under various interference scenarios. The signal peak obtained at the correct Doppler, determined from clean GPS signal, is compared against the detection threshold. The SNRs for different frequency deviations at a modulating frequency of 1 Hz are shown in Figure 6.30.

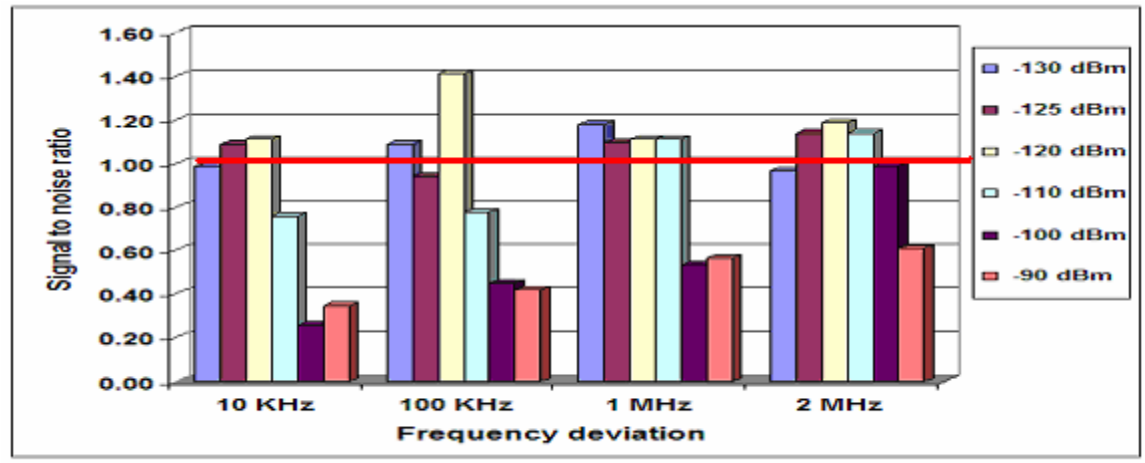

Figure 6.30: SNRs for different frequency deviation at frequency of 1 Hz

The SNR is above one for +20 dB relative interference power. It increases for higher frequency deviations because the noise introduced is less at higher frequency deviations. It drops below one for +25-30 dB relative interference power. The signal peak obtained depends upon the proximity of the correct Doppler with the replica Doppler generated. The SNR variation is found to be similar for different frequency deviations at various modulation frequencies. A frequency deviation below 1 MHz will reduce the SNR below one for +30 dB relative interference power and prevents signal acquisition. The SNRs for different modulating frequencies at a 100 KHz frequency deviation is shown in Figure 6.31. Adaptive predetection integration is able to tolerate a relative interference power of 20 dB. The SNR varies similarly for the different modulating frequencies and gives an indication of the possible interference tolerance. It decreases for higher interference power and jams the receiver.

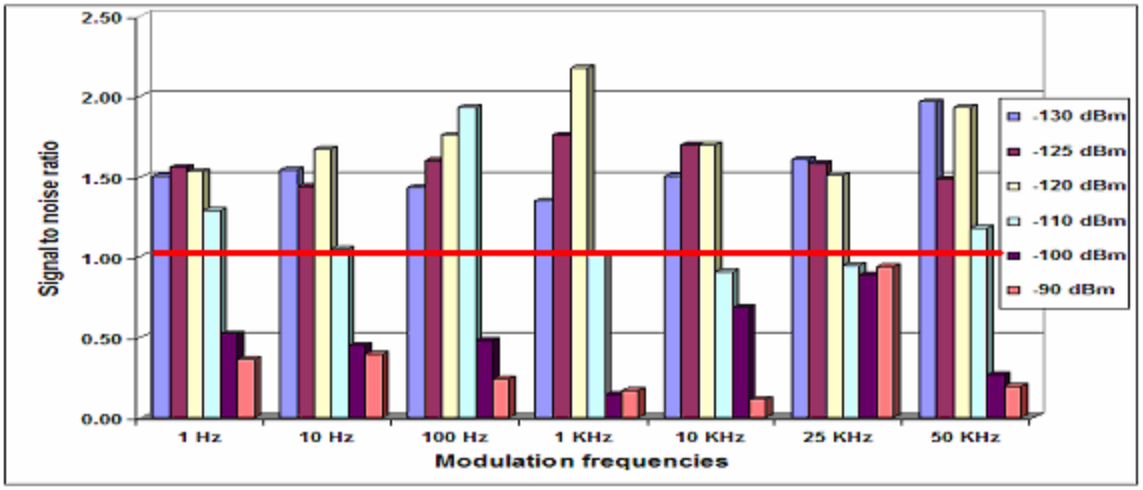

Figure 6.31: SNRs for different modulating frequencies at 10 KHz deviation

The coherent integration period was increased to increase the GPS signal peak. The noise introduced from the FM interference is not Gaussian and increases with the coherent integration time. The noise increases with the coherent integration time and the signal level has to increase by the same ratio to be acquired which is not feasible at all times. The SNR increases for longer coherent integration times and provides more tolerance to the interference. Coherent integration below 4 ms is not sufficient to obtain the correct peak with the minimum interference power analyzed. This is overcome using non-coherent integration. The SNR increases with an increase in the non-coherent integration factor. An increase in the non-coherent integration factor to five provides tolerance to +20 dB relative interference power. A 30 dB relative interference tolerance is provided for higher frequency deviations and lower modulation frequencies for a predetection integration of 100 ms.

6.10.1.3 Acquisition Success Percentage

This section determines the maximum interference power required to distort the GPS signal peak. The acquisition success percentages for different frequency deviations are shown in Figure 6.32. A smaller frequency deviation will distort the GPS signal at a lower interference power. This is because the smaller frequency deviation will cause the FM signal to appear as a CW signal and will introduce more noise. The interference tolerance increases with a higher frequency deviation. A frequency deviation below 100 KHz will distort the GPS signal for less than a +30 dB relative interference power.

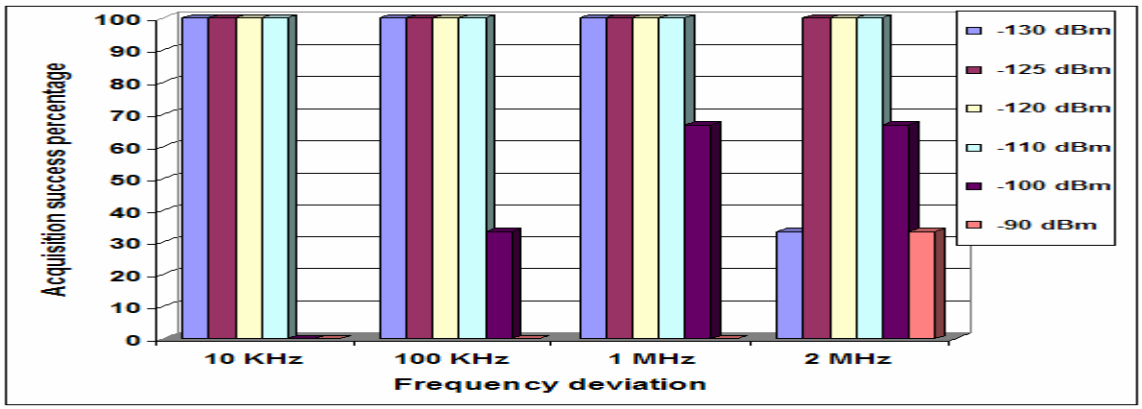

Figure 6.32: Acquisition success percentage for different frequency deviation at 1 Hz modulating frequency

The acquisition process is more robust to FM interference at higher frequency deviations. FM signals with higher frequency deviations will have some signals outside the predetection bandwidth which will reduce the amount of interference present. Thus communication systems using wideband FM signals are less probable to cause interference. The acquisition success percentages for different modulating frequencies are shown in Figure 6.33. Different modulating frequencies are found to affect the GPS

signal in a similar manner. The success percentage is 100% for 20 dB relative interference power which reduces to 70% for 30 dB and drops to zero for 40 dB relative interference power. Acquisition success percentage increases for lower modulation frequencies. The increase is about 30% for modulation frequencies below 1 KHz at various frequencies deviations compared to the modulation frequencies above 1 KHz. Thus communication systems should use a lower modulation frequency but higher frequency deviation. A longer coherent integration time is found to increase the SNR and hence increase the acquisition success percentage.

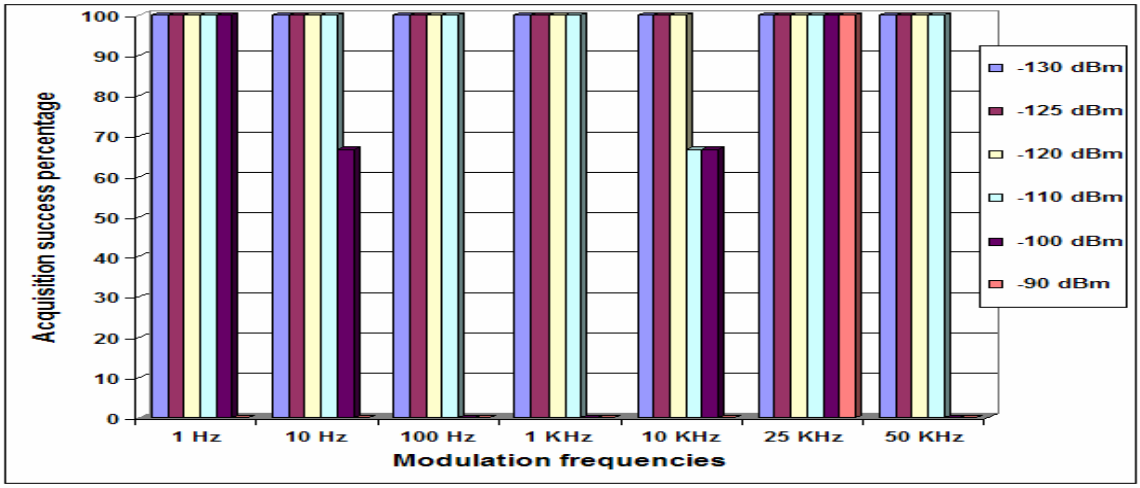

Figure 6.33: Acquisition success percentage for different modulating frequencies at 10 KHz deviation

Coherent integration above 8 ms gives 100% acquisition success for +30 dB relative interference power. The results are similar for the different frequency deviation and modulation frequencies analyzed. The acquisition peak increases with an increase in the non-coherent integration factor which increases the acquisition success percentage. This provides better tolerance to high interference power. A predetection integration time of

100 ms can tolerate a relative FM interference of +40 dB for different modulation frequencies and frequency deviations analyzed.

6.10.1.4 Acquisition Plots

The correlation plots for different FM interference powers are shown in Figure 6.34. These plots are for an FM signal with a modulating frequency of 1 KHz and a frequency deviation of 100 KHz. The plots show the increase of the noise floor which reduces the SNR and prevents acquisition.

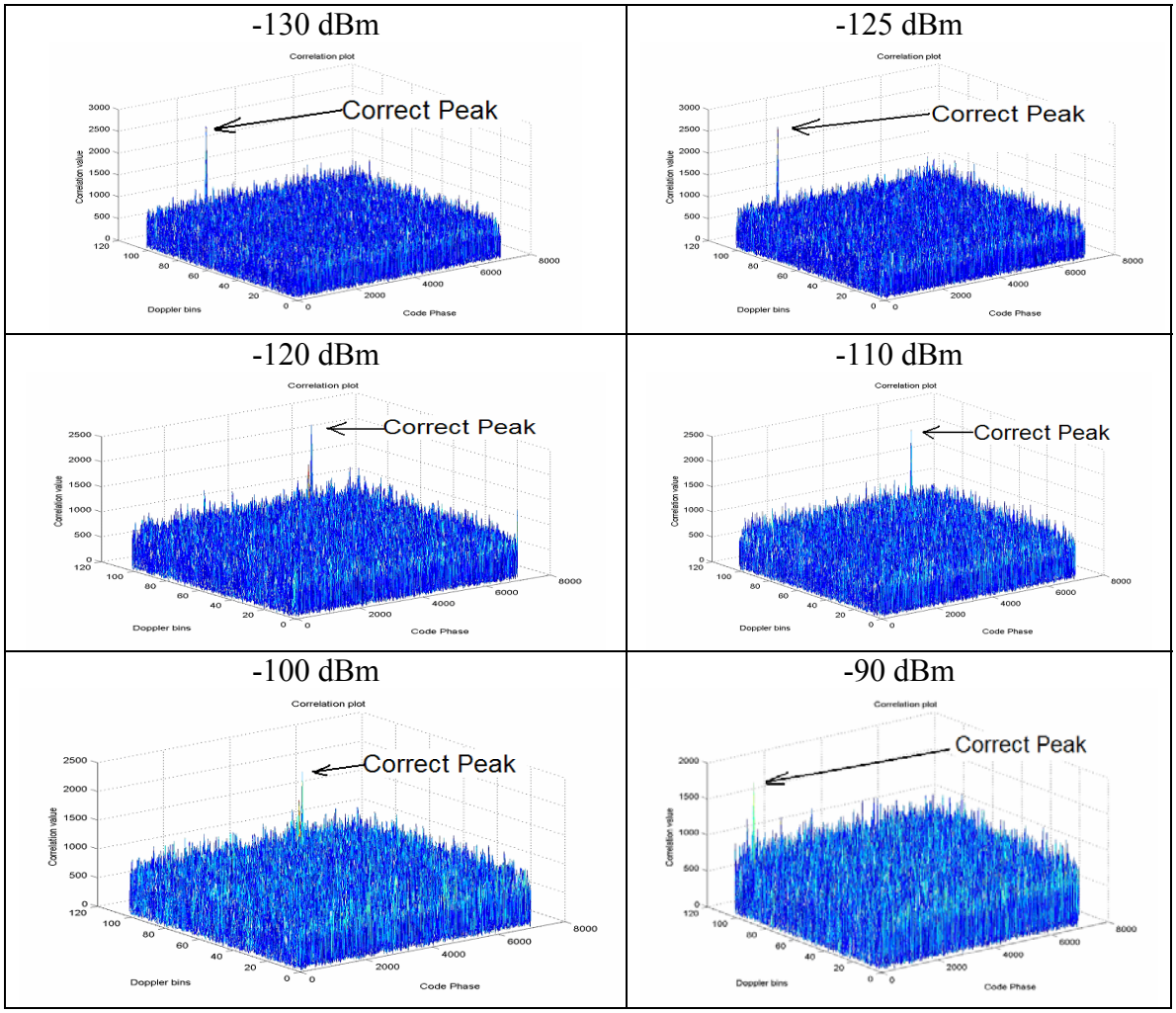

Figure 6.34: Correlation plots for FM interference at different power levels

CHAPTER 7: CONCLUSION AND RECOMMENDATIONS

This research investigated the effect of various acquisition parameters and RFI signals on GPS signal acquisition. In the first part of the research, the acquisition schemes were developed and implemented as a part of the software receiver. These acquisition schemes were compared using different figures of merit. The effects of the sampling frequency and predetection integration time on the GPS signal spectrum were studied in detail.

The second part of the research analyzed the effect of RFI signals on the GPS acquisition process. Different interference signals were simulated using the Agilent signal generator, the GPS simulator and an interference combiner. These interference signals were analyzed for the different signal parameters. An adaptive predetection integration was carried out in GPS acquisition to determine possible interference tolerance. RFI effects were analyzed to determine the amount of noise introduced and their effect on the signal peak.

7.1 Conclusions

The following conclusions can be drawn from the results of the research:

1. The circular convolution scheme provides about 1.5 dB more gain than modified circular convolution which allows acquisition of weaker signals. The modified circular convolution has 50% less processing time for a coherent integration time

above 10 ms compared to the other method. The modified circular scheme requires less memory which is a constraint for embedded systems.

2. Aliasing effect from sampling frequency introduces a signal loss of 2-3 dB and in some cases it causes signal distortion and false locks. The aliasing-free sampling frequency increases with the signal bandwidth. A higher sampling frequency requires more processing memory and time. The sampling frequency should be optimally chosen to avoid the aliasing effect and spectral inversion and to reduce the processing requirements.
3. The predetection integration time determines the gain obtained from the acquisition methods. A coherent integration time above 8 ms is sufficient to acquire the GPS signal strength of -130 dBm. To acquire signal strength of -135 dBm, the coherent integration time has to be above 30 ms.
4. The coherent integration time is limited by the navigation data bit uncertainty and the residual Doppler which can be overcome using non-coherent integration. However non-coherent integration has lesser acquisition gain than coherent integration.
5. A false detection probability of 5-10% provides reliable results under all conditions for 3-sigma correlation noise.
6. C/A-code cross-correlation causes major problems for signal acquisition below a -135 dBm power level.
7. RFI distorts the GPS signal for very low power levels and degrade GPS performance. RF signals severely affect the GPS signal acquisition process and results in false acquisition.

a. A relative CWI power of +10 dB is sufficient to prevent signal acquisition and +15 dB to jam the acquisition process for the CW frequencies considered.
b. A relative swept CWI power of +15 dB is sufficient to prevent signal acquisition and +20-25 dB to jam the acquisition process.
c. A relative broadband noise power of +15 dB is sufficient to prevent signal acquisition and +20 dB to jam the acquisition process.
d. A relative AM power of +15 dB is sufficient to prevent signal acquisition and +25-30 dB to jam the acquisition process.
e. A relative FM power of +20 dB is sufficient to prevent signal acquisition and +35 dB to jam the acquisition process.

These are the average values for all the different scenarios analyzed for each RF signal. However, the actual interference power required to prevent or to jam the acquisition process depends upon the characteristics of the interference signal.

7.2 Recommendations for GPS Acquisition process

Based on the results and conclusions of this research, the following recommendations regarding GPS acquisition and RFI mitigation can be made:

1. The current GPS acquisition schemes have large processing times. This is due to the number of FFT and IFFT points. To reduce the FFT points, averaging of samples can be done. However averaging across the PRN chips will cause distortion. To overcome this, averaging the data in two sets separated by a half code chip is recommended.

2. The present version of the software receiver developed uses the circular convolution scheme for acquisition. Intelligent acquisition was implemented to use the modified circular convolution scheme first to acquire strong GPS signals and then use the circular convolution scheme with a longer coherent integration to acquire weak signals. Similar combinations of acquisition methods can be used to improve acquisition performance.
3. A sampling frequency above 5 MHz, predetection integration time above 8 ms, noise power of 3-sigma and a false detection probability of 10% is suggested for the acquisition process at an IF of 15.42 MHz and IF bandwidth of 2 MHz.

   A sampling frequency above 17 MHz, predetection integration time above 10 ms, noise power of 3-sigma and a false detection probability of 10% is suggested for the acquisition process at an IF of 15.42 MHz and IF bandwidth of 8 MHz.

   The values for the noise power and false detection probability ensure that there is no false acquisition until -135 dBm. The integration time is longer for an 8 MHz bandwidth because of the increased noise in the acquisition process due to wider bandwidth.
4. Possible RFI tolerance using an adaptive predetection integration up to 100 ms was thoroughly tested and the following recommendations can be made:
   a. Swept CW and AM interference are similar in nature and better tolerance can be provided with a 10 ms coherent integration time and a non-coherent integration factor of five.

b. The GPS signal is more tolerant to FM signals among all the signals analyzed. The acquisition process shows better tolerance to a lower modulation frequency and higher frequency deviation. Predetection integration of 40 ms or above is suggested to reduce FM interference effects.

c. Coherent integration of 20 ms or above provides better tolerance to the broadband signal. It is better to keep the non-coherent factor at one for this type of interference.

d. The CW signals are the most damaging of all the signals analyzed. The predetection integration time does not help in tolerating higher interference power. Hence predetection integration for the normal case can be used under CWI.

5. To improve RFI mitigation, preprocessing the frequency spectrum of the input signal to eliminate the undesired frequency components could be explored. The GPS signal spectrum containing interference consists of frequency bins with high power compared to the clean GPS signal spectrum. These frequency bins contain the interference signals which can be filtered out to reduce interference. This will provide a better performance of the acquisition process. Cutright et al. [2003] did some work on the spectrum filtering to reduce interference.

7.3 Recommendations for Future Research

Based on this research, work can be done in following areas:

1. User dynamics were not considered during the analysis. User dynamics are expected to increase the Doppler search range in the acquisition process. They also limit the duration of the predetection integration time since the Doppler varies quickly for high user dynamics. This should be investigated.
2. All the interference analysis was done with an IF bandwidth of 2 MHz. A higher IF bandwidth is expected to reduce interference tolerance because the amount of noise allowed in the acquisition process is larger compared to a 2 MHz bandwidth. The effect of different IF bandwidth needs to be analyzed.
3. The noise power was computed assuming a Gaussian nature of the GPS correlation noise. With an interference signal present, this may not be true and work can be done to characterize the nature of the noise.
4. An improvement in the acquisition sensitivity and time by aiding the acquisition process with various information like the GPS time, ephemeris, almanac and user position could be studied. Data wipe-off methods could be implemented and tested for weak signal acquisition.
5. The advantage of assisted GPS in mitigating interference could be studied

APPENDIX A: Circular convolution method

The Fourier transform decomposes or separates a waveform or function into sinusoids of different frequencies which sum to the original waveform [Brigham, 1988]. It identifies or distinguishes the different frequency sinusoids and their respective amplitudes. The Fourier transform of a function f(x) is defined in Equation (A.1) [Brigham, 1988].

$$F(s) = \int_{-\infty}^{\infty} f(x) e^{-i2\pi xs} dx \qquad \text{A.1}$$

The inverse Fourier transform of F(s) is given by Equation (A.2) [Brigham, 1988].

$$f(w) = \int_{-\infty}^{\infty} F(s) e^{i2\pi ws} ds \qquad \text{A.2}$$

The functions and transforms occupy the two domains referred to as the function and the transform. However, in most applications these domains are called as the time and frequency domains. The time domain correlation property for the Fourier transform is discussed below. The correlation of two signals f(x) and g(x) is defined in Equation (A.3)

$$h(x) = \int_{-\infty}^{\infty} f(u) g(x+u) du \qquad \text{A.3}$$

Taking the Fourier transform of the correlated signal h(x), Equations (A.4) and (A.5) are obtained.

$$H(s) = \Gamma\{h(x)\} \qquad \text{A.4}$$

$$H(s) = \int_{-\infty}^{\infty} h(x) e^{-i2\pi sx} dx \qquad \text{A.5}$$

$$H(s) = \int_{-\infty}^{\infty}[\int_{-\infty}^{\infty} f(u)g(x+u)du]e^{-i2\pi sx}dx \qquad A.6$$

$$H(s) = \int_{-\infty}^{\infty} f(u)e^{-i2\pi s(-u)}\{\int_{-\infty}^{\infty} g(x+u)e^{-i2\pi s(x+u)}dx\}du \qquad A.7$$

$$H(s) = \int_{-\infty}^{\infty} f(u)e^{-i2\pi s(-u)}du \;\; G(s) \qquad A.8$$

$$H(s) = F^*(s)G(s) \qquad A.9$$

where

$F^*(s)$ is conjugate of the Fourier transform F(s).

Equation (A.9) is the statement of the correlation theorem of Fourier transform. If f(x) and g(x) are the same function, the integral in Equation (A.3) is normally called the autocorrelation function. If they differ it is called the cross-correlation function. Thus correlation in the time domain is multiplication of the Fourier transform of the two signals. The correlation interval is spread over the entire range of the function. The acquisition search range is two-dimensional in a GPS receiver. The correlation can be reduced to one-domain by using this correlation property of the Fourier transform. The multiplication of the two signal spectrums gives correlation values over the entire range. Thus correlation of the incoming GPS signal with a local signal at a particular Doppler over the entire code phase range is basically multiplication of the Fourier transforms of the incoming GPS signal and the local signal. Thus a search need not be conducted in the code phase domain. This reduces the search domain to a single-dimension (Doppler search) during acquisition. This method is called circular convolution.

REFERENCES

Agilent Technologies (2003), Understanding Dynamic Signal Analysis, Fundamentals of Signal Analysis Series, Agilent Technologies, Application note 1405-2.

Akopian D., H. Valio and S. Turunen (2002), Fine Frequency Resolution Acquisition Methods for GPS Receivers, Proceedings of ION GPS 2002, Portland, OR, September 24-27, pp. 2515-2523.

Akos D., P.L. Normark, A. Hansson, A. Rosenlind and P. Enge (2001), Real-Time GPS Software Radio Receiver, Proceedings of ION NTM 2001, Long Beach, CA, January 22-24, pp. 809-816.

Alaqeeli A. and J. A. Starzyk, (2001), Hardware Implementation of Fast Convolution for GPS Signal Acquisition Using FPGA, Proceedings of 33rd South-eastern Symposium on System Theory, Athens, OH, March 2001, pp 17-204.

Alaqeeli A. (2002), Global Positioning System Signal Acquisition and Tracking Using Field Programmable Gate Arrays, PhD thesis, Ohio University, November 2002.

Bastide F., D. Akos, C. Macabiau and B. Roturier (2003), Automatic Gain Control (AGC) as an Interference Assessment Tool, Proceedings of ION GPS 2003, Portland, OR, September 9-12, pp. 2042-2053.

Behre C., R. Ornedo, G. Rogeness and T. Moore (2002), Satellite Acquisition for a Strike Missile under Jamming and Time Initialization constraints, Proceedings of ION NTM 2002, San Diego, CA, January 28-30, pp.254-264.

Betz J.W. (2000), Effect of Narrowband Interference on GPS Code Tracking Accuracy, Proceedings of ION NTM 2000, Anaheim, CA, January 26-28, pp.16-27.

Bond K. and J. Brading (2000), Location of GPS Interference using Adaptive Antenna Technology, Proceedings of ION GPS 2000, Salt Lake City, UT, September 19-22, pp. 512-518.

Braasch M., C.A. Snyder and R. Olin (1997), Ranging Accuracy Considerations in GPS Interference Suppression, Proceedings of ION GPS 1997, Kansas City, MO, September 16-19, pp. 1483-1487.

Braasch M.S. and F. Van Graas (1991), Guidance Accuracy Considerations for Real time GPS Interferometry, Proceedings of ION GPS 1991, Albuquerque, NM, September 9-13, pp. 373-386.

Brigham E. O. (1988) The Fast Fourier Transform and Its Applications, Englewood Cliffs, Prentice-Hall Inc., New Jersey, NY.

Brown A., D. Reynolds, D. Roberts and S. Serie (1999), Jammer and Interference Location System – Design and Initial Test Results, Proceedings of ION GPS 1999, Nashville, TN, September 14-17, pp. 137-142.

Brown A., S. Atterberg and N. Gerein (2000), Detection and Location of GPS Interference Sources using Digital receiver Electronics, Proceedings of IAIN World Congress and ION AM 2000, San Diego, CA, June 26-28, pp. 269-274.

Buck T. and G. Sellick (1997), GPS RF Interference via a TV Video Signal, Proceedings of ION GPS 1997, Kansas City, MO, September 16-19, pp. 1497-1502.

Burns J., C. Cutright and M. Braasch (2002), Investigation of GPS Software Radio Performance in Combating Narrow Band Interference, Proceedings of ION AM 2002, Albuquerque, NM, June 24-26, pp. 523-530.

Chansarkar M. (2000), Acquisition of GPS Signals at Very Low Signal to Noise Ratio, Proceedings of ION NTM 2000, Anaheim, CA, January 26-28, pp 731-737.

Choi I. H., S. H. Park, D. J. Cho, S. J. Yun, Y. B. Kim and S. J. Lee (2002), A Novel Weak Signal Acquisition Scheme for Assisted GPS, Proceedings of ION GPS 2002, Portland, OR, September 24-27, pp. 177-183.

Cooper J. and P. Daly (1997), Pre-processing of GNSS Signals Subject to Interference, Proceedings of ION GPS 1997, Kansas City, MO, September 16-19, pp. 1437-1446.

Cutright C., J. Burns and M. Braasch (2003), Characterization of Narrow-Band Interference Mitigation Performance Versus Quantization Error in Software Radios, Proceedings of ION AM 2003, Albuquerque, NM, June 23-25, pp. 323-332.

Erlandson R. and R. Frazier (2002), An Updated Assessment of the GNSS L1 Radio Frequency Interference Environment, Proceedings of ION GPS 2002, Portland, OR, September 24-27, pp. 591-599.

Escobar A. and J. Harper (2001), High Temperature Superconducting Filters for GPS Interference Mitigation, Proceedings of ION NTM 2001, Long Beach, CA, January 22-24, pp. 364-368.

FCC Report (2003), Report and Order and Second Further Notice of Proposed Rulemaking, Report No. FCC 03-290, Washington, DC.
http://hraunfoss.fcc.gov/edocs_public/attachmatch/FCC-03-290A1.pdf

Geyer M. and R. Frazier (1999), FAA GPS RFI Mitigation program, Proceedings of ION GPS 1999, Nashville, TN, September 14-17, pp. 107-113.

Gunawardena S. (2000), Feasibility Study For Implementation Of Global Positioning System Processing Techniques In Field Programmable Gate Arrays, Master of Science thesis, Ohio University, November 2000.

Gupta I. (1984), Effect of Jammer Power on the Performance of Adaptive Arrays, IEEE Transaction, Antennas Propagation, vol. AP-32, pp. 933-938.

Gupta I. and T. Moore (2001), Space-Frequency Adaptive Processing for Interference Suppression in GPS Receivers, Proceedings of ION NTM 2001, Long Beach, CA, January 22-24, pp. 377-385.

Gormov K., D. Akos, S. Pullen, P. Enge and B. Parkinson (2000), Generalized Interference Detection and Localization System, Proceedings of ION GPS 2000, Salt Lake City, UT, September 19-22, pp. 447-457.

Hegarty G., A. J. VanDierendonck, D. Bobyn, M. Tran, T. Kim and J. Grabowski (2000), Suppression of Pulsed Interference through Blanking, Proceedings of IAIN World Congress and ION AM 2000, San Diego, CA, June 26-28, pp. 399-408.

Heppe S. and P. Ward (2003), RFI & Jamming and its Effects on GPS Receivers, Based on communication theory, Navtech seminars course 452, Dahlgren, VA, May 5-6.

Herold F. and J. Kaiser (2002), GPS Interference Mitigation, Proceedings of ION AM 2002, Albuquerque, NM, June 24-26, pp. 473-482.

Hopfield, H.S. (1969) Two-Quartic Tropospheric Refractivity Profile for Correcting Satellite Data. Journal of Geophysics Res., 74(18), 4487-4499.

ICD-GPS-200 (2003), Interface Control Document, Navstar GPS Space Segment and Navigation User Interface, ARINC Research Corporation, El Segundo, CA, January 14.

Iltnis R. and G. Hanson (1999), C/A Code Tracking and Acquisition with Interference Rejection using the Extended Kalman Filter, Proceedings of ION NTM 1999, San Diego, CA, January 25-27, pp. 881-889.

Johannessen R., S. Gale and M. Asbury (1990), Potential interference sources to GPS and solutions appropriate for applications to civil aviation, IEEE AES Magazine, vol. 5, Issue 1, January 1990, pp. 3-9.

Johnston H. (1999), A Comparison of CW and Swept CW Effects on a C/A Code GPS Receiver, Proceedings of ION GPS 1997, Kansas City, MO, September 16-19, pp. 149-158.

Kaplan E.D. (1996), Understanding GPS: Principles and Applications, Artech House Inc., Norwood, MA.

Kunysz W. (2001), Advanced Pinwheel Compact Controlled Reception Pattern Antenna designed for Interference and Multipath Mitigation, Proceedings of ION GPS 2001, Salt Lake City, UT, September 11-14, pp. 2030-2036.

Lachapelle G. (2002), Navstar GPS: Theory and Applications, ENGO 625, University of Calgary, Calgary, AB.

Ledvina B.M., S.P.Powell, P.M.Kintner and M.L.Psiaki (2003), A 12-channel Real-Time GPS L1 Software Receiver, Proceedings of ION NTM 2003, Anaheim, CA, pp. 767-782.

Lin D. M., J. B.Y. Tsui, L. Lee, Y. T. Liou and J. Morton (2002), Sensitivity Limit of A Stand-Alone GPS Receiver and An Acquisition Method, Proceedings of ION GPS 2002, Portland, OR, September 24-27, pp. 2515-2523.

Littlepage R. (1999), The Impact of Interference on Civil GPS, Proceedings of ION AM 1999, Cambridge, MA, June 28-30, pp. 821-828.

Macabiau C., O. Julien and E. Chatre (2001), Use of Multicorrelator Techniques for Interference Detection, Proceedings of ION NTM 2001, Long Beach, CA, January 22-24, pp. 353-363.

MacGougan G. (2003) High Sensitivity GPS Performance Analysis in Degraded Signal Environments, UCGE #20176, Department of Geomatics Engineering, University of Calgary, Calgary, AB.

Madhani P. and P. Axelrad (2001), Mitigation of the Near-Far Problem by Successive Interference Cancellation, Proceedings of ION GPS 2001, Salt Lake City, UT, September 11-14, pp. 148-154.

Maenpa J. E., M. Balodis, G. Walter and J. Sandholzer (1997), New Interference Rejection Technology from Leica, Proceedings of ION GPS 1997, Kansas City, MO, September 16-19, pp. 1457-1466.

Manz A., K. Shallberg and P. Shloss (2000), Improving WAAS Receiver Radio Frequency Interference Rejection, Proceedings of ION GPS 2000, Salt Lake City, UT, September 19-22, pp. 471-479.

Moore T. and I. Gupta (2003), The Effect of Interference Power and Bandwidth on Space-Time Adaptive Processing, Proceedings of ION AM 2003, Albuquerque, NM, June 23-25, pp. 337-346.

Ndili A. (1994), GPS Pseudolite Signal Design, Proceedings of ION GPS 1994, Salt Lake City, UT, pp. 1375-1382.

Paddan P., P. Naish and M. Phocas (2003), GPS radio IP design for cellular applications, GPS World, February 2003, pp 30-45.

Parkinson B.W., T. Stansell, R. Beard and K. Gromov (1995), A History of Satellite Navigation, Journal of Institute of Navigation, vol. 42, Special Issue 1, pp. 109-164.

Peterson R., R. Ziemer and D. Borth (1995), Introduction to Spread Spectrum Communications, Prentice Hall Inc., New Jersey, NY.

Pietilä S. and J. Syrjärinne (2000), Improved Method for Satellite Acquisition, Proceedings of ION GPS 2000, Salt Lake City, UT, September19-22, pp. 1957-1961.

Ray J. (2003), Advanced GPS Receiver Technology, ENGO 699.73, University of Calgary, Calgary, AB.

RTCA (2001), Minimum Operational Performance Standards for Global Positioning System/Wide Area Augmentation System Airborne Equipment, Document no. DO-229C, RTCA Inc., Washington, DC, November 28.

Saasamoinen, J. (1971) Atmospheric Correction for the Troposphere and Stratosphere in Radio Ranging of Satellite. International Symposium on the Use of Artificial Satellite, Henriksen (ed.), 3rd Washington, 247-251.

Sastry S. (1997), Analog Modulation Schemes, MIT Media laboratory, Massachusetts Institute of Technology, Cambridge, MA.
http://www.media.mit.edu/physics/pedagogy/fab/fab_2002/help_pages/networking_resources/more%20networking/robotics.eecs.berkeley.edu/_sastry/ee20/modulation/node1.html

Sayed A.H. (2004), Sampling and Aliasing Overview, Digital Signal Processing laboratory, Electrical Engineering department, Univeristy of California at Los Angeles, Los Angeles, CA.
http://www.ee.ucla.edu/~dsplab/sa/over.html

Shau-Shinu J. and P. Enge (2001), Finding Source of Electromagnetic Interference (EMI) to GPS Using Network Sensors, Proceedings of ION NTM 2001, Long Beach, CA, January 22-24, pp. 533-540.

Shashidhar K. (2003), GPS Signal Tap User Guide, Accord Software & Systems Pvt. Ltd., India, www.accord-soft.com.

Spilker J.J. Jr. and B.W. Parkinson (1996), Overview of GPS Operation and Design, Global Positioning System: Theory and Applications, Vol. I, American Institute of Aeronautics and Astronautics Inc., Washington, DC.

Spirent communications (2003), User Manual for the GSS 4765 Interference Simulation System operation with SimGEN for windows, Issue 1.0, Spirent Communications Ltd., pp. 4.1-4.12.

Stenbit J. (2001), Global Positioning System Standard Positioning Service Performance Standard, Command, Control, Communications, and Intelligence, Department of Defense, Washingtion, DC.

Tsui Y. and J. Bao (2000), Fundamentals of Global Positioning System Receivers: A Software Approach, John Wiley & Sons Inc., New York, NY.

Tsui J. B. Y. and D. M. Lin (2001), An Efficient weak signal acquisition algorithm for software GPS receiver, Proceedings of ION GPS 2001, Salt Lake City, UT, September 11-14, pp .115-136.

Vaccaro J. and R. Fante (2000), Ensuring GPS Availability in an Interference Environment, Proceedings of ION GPS 2000, Salt Lake City, UT, September 19-22, pp. 458-461.

VanNee D.J.R. and A.J.R.M. Conen (1991), New Fast GPS code acquisition technique using FFT, IEEE Electronic letters, Vol. 27, No, 2, pp. 158-160.

Ward P. (1996), GPS Receiver Search Techniques, IEEE proceedings of Position Location and Navigation Symposium, Atlanta, GA, April 22-26, pp. 604-611.

Ward P. (1998), Performance Comparisons between FLL, PLL and a Novel FLL-Assisted-PLL Carrier Tracking Loop under RF Interference Conditions, Proceedings of ION GPS 1998, Nashville, TN, September 15-18, pp. 783-795.

Wells D.E., N. Beck, D. Delikaraoglou, A. Kleusberg, E.J. Krakiwsky, G. Lachapelle, R.B. Langley, M. Nakiboglou, K.P. Schwarz, J.M. Tranquilla, and P. Vanicek (1986) Guide to GPS Positioning, Canadian GPS Associates, Fredericton.

Zawistowski T. and P. Shah (2001), An Introduction to Sampling Theory, Department of Electrical and Compute Engineering, University of Houston, Houston, TX. http://www2.egr.uh.edu/~glover/applets/Sampling/Sampling.html